



University of Évora

ARCHMAT

(ERASMUS MUNDUS MASTER IN ARCHaeological MATerials
Science)

Mestrado em Arqueologia e Ambiente (Erasmus Mundus –ARCHMAT)

Technological characterization of molded Islamic pottery from Iberian Peninsula

by

Milan Marković (m34320)

Professor José Antonio Paulo Mirão

(Supervisor – University of Évora)

Doctor Susana Gomes

(Co-Supervisor – Campo Arqueológico de Mértola)

Évora, September 2016



A Tese não inclui as Críticas e sugestões do Jur

ACKNOWLEDGEMENTS

Foremost, I would like to express my sincere gratitude to all the people who have devoted their time to make this project successful. I would first like to thank my thesis supervisor professor José Mirão for the continuous support of my MA study and research, for his patience, motivation, enthusiasm and immense knowledge. His guidance helped me in all the time of research and writing of this thesis. Besides my supervisor I would like to thank the rest of my thesis committee: Doctor Susana Gomez and Doctor Nick Schiavon for their encouragement, insightful comments and hard questions.

I would like to extend my gratitude to the Hercules laboratory and its staff members Massimo Beltrame and Pedro Barrulas, for their unconditional support and valuable advices.

My sincere thanks also goes to Dr. Thilo Rehren, Dr. Myrto Georgakopoulou, Dr. Jose Carvajal, PhD Jelena Živković and the rest of the UCL Qatar staff for offering me an opportunity to carry out a part of my research in their laboratories in Doha as a Visiting Researcher.

I am also indebted to my fellow ARCHMAT colleagues: Leonor Costa, Francisco Centola, Drita Abazi, Whitney Jacobs, Diego Armando Badillo, Ivona Posedi, Aman Maldewo, Carla Soto, Indre Zalaite, Guilhem Mauran and Dauren Adilbekov, for the stimulating discussions, for the sleepless nights we were working together before deadlines, and for all the fun we have had in the last two years.

Last but not the least, I would like to thank my family: my father Živojin Marković and my mother Nataša Marković, my brothers Nikola and Rastko Marković and my sister Katarina for their encouragement and support throughout this project.

TABLE OF CONTENTS

ACKNOWLEDGEMENTS	i
List of Figures	iv
List of Tables	vi
Abstract	1
Resumo	2
CHAPTER 1: INTRODUCTION	3
1.1. A brief introduction to pottery	15
1.2. Introduction to ceramic archaeometry and paste analysis.....	16
1.3. Objectives and main goals of this research.....	5
1.4. Historical background.....	6
1.5. Archaeological context and sample description.....	11
1.6. Archaeometric techniques and pottery studies – review.....	18
1.6.1. Textural analysis	19
1.6.2. Mineralogical analysis	20
1.6.3. Petrographic analysis	22
1.6.4. Chemical analysis	23
1.7. Working principles of applied analytical techniques	24
1.7.1. Scanning Electron Microscopy (SEM)	24
1.7.2. X – Ray Fluorescence	27
1.7.3. X – Ray Diffraction	28
1.7.4. Inductively Coupled Plasma – Mass Spectrometry (ICP-MS).....	30
CHAPTER 2: MATERIALS AND METHODS	33
2.1. Sample selection	34
2.2. Methodology	35
2.2.1. Scanning Electron Microscopy – Energy Dispersive Spectroscopy (SEM-EDS)	35
2.2.2. X-Ray Diffraction (XRD)	36
2.2.3. X-Ray Fluorescence (XRF)	37
2.2.4. Laser Ablation - Inductively Coupled Plasma - Mass Spectrometry (ICP-MS)	37
CHAPTER 3: RESULTS AND DISCUSSION.....	40
3.1. Molded ceramic with slip.....	41
3.1.1. Specimen CR/MD/004.....	41
3.1.2. Specimen CR/MD/003.....	49

3.1.3. Specimen CR/MD/005	54
3.2. Molded glazed ceramic	61
3.2.1. Specimen CR/DR/0023	62
3.2.2. Specimen CR/DR/0002	75
3.3. Laser Ablation - Inductively Coupled Plasma – Mass Spectrometry (ICP – MS)	84
CHAPTER 4: FINAL REMARKS	90
BIBLIOGRAPHY	97

List of Figures

Figure 1. The expansion of Islam in the west during first decades of VIII century (Robinson C. 2011. The New Cambridge history of Islam)	7
Figure 2. The Abbasid empire in c. 800 AD (Robinson C. 2011. The New Cambridge history of Islam)	8
Figure 3. Area of origin of the Almohads and expansion of the Almohad state (Photo taken from Wikipedia, http://bit.ly/2c2n4hv)	10
Figure 4. Samples CR/MD/003; CR/MD/004 and CR/MD/005, respectively (Gomez 2004)	12
Figure 5. SAMPLES CR/DR/0002 AND CR/DR/0023 RESPECTIVELY (GOMEZ 2004)	14
Figure 6. Schematic representation of SEM (Image taken from http://goo.gl/zZXHy6) and BSE image of ceramic sample, respectively	24
Figure 7. SEM-EDS used for elemental mapping of the sample surface	25
Figure 8. Example of pXRF with vacuum pump, tripod and computer for data analysis (image taken from http://goo.gl/kkzRVX)	27
Figure 9. Schematic representation of X-Ray Diffraction Apparatus (image taken from http://goo.gl/EucASc)	28
Figure 10. Schematic representation of Bragg's law (image taken from http://goo.gl/ZjPIWm)	29
Figure 11. BSE image of sample CR/MD/004 with visually distinguishable body and the slip	42
Figure 12. BSE image of sample's CR/MD/004 body, area analysis	43
Figure 13. BSE image of sample's CR/MD/004 slip area analysis	43
Figure 14. X-ray powder diffraction spectra of CR/MD/004	47
Figure 15. BSE image of sample CR/MD/003 body	49
Figure 16. BSE images of the sample CR/MD/005 and body area analysis	50
Figure 17. X-ray powder diffraction spectra of CR/MD/003	54
Figure 18. BSE image of sample CR/MD/005 body	55
Figure 19. Cross section of the sample CD/MD/005	55
Figure 20. BSE images of the sample CR/MD/005 and body bulk analysis	57
Figure 21. BSE image of the sample CD/MD/005 and area analysis of the clay	58
Figure 22. X-ray powder diffraction spectra of CR/MD/005	60
Figure 23. Vessels CR/DR/0002 and CR/DR/0023, respectively	61
Figure 24. BSE image of sample CR/DR/0023 with visually distinguishable body and the glaze	62
Figure 25. Point 1 and 2 respectively, location and their elemental composition	65
Figure 26. PbO vs Na ₂ O+K ₂ O plot	67
Figure 27. SEM photomicrographs of body-glaze interfaces for transparent high lead glazes showing (upper) the high concentration of potassium-lead-aluminium-silicate crystals which are characteristically formed at the interface when the glaze suspension is applied to an unfired body and (lower) the absence of potassium-lead-	

<i>aluminum-silicate crystals at the interface which is characteristic of the application of the glaze suspension to a biscuit-fired body (Tite 1998)</i>	69
<i>Figure 28. Presence of air bubbles</i>	70
<i>Figure 29. X-ray powder diffraction spectra of CR/MD/0023</i>	71
<i>Figure 30. BSE image of the sample CR/MD/0023 and area analysis of the clay</i>	72
<i>Figure 31. Fragments MB0/5A1a, M/82/6c3a, M/79/AA1B respectively</i>	75
<i>Figure 32. BSE image of M/79/AA1B body fabric as an example of the inclusion characteristics</i>	76
<i>Figure 33. BSE image of exterior glaze, sample M/82/6c3a</i>	79
<i>Figure 34. XRD spectrums of fragments MB0/5A1a, M/82/6c3a, M/79/AA1B, respectively</i>	82
<i>Figure 35a,b. Ternary plot of: (a) Al₂O₃, CaO, Fe₂O₃; and (b) Al₂O₃, CaO, Na₂O + K₂O (all in oxides %) showing two ceramic groups within Mertola ; the non-calcareous ceramic group and highly calcareous pottery assemblage</i>	87
<i>Figure 36. Cr vs Cs bivariate plots of ICP-MS data. Note values are given in ppm</i>	87
<i>Figure 37. Rb vs Sr bivariate plots of ICP-MS data. Note values are given in ppm</i>	88

List of Tables

<i>Table 1. The bulk body and slip SEM-EDS analysis, sample CR/MD/04, normalized to 100 wt%. _____</i>	<i>44</i>
<i>Table 2. Chemical composition of Zaragoza ceramic samples (slip and body chemical composition) (Arantegui P., Castillo R., 2000) _____</i>	<i>45</i>
<i>Table 3. SiO₂/Al₂O₃ ratios of clay body and slip _____</i>	<i>49</i>
<i>Table 4. The body area SEM-EDS analysis, sample CR/MD/003, normalized to 100 wt%. _____</i>	<i>51</i>
<i>Table 5. Si/Al ratios of the clay body _____</i>	<i>52</i>
<i>Table 6. The bulk body SEM-EDS analysis, sample CR/MD/005, normalized to 100 wt%. _____</i>	<i>57</i>
<i>Table 7. Si/Al ratios of the clay body _____</i>	<i>58</i>
<i>Table 8. The bulk body SEM-EDS analysis, sample CR/DR/0023, normalized to 100 wt%. Note that weight proportions represent normalized weights. Normalized weights have been converted to Oxides _____</i>	<i>63</i>
<i>Table 9. SEM – EDS elemental concentrations of feldspars and amphibole in sample CR/DR/0023 _____</i>	<i>64</i>
<i>Table 10. The area analysis of the glaze, sample CR/DR/0023, normalized to 100 wt%. Note that weight proportions represent normalized weights. Normalized weights have been converted to Oxides _____</i>	<i>66</i>
<i>Table 11. Si/Al ratios of the clay body _____</i>	<i>72</i>
<i>Table 12. The area body SEM-EDS analysis, sample CR/DR/0002, normalized to 100 wt%. Note that weight proportions represent normalized weights. Normalized weights have been converted to Oxides _____</i>	<i>78</i>
<i>Table 13. SEM – EDS elemental concentrations of feldspars in samples MB0/5A1a, M/82/6c3a and M/79/AA1B _</i>	<i>78</i>
<i>Table 14. The area analysis of the glazes, samples M/79/AA1B M/79/AA1B and the corresponding PbO vs Na₂O+K₂O plot _____</i>	<i>80</i>
<i>Table 15. Average concentration values of unglazed (CR/MD/003-005) and glazed pottery from Mértola. Oxides are given on % while minor and trace elements are in ppm _____</i>	<i>85</i>

Abstract

The thesis examines the technical aspects of unglazed molded ceramics from Mértola, in the context of Islamic archaeology of the Iberian Peninsula (Almohad period, end of 12th and the beginning of 13th century). Ceramics of the time period under discussion (12th – 13th century) are understudied, including in what concern to shaping and firing of ceramic vessels, the origin of raw materials used in ceramics and glazes, and decoration methods such as slip painting and/or colored glazes. Moreover, the use of archaeometry tools is rare. Along with providing a general picture of molded ceramic production in Mértola, this work provides a new dimension to the discipline of Islamic ceramic studies by the analytical tool used and demonstrating the importance of archaeological ceramics of the western peripheries to the understanding the production of ceramics and the transmission of knowledge and cultural traditions within the Islamic caliphate.

The chemical and mineralogical characterization of 12th/13th century Almohad unglazed molded ware from Mértola was accomplished through multi – analytical approach combining SEM, Powder/xRD and LA-ICP-MS methods. In this paper unglazed and glazed samples were analyzed but the attention was given to unglazed specimens, while the glazed samples were used for the comparison with the previous group in order to determine possible similarities or dissimilarities, thus providing enough data to discuss about technical aspects and potential provenance.

Resumo

A tese debruça-se sobre os aspetos técnicos de cerâmica de molde não-vidrada de Mértola, no contexto da arqueologia islâmica da Península Ibérica (período Almóada, final de XII e início do século XIII). A cerâmica do período em discussão (séculos XII-XIII) é pouco estudada inclusive no que concerne ao fabrico e à cozedura, à de fonte de matérias-primas, na pasta ou nos esmaltes e aos métodos de decoração, como pintura, presença de engobes ou esmaltes. Além disso, o uso de ferramentas de Arqueometria é raro. Para fornecer uma visão geral da produção de cerâmica moldada em Mértola, este trabalho oferece uma nova dimensão para a disciplina de cerâmica islâmicas pelas ferramentas analíticas utilizadas. Demonstrando a importância da cerâmica arqueológica da periferia ocidental para a compreensão da produção cerâmica e a transmissão de conhecimentos e tradições culturais no califado islâmico.

A caracterização mineralógica e química das cerâmicas de molde e não-vidrada, Almóada, dos séculos XII-XIII de Mértola foi realizada através de uma abordagem multi-analítica que combina métodos de SEM-EDS, uXRD e LA-ICP-MS. Neste trabalho, as cerâmicas vidradas e não-vidradas foram analisadas conjuntamente, dando mais atenção aos espécimes não vidrados. As amostras de cerâmicas vidradas foram utilizados para a comparação com o grupo anterior, a fim de determinar as possíveis semelhanças ou diferenças, proporcionando, assim, dados suficientes para discutir os aspetos técnicos e o potencial de proveniência das cerâmicas não vidradas.

CHAPTER 1: INTRODUCTION

1.1. Objectives and main goals of this research

This study aims to investigate the production technology of a very rare and specific type of Islamic molded pottery found in Mértola (Portugal) in the context of Islamic archaeology of the Iberian Peninsula (Almohad period, end of 12th and the beginning of 13th century), questioning the origin of raw materials (clay and non-plastic materials), the manufacturing processes and stylistic influences. However, specialized studies of Islamic pottery have been a neglected subject in the European archaeology, this study will try to contribute to the development of a broader discussion focused in this specific and rare Islamic ceramic group. Therefore, main focus of this work will be to determine production technology of unglazed Molded Ware through the reconstruction of technological sequences or *chaînes opératoires* (selection and processing of the raw materials, forming, surface treatment, decoration and firing conditions). Furthermore, the outcome of this study will be compared with the results obtained from the same type of methods on glazed molded samples from Mértola and other southern Portugal Islamic archaeological sites, thus leading to a better understanding of the production of this specific and rare type of Islamic pottery in the southwest part of the Iberian Peninsula. The final aim is to contribute to the general knowledge of the population that used this type of ceramic technology, in terms of what were their technological choices and whether pottery was reserved for the higher social classes (if we consider the fact that this type of pottery is exceedingly rare in the whole Iberian Peninsula). Moreover, one of the research questions will be to determine what the provenance of this scarce archaeological finds was in order to obtain information about whether they were locally produced or imported through comparison between unglazed and glazed samples from Mértola. A multi-analytical approach which includes the study of mineralogical composition through Powder X-ray diffraction and μ XRD, as well as chemical composition via Inductively Coupled Plasma – Mass Spectrometry, X-Ray Fluorescence and Scanning Electron Microscope – Energy Dispersive Spectroscopy has been integrated for the purposes of this study.

1.2. Historical background

In the spring of 711, a mainly Berber expeditionary force commanded by Tariq ibn Ziyad, a subordinate of the Umayyad governor of North Africa, crossed the Straits of Gibraltar and landed in Baetica. On hearing the news Rodrigo, the Visigoth king (710–11), who was campaigning far to the north, summoned his host to assemble at Cordoba and hastened south. Tariq awaited Rodrigo near Algeciras, and the two armies eventually met, probably in July 711, in southern Baetica somewhere in the vicinity of Medina-Sidonia. In the fateful battle that followed, Tariq's forces were overwhelmingly victorious. Rodrigo was killed – either in the battle itself or soon afterwards – along with most of his noble entourage and household troops. Tariq thereupon rapidly advanced into the heart of the peninsula, encountering little opposition. In 712, the Umayyad governor, Musa ibn Nusayr, realizing the scale of Tariq's success, he crossed the strait to take personal command, bringing another army with him. Toledo was quickly occupied, its Visigothic count and most of the inhabitants having fled. By 716 Musa, his son Abd al-Aziz and Tariq between them had subdued virtually all core strategic and population centers in Visigothic Iberia. Though one or two cities had to be reduced by siege, resistance was uncoordinated and ultimately ineffectual. Why the Visigothic kingdom was overwhelmed so swiftly is not easy to explain. The fact is that the invasion of Tariq in 711 was not as sudden and unexpected as sometimes depicted. For some years, Visigothic leaders had known and worried about the rapid westward advance of the Arabs across North Africa, their expulsion of the Byzantines in the 690s and their subjugation of the Berber tribes in Morocco between 698 and 710. There are also indications that the battle between Tariq and Rodrigo was not the first clash of Christians with Muslims on peninsular soil, but the culmination of an ongoing process. Nevertheless the subjugation of the peninsula was achieved largely by using the standard tactics of earlier Arab conquests.

After the capitulation of the Visigothic heartland the subjugation of outlying regions like the future Portugal was only a matter of time. It was eventually Musa himself who invaded Lusitania, probably in 713. Most cities of the Algarve and Baixo Alentejo quickly submitted to him, though Mérida, a stronghold of Rodrigo's supporters, surrendered only after a siege lasting several months. Abd al-Aziz then occupied Alto Alentejo and Estremadura, while Musa took the Beiras. By the time both leaders had left for Damascus in or before early 715, their work in western Iberia

was all but complete. Portugal had been effectively incorporated into the Umayyad Empire, along with nearly all the rest of the Iberian Peninsula (Figure 1).

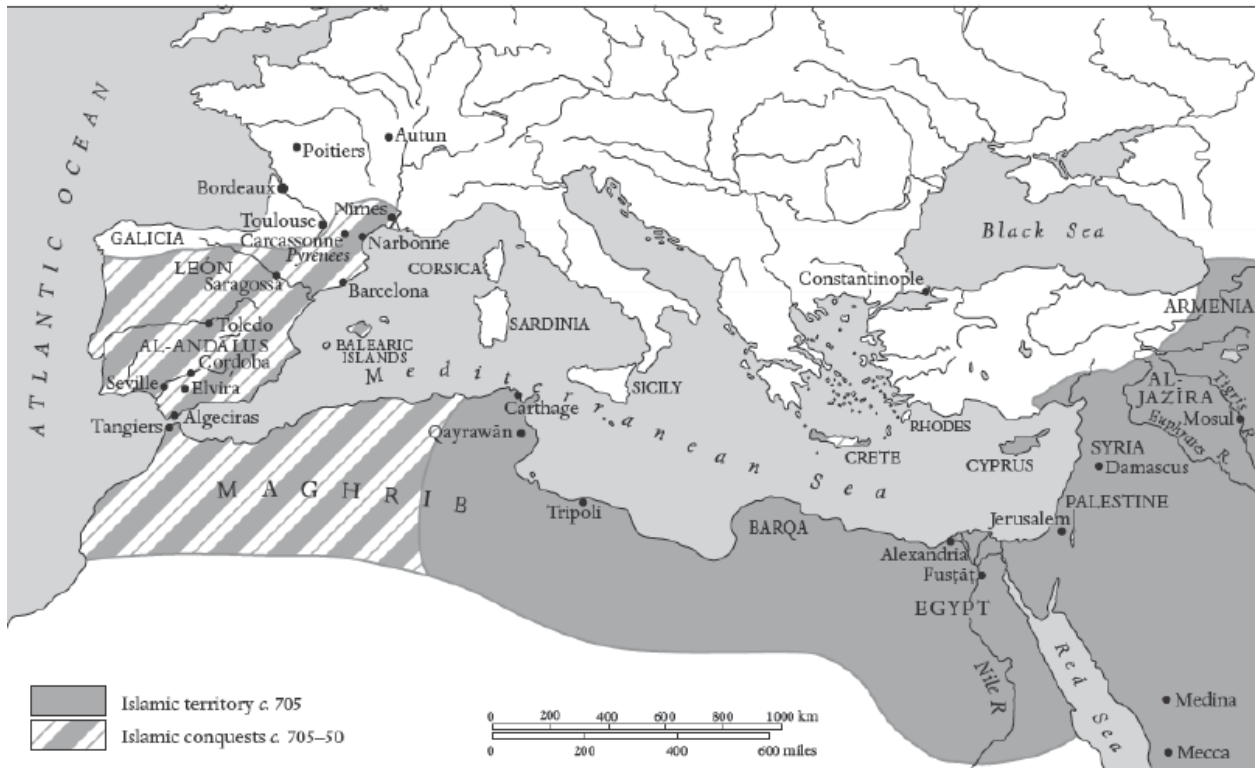


FIGURE 1. THE EXPANSION OF ISLAM IN THE WEST DURING FIRST DECADES OF VIII CENTURY (ROBINSON C. 2011. THE NEW CAMBRIDGE HISTORY OF ISLAM)

For about a generation after the conquest, al-Andalus was treated as a dependency of Umayyad North Africa. It was ruled by a military governor appointed from Kairouan, but under the ultimate authority of the caliph in Damascus. However, in the 730s this long, tenuous chain of command was weakened first by a Berber revolt in the Maghrib, then by a bitter feud between peninsula-based and Syrian Arabs in al-Andalus itself. Links were further strained in the late 740s when the Umayyad caliphs were overthrown and replaced by the Abbasids, a Persian dynasty (Figure 2).

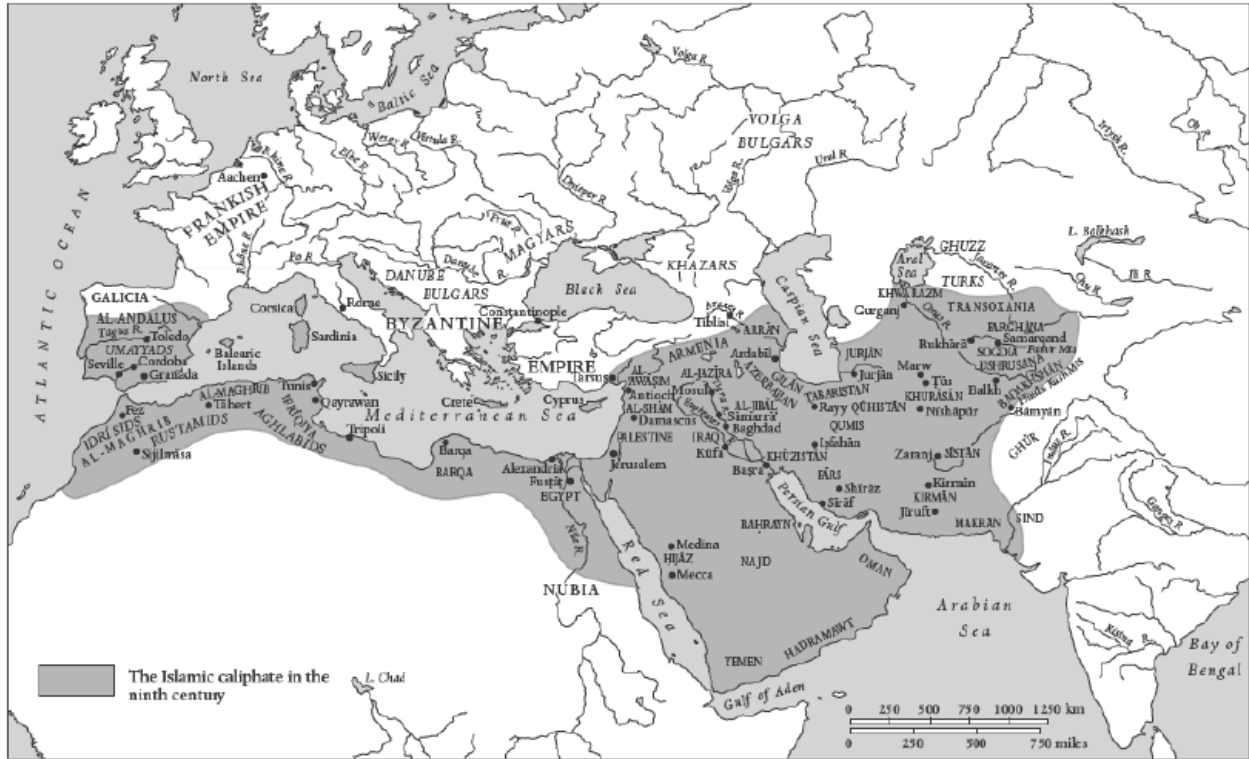


FIGURE 2. THE ABBASID EMPIRE IN C. 800 AD (ROBINSON C. 2011. THE NEW CAMBRIDGE HISTORY OF ISLAM)

The Abbasids founded a new capital at Baghdad, more distant than ever from al-Andalus. The ousted Umayyad family was systematically hunted down and slaughtered. However, one young prince escaped and took refuge in al-Andalus. In Cordoba in 756 he proclaimed himself emir of an independent Umayyad state, and his authority was soon accepted throughout al-Andalus. He became known to history as Abd al-Rahman I (756–88). From the time of Abd al-Rahman I until the late tenth century the emirs at Cordoba were, with few exceptions, able and successful rulers. Internally they had to balance many competing interests – tribal, ethnic and religious – while simultaneously defending the realm against external enemies. The outstanding Umayyad rulers of al-Andalus during this period were Abd al-Rahman III (912–61) and al-Hakem II (961–976).

After the death of al-Hakem II in 976 the fortunes of the caliphs of Cordoba rapidly declined. Al-Hakem was succeeded by his twelve-year-old son, who became a puppet in the hands of his formidable chief minister, al-Mansur. From 980 till his death in 1002 al-Mansur, a ruthless

autocrat but also a military commander of great ability, completely dominated affairs in al-Andalus. He won a series of crushing victories against the Christian north, unprecedented since the conquest, and succeeded in subjugating most of the Maghrib. However, to maintain his dictatorship he effectively dismantled the Umayyad state bureaucracy and replaced it with his own followers. He also relied heavily on Berber fighters imported from Morocco. These North Africans later became involved in a series of bloody revolts and attacks on the local Andalusian population, especially in key cities, giving rise to widespread Berberophobia. In short, by emasculating the caliph's authority al-Mansur contributed decisively to the subsequent disintegration of al-Andalus in the early eleventh century.

The death of al-Mansur and the collapse of caliphal power brought political chaos to al-Andalus on a scale not previously experienced. A period known as the *fitna* or anarchy ensued – and its violent internal struggles fractured al-Andalus, at one stage, into as many as sixty petty kingdoms or taifas. Most taifas were short-lived, though a few became semi-permanent. Gharb al-Andalus was eventually split into the two large taifas of Badajoz and Seville plus the four smaller ones of Faro, Mértola, Silves and Huelva. Of these, by the mid-eleventh century only Badajoz and Seville survived, having absorbed all their lesser neighbors between them. Most of southern and central Portugal was in the taifa of Badajoz, which was ruled by the Banu-al-Aftas, a wealthy Berber family with extensive lands in the Lisbon and Santarém regions as well as round Badajoz itself.

After the death of al-Mansur the northern Christians quickly regained their self-confidence and – ominously for the taifas – started their attacks on Muslim territory. Ill-equipped to resist, the taifa princes began buying off Christian leaders with a form of tribute or protection money called *párias*. Soon in this way vast sums of gold were being paid to the kings of Leon-Castile and other powerful Christian figures, and the arrangement became institutionalized to such extent that the eleventh century in Iberia has been called the age of *párias*. The system eventually broke down after Toledo fell to the Castilians in 1085, prompting the remaining taifa rulers to appeal for intervention to the Almoravids, a militant Islamic dynasty that had recently seized power in Morocco. In 1086, the Almoravids crossed the Straits of Gibraltar in force and quickly defeated the king of Leon-Castile near Badajoz. But Yusuf ibn Tashufin, the leader of these tough tribesmen

from the Western Sahara, then decided to depose the ineffectual taifa princes and incorporate their realms into his own emirate. This was done, and for a time the Almoravids appeared to re-animate peninsular Islam. However, the revival proved relatively short lived. By the 1120s, the Almoravids were losing their power base in Morocco, and within a few years were obliged to abandon al-Andalus.

The reason was that new Berber Muslim movement was founded in the 12th century on Moroccan soil, the so-called Almohad Caliphate (Fierro 2011). The Almohad movement was started by Ibn Tumart among the Masmuda tribes of southern Morocco. The Almohads first established a Berber state in Tinmel in the Atlas Mountains in roughly 1120. They succeeded in overthrowing the ruling Almoravids in governing Morocco by 1147, when Abd al-Mumin al-Gumi (r. 1130–1163) conquered Marrakech and declared himself Caliph. They then extended their power over all of the Maghreb by 1159. Al-Andalus followed the fate of North Africa and all Islamic Iberia was under Almohad rule by 1172 (Figure 3).

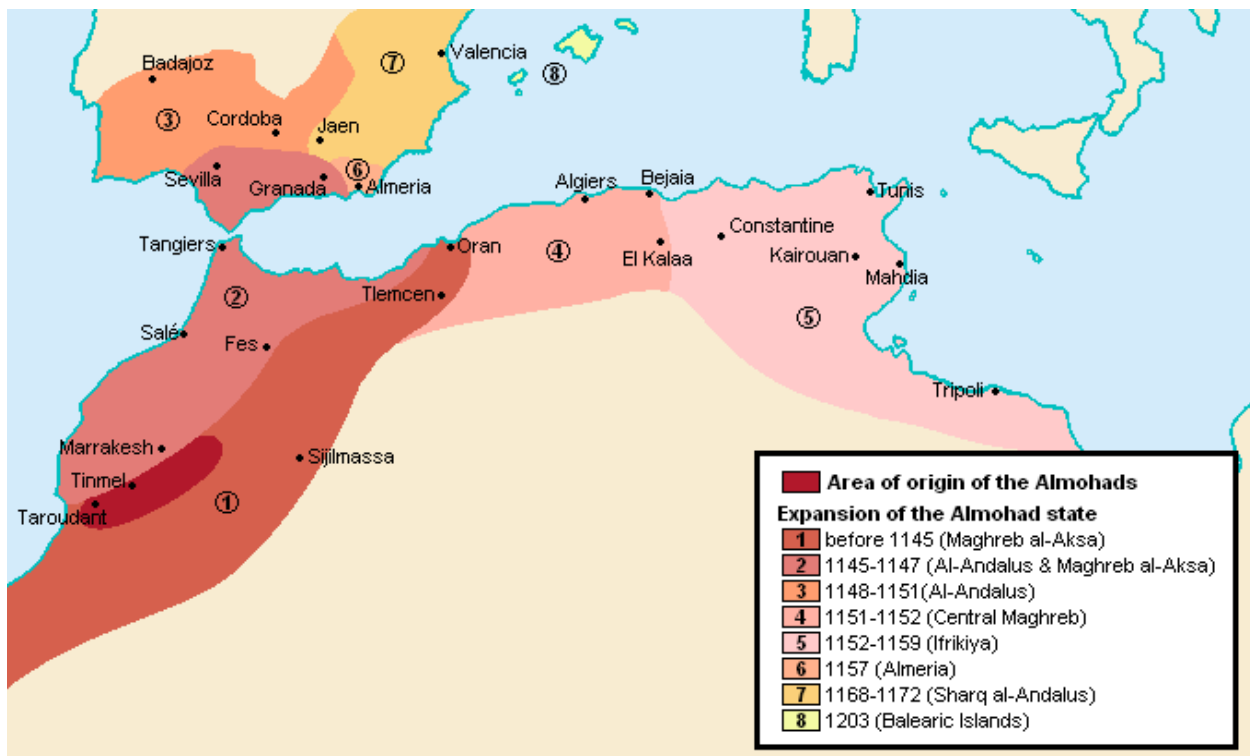


FIGURE 3. AREA OF ORIGIN OF THE ALMOHADS AND EXPANSION OF THE ALMOHAD STATE (PHOTO TAKEN FROM WIKIPEDIA, [HTTP://BIT.LY/2C2N4HV](http://bit.ly/2c2n4hv))

The Almohad dominance of Iberia continued until 1212, when Muhammad III, "al-Nasir" (1199–1214) was defeated at the Battle of Las Navas de Tolosa in the Sierra Morena by an alliance of the Christian princes of Castile, Aragon, Navarre and Portugal. Nearly all of the Moorish dominions in Iberia were lost soon after, with the great Moorish cities of Cordova and Seville falling to the Christians in 1236 and 1248 respectively (Fierro 2011, Torres 1992).

1.3. Archaeological context and sample description

Unlike the Roman Period, where molded ceramics production was widespread, the middle Ages were characterized by a general abandonment of the technique in most of the former Empire's territories. The Iberian Peninsula is no exception; we only know a few examples from early medieval times, especially from the VII c. We can consider the '*terra sigillata hispanica tardia*' (late Hispanic terra sigillata) as the last series of molded ceramics in the Peninsula. However, there seems to be an intensification of the use of molds in the Iberian Peninsula from the XII c., both in Muslim and Christian territories (Gomes 2000). Where the former is concerned, we can distinguish three groups of Almohad molded ceramics; pieces with a red slip, glazed pieces with a metallic reflection and lamps with flat printed discs.

The first group, of molded ceramics with a red slip in Mértola, corresponds to what Retuerce refers to as 'scarlet ceramics' (Gomez 2000). Thirty-eight fragments, corresponding to five different pieces, have been found in Mértola (for the purposes of this study, three samples, fig. 4, from this pottery assemblage will be analyzed because the other two are part of the permanent museum exhibition in Mértola). For the time being, between twelve and fifteen molded ceramic samples are recovered from various archaeological sites across the Iberian Peninsula (Calatrava, Malaga, Zaragoza).



FIGURE 4. SAMPLES CR/MD/003; CR/MD/004 AND CR/MD/005, RESPECTIVELY (GOMEZ 2004)

The clays are reddish, going from orange to reddish brown, with a scaly texture. In a single case the wall of the piece is gray, almost black, giving evidence of a baking that alternated oxidation and reduction processes (Gomez 2000) (inventory no. CR/MD/0005). Referring to the manufacturing process, the pieces were initially shaped and then printed with the mold. Where the neck is preserved, the lines of the lathe are perfectly visible, although it is possible that the neck was shaped independently and attached to the body later on. Bivalve molds must have been used due to the curvature of the pieces, which would impede the removal of the mold without breaking it. The presence, in most pieces, of a smooth band in the widest point, with a coarse surface, leads us to think that there was a mold for the upper part of the piece and another one for the lower part. In some cases, the lower body mold had a small hole in the base, where the potter would press the piece to unmold it. This justifies the presence of an irregular depression on the base of the pieces (see CR/MD/0003). Another indication of the use of bivalve molds is a defect found on one of the pieces (CR/MD/0004) which seems to have been stretched while removing the mold, breaking the decorative pattern. The molding was done, generally, with little care leaving the motives blurred. This defect could be caused by not cleaning the molds or an uneven pressure of the clay on the mold. The interior of the pieces has imprints of the fingerprints of the potters. These are very faint

since the interior of the pieces was smoothed to hide such marks. The walls of these pieces are very thin, with an average thickness of 2mm and rarely thicker than 3mm. In consequence, the pieces are extremely fragile and fragmented. Most of the pieces have a reddish slip, generally in bad state, except for one piece where no slip is seen (CR/MD/004). On this piece was found a horizontal line of white paint on top of a narrow trim. All the pieces correspond to small jars with globular bodies. In the three pieces where the bottom is preserved, it is slightly concave. Only for piece CR/MD/0001 the start of the neck is preserved, which appears to be cylindrical or reverse tapered. No complete handles have been identified, but in two cases the beginning of the handle can be seen still attached to the body. This element is added after the molding and is not considered in the decorative composition since it interrupts the decorative motif abruptly. The functionality of the pieces is doubtful due to their fragility. In any case, they would be used as tableware or as liquid containers (Gomez 2000).

Regarding glazed specimens, a total number of minimum three ceramic vessels (while the maximum number is five) were recovered in Mértola complex during numerous archaeological excavations (CR/DR/0001, CR/DR/0002 and CR/DR/0023; figure 5). Recovered vessels relate to a type of jars with molded edges, inverted fructoconical neck, globular body and vertical handles with oval cross-section. The clays of these pieces are diversified although being quite refined (For the purposes of this study, only vessels CR/DR/0002 and CR/DR/0023 will be examined, because the other one is the part of museum exhibition). In terms of their color and texture, the vessels are not constant: they vary from white and very compact clays, (piece number of inventory CR/DR/0003), to red clays (pieces with inventory number CR/DR/0001, CR/DR/0002, CD/DR/0023) and ochers (piece with inventory number CR/DR/0004) with porous textures and less compact. In relation to the process of manufacture, pieces were made with application of hybrid technique in which only the body is molded while the other pottery parts were made with a fast wheel. As in the “scarlet” ceramics, is probable that the jar’s body were initially wheeled to be after printed the decoration through mold. The clay would be pressed against the mold with some kind of blunt instrument.

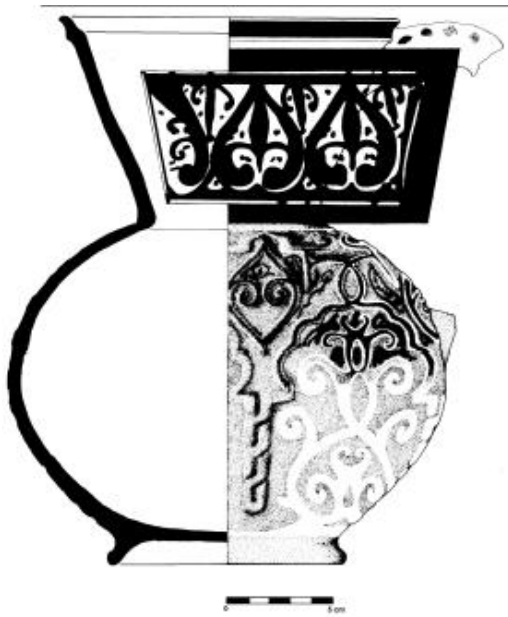


FIGURE 5. SAMPLES CR/DR/0002 AND CR/DR/0023 RESPECTIVELY (GOMEZ 2004)

1.4. A brief introduction to pottery

Archaeological ceramics are clay-rich inorganic artefacts that were produced, used and discarded by past societies. They include pottery, figurines, bricks, tiles, kilns, crucibles, molds, clay writing tablets and a range of other functional objects (Quinn 2013). Pottery itself is a valuable set of data of the ancient world, certainly one of the richest provider of data and information in archaeological studies. Pottery is fundamental in archaeology due to its typological variety, abundance, spread and virtual indestructibility. For these reasons pottery is one of the most important material source of information about previous societies and it represent a dating instrument that cannot be easily superseded (Barilaro et al. 2008). In this context, one of the most significant changes that occurred within archaeology has been the recognition of the active role that material culture plays in the construction and reproduction of social relations and cultural values among human communities. A king's crown is not just a royal emblem; its production and use is the direct result of royal power and authority and it also provides a major focus for the social recognition and reproduction of that power. Within this approach, several anthropologists and sociologists have emphasized how technologies can be analyzed as cultural choices which depend as much on the social, economic and ideological setting as any functional criteria (Sillar 2000: 2). The role of the chemical and physical sciences in technological studies is extremely significant in the case of those technologies (such as pottery, metal and glass) involving significant chemical and structural alteration of the raw materials in the process of artefact manufacture (Tite 1991: 145). Among the archaeological artefacts, pottery and more generally, shards are one of the most studied artefacts and as consequence ceramics have been put in major focus of archaeological science studies from their beginnings in the mid XX century. The practice of archaeology itself has been utterly transformed over the last twenty years by an infusion of new (or greatly improved) scientific methods. These have made it possible to ask many new questions, and have produced a marked revival of interest in archaeological questions that had previously lapsed for lack of firm evidence. Because of their archaeological significance, many different analytical techniques were used to determine the age, the elemental and mineralogical composition of ancient ceramics in

order to identify their origin (local vs. non-local manufacture), the raw materials and the firing process used for their manufacturing.

1.5. Introduction to ceramic archaeometry and paste analysis

Paste analysis is vital in the study of archaeological ceramics and we can roughly distinguish it between archaeological (observations regarding modeling techniques typology, style and surface treatments) and archaeometrical analysis (production technology, technological choices, distribution patterns, provenance). Although in practice both types of approaches are usually combined, for the purpose of this work, this study will be centered mainly on the archaeometric study.

Archaeological studies of pastes and fabrics are fundamental to the classification and characterization of pottery, providing relevant data, among other aspects, about its production, function and social meaning. Archaeometry encompasses a group of analytical techniques applied in the study of material culture with the aim to obtain a quantitatively and qualitatively rich and diverse corpus of data. The data collected with these techniques provide relevant information concerning the ceramic technology of past societies that eventually permits us to approach the way these societies conceptualized, produced, used, maintained, exchanged and stored their pottery. Furthermore, archaeometry is based on the necessary interdisciplinary relationship between diverse branches of the natural and social sciences. This relationship is essential in the material study of the past, since, from artefacts, researchers have to face questions that go beyond the limits of the tangible and pertain instead to abstract and social concerns. In short, with the application of techniques and methods from the natural sciences such as physics, chemistry and earth sciences it aims at dealing with the enquiries associated with human and social sciences (Albero 2014).

Therefore, studies focused on archaeological ceramics have been substantially enriched by the implementation of chemical and mineralogical analyses. This improvement has enabled us to transcend the analytical scales and the information that used to be obtained by traditional macroscopic methods or the typological classification of the vessels. Thus, the use of archaeometric analytical techniques has allowed us to increase the data available concerning the

material culture of past societies (Albero 2014, Jones 2002). The advantages of ceramic archaeometry for addressing many archaeological enquiries resulted, especially since the 1980s, in the consolidation and continued improvement of research methodologies based on physicochemical analysis. At the same time, we have witnessed the emergence of new analytical techniques, which allow a more accurate approach to the manufacturing techniques and the composition of the artefacts.

However, the use of archaeometric analyses does not necessarily involve deeper interpretations of material culture or further knowledge regarding past societies. In this way, a solid theoretical framework (of which archaeometry is a methodological tool) is an absolutely indispensable starting point to properly approach past societies. In consequence, the archaeometric characterization of pottery technology must start from a number of basic assumptions related to specific archaeological and historical concerns. Therefore, the research should start by setting the theoretical framework that is going to determine the methodology and, particularly in ceramic archaeometry, the combination of several analytical techniques used to collect data (Jones 2002, Jones 2004).

However, it cannot be forgotten that any explanation of the past should base on the thorough study of the archaeological artefacts, their manufacturing processes and the analysis of the contexts of their production and use. This stage of the research is absolutely necessary, since the archaeological background is, in its essence, material. It is at this level of analysis where archaeometry can play a decisive role. In practice, archaeometry is an analytical option that potentially allows obtaining large amounts of information from each sample tested. The sheer volume of information provided makes it possible to deal not only with a diversity of phenomena but also with the complexity embedded in material culture.

1.6. Archaeometric techniques and pottery studies – review

Macroscopic approaches of the ceramic record are essential in any archaeological research and indispensable in the study of many aspects of pottery such as modelling techniques, typology, surface treatments, firing process, decorative patterns and style. However, the application of microscopic and compositional analyses is also necessary to approach in depth the technology and provenance of ceramic pastes and fabrics. These analyses allow further classifications of the vessels that can be meaningfully related to different technological dynamics and distribution patterns.

A number of archaeometric studies have clearly demonstrated the applicability of multianalytical diagnostic techniques in the investigation of pottery. From an analytical viewpoint, the archaeometric characterization of the petrographic, mineralogical, textural and chemical composition of the paste makes available a basis for the creation of ceramic fabrics and compositional groups associated with specific technological features. To achieve this goal, it is required to study the matrix, inclusions and tempers that compose the ceramic body in order to determine a pottery fabric. In this sense, the systematic use of several analytical methods and techniques that provide complementary information allows us to approach the study of the ceramic as a whole. Thus, the study of the pottery can be initiated, for example, by means of the macroscopic observations (as modelling techniques, typology, surface treatments, firing process, decorative patterns and style) of the record in order to subsequently undertake mineralogical, petrographic, textural and chemical analysis (Albero 2014).

In the following sections textural, petrographic, mineralogical and chemical analyses in ceramic studies will be approached. Such analyses are widely used in the characterization of the ceramic at different stages. Thus, the usefulness of each one of these analyses in the study of raw material origin, paste preparation, modelling techniques, surface treatments, firing process or post-depositional alterations is going to be highlighted.

1.6.1. Textural analysis

The minerals and rock fragments occurring in pastes are provided by various transport processes and deposited in different sedimentary environments and they therefore experienced dissimilar erosion cycles. The depositional environment and the erosion by water flows as well as other erosive agents determine changes in the morphology and grain size distribution of the sediment used to produce the pottery. In this way, each sedimentary deposit has characteristic grain morphology and size that distinguishes it from others. The raw materials used in pottery production are composed by clay matrix, inclusions and tempers. The clay matrix is a more or less continuous phase in which other components such as mineral or organic inclusions and tempers are retained. Inclusions are non-plastic particles naturally occurring in clays, while tempers are non-plastic materials intentionally added to the paste by potters. Despite this distinction, the two last components are both part of the coarse fraction of the paste. In this way, texture analysis mainly refers to the percentage of fine and coarse fractions occurring in the paste and especially to the characterization of its inclusions and tempers by means of variables such as frequency, grain size, particle shape, sorting and roundness.

The particle grain size distribution of the non-plastic components and their sorting degree are key variables in textural analysis of archaeological ceramics. The estimation of “unimodal” or “bimodal” grain size distributions within the coarse fraction can be crucial to identify the presence of tempers in the paste.

Summing up, the determination of textural parameters has become one of the bases in the characterization of clay raw materials and archaeological ceramics. Thus, it is usual to perform granulometric and morphologic studies in order to identify several human actions involved in raw materials procurement and paste preparation.

1.6.2. Mineralogical analysis

The mineralogical composition of ceramics and clays is usually studied by X-ray powder diffraction (XRD). This method involves an X-ray beam of a fixed wavelength which come in contact with a polymineralic sample, usually previously grinded to powder, on which the intensity of the diffracted X-rays is measured in different angular conditions between the x-ray source, the sample and the detector. Interpretation of X-ray diffraction patterns provides the broad mineralogical composition of the ceramics. Therefore, this method makes available information related to some features and properties of the pottery as well as other technological aspects such as their provenance or firing temperature. That is the reason why the use of this technique for archaeological purposes is quite widespread in ceramic studies and is applied since the last century, both in the mineralogical analysis of archaeological artefacts and for clay raw materials. As already mentioned, mineralogical analysis by XRD permits us to identify the main crystalline phases occurring in ceramics and clays. Moreover, the detection of certain mineral phases, such as the clay minerals, is only available by this method, especially if oriented aggregate mounts are performed. Qualitative estimations achieved through the identification and intensity quantification of primary and secondary diffraction peaks present in the diffractograms allow the classifying of samples into groups according to their mineralogical features (Tite 2008).

Many other analytical techniques give complementary information and are usually employed in the study of archaeological objects. Specifically, spectroscopic techniques are very valuable assets to achieve a detailed data of archaeological artefacts of the past. For bulk characterization of archaeological shards, Fourier Transform Infrared (FT-IR) absorbance spectroscopy is usually preferred to other analytical techniques, such as X-Ray Diffraction (XRD) as an example, for its non-invasiveness (certainly, a sampling of the object is needed around 2mg of analyzed material) if the materials are amorphous. What are the principles of FT-IR? Basically, it involves the absorption of electromagnetic radiation in the infrared region of the spectrum which results in changes in the vibrational energy of molecule. Since, usually all molecules will be having vibrations in the form of stretching and bending., the absorbed energy will be utilized in changing the energy levels associated with them (Rajarathnam 2010). Then, by collecting the infrared spectra at multiple frequencies and applying Fourier transform mathematical operation, unique

spectrum for a specific archaeological artefact can be created. Therefore, FT-IR spectroscopy is a common and well-established tool for the ceramic body identification (Barilaro 2008) used for uncovering data regarding raw material used and temperature of firing and firing condition of the particular vessel (Kiruba 2015). It is very crucial to note that FT-IR allows us to investigate changes in both crystalline and amorphous fired clays as a function of the firing temperature (Zerai 2015). Thus, FT-IR offers a versatile analytical tool, which is fast and easy to use, and in which sample preparation is minimal or unnecessary, for characterizing micro and macro-samples (Pollard et al. 2011).

Another spectroscopic technique which is very useful in pottery studies is Raman spectroscopy. Raman spectroscopy is a scattering technique and it owes its name to the Indian scientist C.V. Raman (1888-1970) who in 1928. discovered something he simply called “new radiation” after years of experiments on the scattering of light. As noted, Raman spectroscopy depends on scattering of radiation and as radiation passes through the sample certain part is scattered by the molecules present in the sample as a result of a weak interaction between the radiation and the molecule. Due to initial scattering photons are occasionally scattered with more or less energy which as a result creates spectral lines which are unique for each molecule (Pollard et al. 2011). These characteristics make it an exceptional method for unambiguously identifying materials in any physical form: gases, liquids, solutions, and crystalline or amorphous solids. Raman spectroscopy has thus become an established technique for the study of cultural heritage materials over the past 20 years.

1.6.3. Petrographic analysis

The use of petrographic analysis in archaeology was first documented in the second half of the nineteenth century and has since become a widely used technique, especially in ceramic analysis. This optical microscopy method permits us to identify the minerals, rock fragments and other materials (e.g., organic matter or microfossils) which are present in the coarse fraction of the sample. In addition, the texture, porosity, orientation, frequency and morphology of each of these components in the paste are usually recorded. This technique also focuses on certain aspects of the fabric microstructure, thus referring to the characteristics of the clay matrix too. Therefore, the petrographic study of ceramics provides information on two parameters: the phase composition of the inclusions or tempers and the structure of the ceramic fabric. The complementarity of both parameters allows the determination of specific *petrofabric*s, taxonomic categories that distinguish between ceramic groups depending on their particular composition, technology and origin (Quinn 2013; Tite 2008).

Petrological analysis is performed by means of a petrographic microscope using polarized transmitted light which incorporates also a polarizer filter, a removable polarizer filter called the analyzer and a rotating stage. These filters allow seeing the thin section in plane polarized light (PPL) and cross polarized light (XPL), where the waves, in contrast to ordinary light, vibrate in only one plane.

Petrographic study will not be conducted in this research due to few very important scientific reasons: extremely rare type of Islamic pottery in the Iberian Peninsula, therefore we need to preserve as much as we can for future studies, and very fine fabric was shown under the stereomicroscope.

1.6.4. Chemical analysis

Chemical analyses are used for various purposes in archaeology and there are many techniques to approach the chemical composition of the artefacts. The most widespread methods in ceramic studies are Instrumental Neutron Activation Analysis (INAA), X-Ray Fluorescence (XRF) and, more recently, Inductively Coupled Plasma Mass Spectrometry (ICP-MS). However, other techniques such as X-ray Emission Induced by Protons (PIXE) or even Scanning Electron Microscopes combined with Energy Dispersive X-ray Spectroscopy (SEM-EDX/EDS) have also been used.

In ceramic studies, chemical analyses are particularly useful in the study of the provenance of raw materials, manufacturing technology and the identification of post-depositional alterations. Thus, analyses centered on establishing the chemical composition of materials supplement other studies that address the petrological, mineralogical and textural composition of pottery vessels. With all these chemical methods, differences in the composition of the samples that allow grouping the ceramics can be characterized with more or less accuracy. These groups relate to the different geochemical origin of the vessels, even in areas that are quite uniform in mineralogical terms. Often, in these cases, petrographic and mineralogical approaches may be useless to group the samples and determine their provenance. Therefore, the application of chemical analysis is expected to be particularly useful to distinguish pottery assemblages coming from geological environments that are quite similar.

We must be aware of the accuracy and limitations of the techniques used to establish chemical reference groups. We have to consider the sensitivity of the instruments as well as the degree of reproducibility, compatibility and correspondence of the results with other analyses developed following other procedures and techniques or performed by other laboratories. In this sense, methods such as INAA, XRF or ICP-MS usually have a high sensitivity and enable us to record over 20 elements. In addition, most of these elements can be quantified in parts per million (ppm) or even in parts per billion (ppb). These techniques provide very precise and reliable data regarding the concentrations of major, minor and trace elements, including rare earth elements. Thus, when properly used, these techniques characterize with significant accuracy the ceramics

and establish solid reference groups. In contrast, other techniques such as SEM-EDX only record a few elements, since their detection limits are up to 0.3% of the total sample weight.

1.7. Working principles of applied analytical techniques

1.7.1. Scanning Electron Microscopy (SEM)

The scanning electron microscope has many similarities to the optical microscope with the main difference being that a beam of electrons, instead of visible light, is used to illuminate the object. Hence, the finer detail being studied, the shorter the wavelength of the illuminating source must be to reveal it. The wavelengths associated with electrons are much shorter than the wavelengths for visible light and so if a beam of electrons, rather than a beam of visible light, is used to illuminate the sample a much higher resolution can be achieved (Figure 6). Thus the SEM is a powerful tool for the study of the surface detail and microstructure of a wide variety of materials (Parkes 2015: 185).

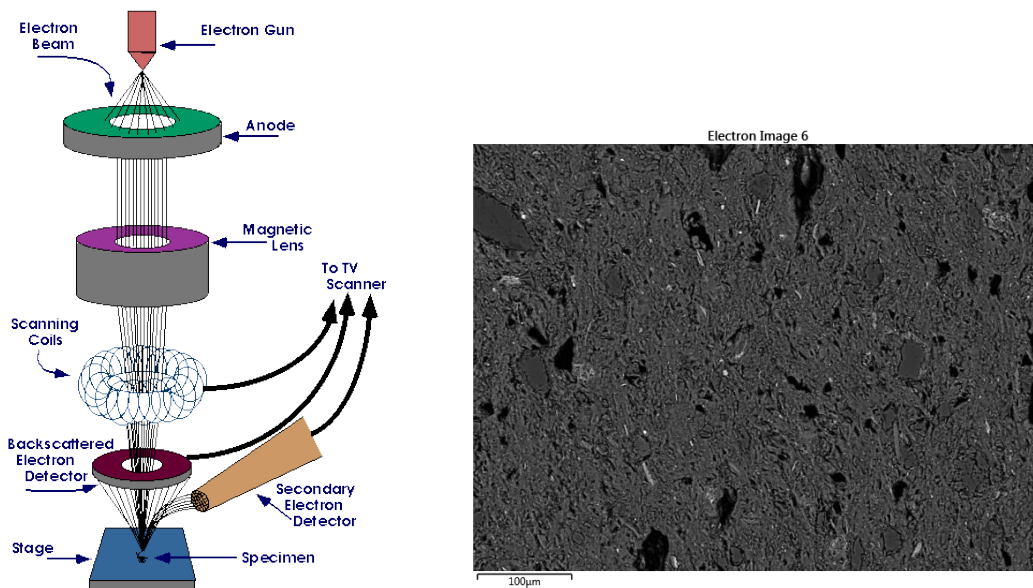


FIGURE 6. SCHEMATIC REPRESENTATION OF SEM (IMAGE TAKEN FROM [HTTP://GOO.GL/ZZXHY6](http://goo.gl/zzXHy6)) AND BSE IMAGE OF CERAMIC SAMPLE CR/MD/004, RESPECTIVELY

When the beam of electrons used to illuminate, the object being studied reaches the surface of that object several things can happen. Firstly, some of the primary electrons are deflected from the surface by the sample atoms and such electrons are known as backscattered electrons. The probability of an electron being backscattered depends on the atomic weight of the atoms it hits, with heavy atoms being more likely to deflect electrons back than light atoms. These backscattered electrons can be detected and by observing how the numbers of backscattered electrons vary over the surface being studied, it is possible to build up a picture of how the elements are distributed in that surface.

As a result of the collisions of the primary electrons the sample atoms lose electrons. Some of these secondary electrons, which have lower energies than the primary electrons, then escape from the surface of the object. The number of secondary electrons detected from any given point depends on the angle between the primary electron beam and the part of the surface hit by the beam, so by comparing the number of electrons detected from different parts of the surface it is possible to build up a detailed 3-D like picture of the microstructure of the surface.

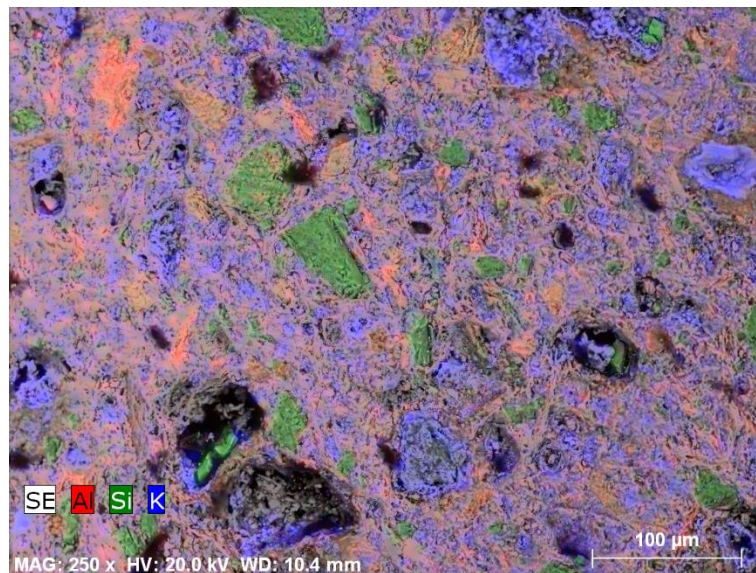


FIGURE 7. SEM-EDS USED FOR ELEMENTAL MAPPING OF THE SAMPLE CR/DR/0002 SURFACE

For the spectroscopy of X-rays in the SEM, two fundamentally different techniques are available, namely the so-called wavelength dispersive and the energy dispersive systems. Wavelength dispersive systems have excellent wavelength – and hence energy – resolution, which

often facilitates a quantitative evaluation for elements with close lying X-ray peaks. But it requires very polished surfaces therefore wavelength dispersive analyzers are therefore rarely used in SEM systems in the study of rough surfaces common in cultural heritage materials. They are, however, a standard analytic device in electron microprobes, in which the focused electron beam is mainly used for quantitative point element analysis of polished sections of minerals and other materials. On the other hand, Scanning Electron Microscope combined with Energy Dispersive System simultaneously measure the whole X-ray spectrum and hence provide a quick determination of the element composition of the target (Froh 2004). Compared to wavelength dispersive, the energy resolution is inferior, but tilted and rough surfaces and the movement of the emitting spot over the target surface do not so strongly adversely affect the X-ray analysis detection. (Froh 2004, Parkes 2015). The signal of the characteristic X-rays of specific elements may also be used for producing elemental maps (Figure 7).

SEM studies have been carried out on a wide variety of materials for a range of purposes: pottery and ceramic being one of the most studied material (Parkes 2015, Tite 2008). Tite mentions mainly three types of information that can be obtained from SEM: information on the raw materials used, information on firing procedures, and information on surface decoration, i.e., the application and nature of slips and glazes.

Another type of electron microscope is VP-SEM in which interactions of electrons in the gas and the subsequent formation of positive ion by-products are particularly useful in allowing insulating specimens to be imaged without the need for a conductive coating. However, there are many interdependent parameters involved and we must always consider how a change in even one parameter will affect resultant images or spectra (Stokes 2008). VP-SEM differs from traditional SEM in that the instrument chamber is operated at higher pressures (~10 Pa to 3,000 Pa) which allows for imaging and analysis of samples without the need to apply a conductive coating. This is convenient for when it is undesirable to coat a sample or the sample is too large for the coating systems. With VPSEM, we can examine a sample's topography, structure, and its elemental composition under magnifications of ~10X to ~20,000X. Multiple electron and x-ray detectors can be employed to expose even more information about the characteristic of a sample. VP-SEM produces a finely-focused electron beam and scan it across the sample. When the electron beam

hits the sample, it generates secondary electrons and backscattered electrons. Various detectors collect these signals and they are displayed on a computer monitor as well as captured in high resolution digital images.

1.7.2. X – Ray Fluorescence

X-ray fluorescence is now a well-established method of analysis both in the laboratory and industry. The fact that the method is essentially non-destructive makes it particularly attractive for the analysis of archaeological and museum artifacts (Hall 1960, Shackley 2011).

XRF spectrometry is based on the principle that primary X-rays (from an X-ray tube or radioactive source) are incident upon a sample and create inner shell (K, L, and M lines) vacancies in the atoms of the sample. These vacancies de-excite by the production of a secondary (fluorescent) X-ray whose energy that it is characteristic of the elements present in the sample. Some of these characteristic X-rays escape from the sample and are counted and their energies and intensities measured (Figure 8). Comparison of these energies with known values for each element allow the elements present in the sample to be identified and quantified in ceramics of known and unknown provenance (Pollard 2008, Pollard 2011, Shackley 2011).



FIGURE 8. EXAMPLE OF PORTABLE XRF WITH VACUUM PUMP, TRIPOD AND COMPUTER FOR DATA ANALYSIS (IMAGE TAKEN FROM [HTTP://GOO.GL/KKZRVX](http://goo.gl/kkzrvx))

When primary X-rays strike the sample two processes take place – scattering and absorption – of which absorption is usually the dominant process. Scattering may be elastic (coherent or Rayleigh scattering), in which case the scattered ray has the same wavelength (energy) as the primary beam, or inelastic (incoherent or Compton scattering), which results in longer wavelength (lower energy) X-rays. Coherent scattering results in the primary spectrum of the X-ray tube being “reflected” into the detector, which is why the lines characteristic of the X-ray tube target material appear in the resulting spectrum. Incoherent scattering sometimes gives rise to a broadened inelastic peak on the lower energy side of the coherently scattered characteristic tube lines, as well as contributing to the general background (Pollard 2008, Pollard 2011, Shackley 2011). There are two forms of X-ray spectrometers, which differ in the way in which they characterize the secondary radiation – wavelength dispersive (WD), which measures the wavelength, and energy dispersive (ED), which measures the energy of the fluorescent X-ray.

1.7.3. X – Ray Diffraction

X-ray diffraction uses X-rays of known wavelengths to determine the lattice spacing in crystalline structures and therefore directly identify crystalline chemical compounds. This is in contrast to the other X-ray method discussed earlier (XRF) which determine concentrations of constituent elements in artifacts (Figure 9).

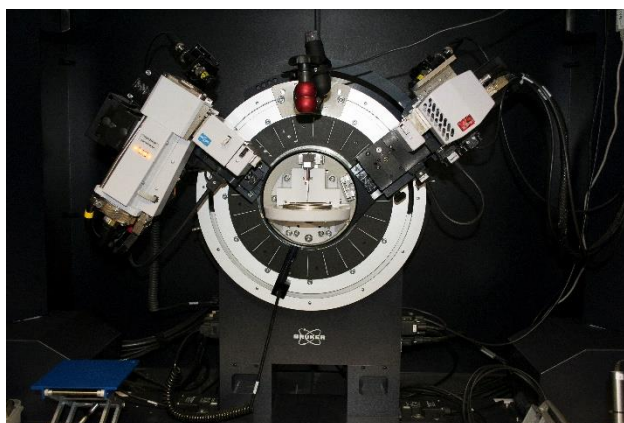


FIGURE 9. SCHEMATIC REPRESENTATION OF X-RAY DIFFRACTION APPARATUS

Powder XRD, is the most widely applied method for identification of inorganic materials, and, in some cases, can also provide information about mechanical and thermal treatments during artifact manufacture (Pollard 2011). In recent years, there has been a long debate about how to determine the maximum firing temperature of archaeological pottery (Tite 2008). It is agreed in the literature that the simplistic ‘open firing’ versus ‘kiln firing’ discussion leaves out much of the complexities of the firing procedure, although either of these assumptions may be viable or at least practical archaeological approximations (Pollard 2008). In general, the analytical methods applied to determine firing temperatures involve establishing a relationship between the firing temperature and changes in mineralogy and the use of X-ray diffraction for mineralogical characterization of ancient ceramics has been demonstrated in various studies (Albero 2014, Pollard 2011).

In powder X-ray diffraction measurements, the solid sample is irradiated by a collimated beam of monochromatic X-rays of known wavelength. A proportion of these are diffracted at angles which depend on the crystal structure of the specimen. The wavelength of the incident radiation must be of the same magnitude as the distance between the scattering points and a typical choice of X-ray wavelength is 1.54059 Å, the $K\alpha$ radiation of copper. The X-rays penetrate in the crystal and are “reflected” from the successive atomic layers in the crystal lattice creating constructive and destructive interference from successive layers. The path difference (i.e., the difference in distance traveled) between “reflections” at an angle of θ from successive layers of atoms separated by a spacing of d is equal to $2d\sin\theta$ to have constructive interferences. A maximum in the reflected X-ray intensity therefore occurs at this angle if the contributions from successive planes are in phase, the condition for which is given by the Bragg relationship (Figure 10):

$$n\lambda = 2d\sin\theta$$

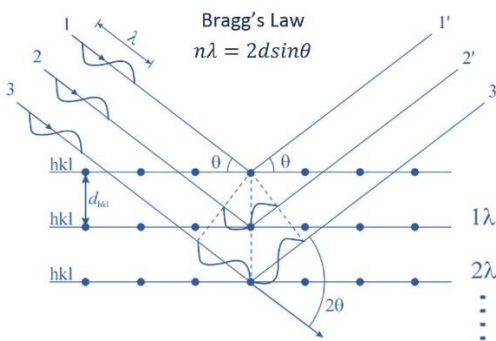


FIGURE 10. SCHEMATIC REPRESENTATION OF BRAGG'S LAW (IMAGE TAKEN FROM [HTTP://GOO.GL/ZjPIWM](http://goo.gl/ZjPIWM))

where n is an integer (the order of the diffraction) and λ is the wavelength of the incident X-rays. Therefore, a crystalline specimen will produce a series of reflected X-ray intensity maxima (a diffraction pattern) at angles determined by the spacing between crystal planes of its constituent minerals. The diffraction pattern is characteristic of the minerals present, and can be used to identify them. The intensity of the diffracted beam is dependent on the quantity of the corresponding crystalline material in the sample and therefore relative amounts of different minerals can also be determined. As for the μ XRD, micro X-ray diffraction analysis is a structural analysis technique which allows for the examination of very small sample areas. Like conventional XRD instrumentation, μ XRD relies on the dual wave/particle nature of X-rays to obtain information about the structure of crystalline materials. Unlike conventional XRF, which has a typical spatial resolution ranging in diameter from several hundred micrometers up to several millimeters, μ XRD uses X-ray optics to focus the excitation beam to a small spot on the sample surface so that small features on the sample can be analyzed.

1.7.4. Inductively Coupled Plasma – Mass Spectrometry (ICP-MS)

Inductively Coupled Plasma Mass Spectrometry is an analytical technique used for chemical elemental analysis. An ICP-MS combines a high temperature ICP (Inductively Coupled Plasma) source with a mass spectrometer. The ICP source converts the atoms of the elements of the sample to ions and then these ions are separated by the mass spectrometer and detected in the final detector. During the past several years, in the field of provenance studies and the analysis of trace elements, this technique had become essential for archaeologist who tend to use this technique primarily because of the advantages it provides in terms of a large analytical dynamic range and largely interference free spectra (Kennett et al. 2004).

The sample is typically introduced into the ICP plasma as an aerosol, either by aspirating a liquid or dissolved solid sample into a nebulizer or using a laser to sample solid samples, converted in small particles. Once the sample is introduced into the ICP torch, it is completely desolvated and the elements are converted first into gaseous atoms and then ionized towards the end of the plasma. Once the elements in the sample are converted into ions, they are then brought

into the mass spectrometer via the interface cones. The interface region in the ICP-MS transmits the ions traveling in the argon sample stream at atmospheric pressure (1-2 torr) into the low pressure region of the mass spectrometer. The sampler and skimmer cones are metal disks with a small hole (~1mm) in the center. The purpose of these cones is to sample the center portion of the ion beam coming from the ICP torch. A shadow stop or similar device blocks the photons coming from the ICP torch, which is also an intense light source. Due to the small diameters of the orifices in the sampler and skimmer cones, ICP-MS has some limitations as to the amount of total dissolved solids in the samples. Generally, it is recommended that samples have no more than 0.2% total dissolved solids (TDS) for best instrument performance and stability. If samples with very high TDS levels are run, the orifices in the cones will eventually become blocked, causing decreased sensitivity and detection capability and requiring the system to be shut down for maintenance. This is why many sample types, including digested soil and rock samples must be diluted before running on the ICP-MS. The ions from the ICP source are then focused by the electrostatic lenses in the system. The ions coming from the system are positively charged, so the electrostatic lens, which also has a positive charge, serves to collimate the ion beam and focus it into the entrance aperture or slit of the mass spectrometer. Once the ions enter the mass spectrometer, they are separated by their mass-to-charge ratio. The most commonly used type of mass spectrometer is the quadrupole mass filter. In this type, 4 rods (approximately 1 cm in diameter and 15-20 cm long) are arranged as in Figure 3. In a quadrupole mass filter, alternating AC and DC voltages are applied to opposite pairs of the rods. These voltages are then rapidly switched. The result is that an electrostatic filter is established that only allows ions of a single mass-to charge ratio (m/e) pass through the rods to the detector at a given instant in time. So, the quadrupole mass filter is really a sequential filter, with the settings being change for each specific m/e at a time. However, the voltages on the rods can be switched at a very rapid rate. The result is that the quadrupole mass filter can separate up to 2400 amu (atomic mass units) per second. This speed is why the quadrupole ICP-MS is often considered to have simultaneous multielemental analysis properties. The ability to filter ions on their mass-to-charge ratio allows ICP-MS to supply isotopic information, since different isotopes of the same element have different masses.

CHAPTER 2: MATERIALS AND METHODS

2.1. Sample selection

The main focus of this study will be aimed on the technological characterization of unglazed molded Islamic pottery from Mértola (Portugal) – samples CR/MD/003, CR/MD/004 and CR//MD/005. This type of pottery was quite widespread during Roman times documented on practically every bigger Roman archaeological site (e.g. terra sigillata) even on the territory of present-day Iberian Peninsula. However, with the fall of the Empire, this type of pottery ceases to occur in the archaeological context almost completely at the end of the 8th century in the Iberian Peninsula. Unexpectedly, this kind of pottery (with the application of mold) starts again to appear sporadically in archaeological context during Almohad rule in 12th century in the area of today's southern Portugal and still remains unknown whether the vessels are the result of import or local production. On the other hand, for the time being, only five unglazed molded samples are found on the entire territory of the Iberian Peninsula and as previously noted only three of them will be subjected to scientific analysis. In order to accomplish the pre-defined research goals (technological characterization of unglazed molded Islamic pottery) it is essential to compare them with another type of Islamic pottery – glazed molded pottery. Molded glazed Islamic ware is far more represented in archaeological context of 12th/13th century Almohad state (archaeological sites in both Portugal and Spain). Correspondingly, in Mértola a number of this of molded glazed pottery was found and for the purposes of this study samples CR/DR/0002 and CR/DR/0023 will be incorporated in this research as a means of comparing them with unglazed samples in order to answer some very important archaeometric questions, such as whether unglazed samples have similar origin as glazed ones (are they from the same workshop, production center) and was the production technology the same.

For the purposes of characterization of molded pottery from the Iberian Peninsula, in total seven samples from Mértola (Portugal) were used in this study, three unglazed and four glazed. Samples were obtained from Campo Arqueológico de Mértola. At the time of conducting this study, these vessels are the only known examples of unglazed molded ware from Portugal. And as for glazed pottery, there are known examples in archaeological sites in both Portugal and Spain, from various Islamic cities from that time period.

2.2. Methodology

In order to establish petrographic, mineralogical and compositional characterization of molded ware from the Iberian Peninsula, an integrated analytical approach based on the use of non-invasive and micro-invasive techniques was performed. It is important to note that whenever it was possible, non-invasive approach was used in this study in order to preserve as much as possible these rare archaeological artefacts for future studies.

This study was done as a joint project between University of Évora in Portugal and Department for Islamic Archaeology in UCL Qatar, therefore various types of equipment were used in this study as well as different methodological approaches.

2.2.1. Scanning Electron Microscopy – Energy Dispersive Spectroscopy (SEM-EDS)

SEM-EDS analysis was performed both in Hercules laboratory and in UCL Qatar. In the laboratories in UCL Qatar, for the purposes of SEM analysis, micro – sampling technique was applied on representative pottery parts (Artioli 2010: 94). The samples were mounted in a resin and left to dry overnight. The next day they were polished with increasingly fine grades of diamond paste from 3 μ m to 1/4 μ m grade. After polishing process, samples were coated with a thin layer of carbon in order to be electrically conductive (Pollard & Heron 2008: 49). The scanning electron

microscope (JEOL JSM 6610LV) with attached EDS detector (Oxford Instruments X-man) was used for body and red slip analysis in the high vacuum conditions and accelerating voltage of 20kV. Secondary electron images were used for surface topography, while backscatter electron images were used for structural information (Pollard & Heron 2008: 46). For all three unglazed samples from Mértola, bulk and spot analysis were done in all segments of the ceramics, with regular calibration of the instrument performance (accuracy and precision) on cobalt piece. The data were prepared using Aztec software.

In Hercules laboratory, samples (glazed samples) were analyzed in variable pressure mode. Variable Pressure Scanning Electron Microscope HITACHI S-3700N operated with an accelerating voltage of 20kV in order to collect X-Ray emissions from heavier elements like Pb. Glazed samples were analyzed under an air pressure of 40 Pa in the chamber and thanks to the extensive size of it, it was possible to put the whole specimen on the sample holder in SEM-EDS apparatus without destroying it. Chemical microanalysis was done in the same conditions, using a Bruker XFlash 5010 *Silicon Drift Detector* (SDD) with a resolution of 126eV at Mn K α . The EDS tasks and the quantification were achieved through the Esprit 1.9 software from Bruker Corporation.

2.2.2. X-Ray Diffraction (XRD)

XRD analysis were performed in Hercules laboratory, University of Evora. For the purposes of this study, both XRD and uXRD analysis was performed. For the regular powder XRD, sample preparation required an approximately 2g of powdered sample prepared using a mortar and pestle. Subsequently they were packed in a cavity mount in order to be put in the sample holder of the diffractometer apparatus. As for the uXRD, analysis was performed straight on the specimens without any prior sample preparation. Samples were simply put on the sample holder of the diffractometer apparatus and the analysis was done using Bruker AXS D8 Advance diffractometer with DAVINCI design, equipped with Cu K α radiation source, a Göbel mirror assembly and LynxEye 1D detector, and operating with DIFFRAC.SUITE software package. It is important to note that in order to switch between regular XRD and uXRD, configuration had to be changed.

The powder XRD analyses were conducted using Brüker AXS D8 Advance with DAVINCI design diffractometer housed at Hercules Lab, equipped with a LynxEye 1D detector. Cu K α radiation was used for the study and operating with a DIFFRAC.SUITE software package. All the diffraction patterns were collected from 3° to 75° 2 θ at a step size of 0.05° 2 θ , with a working voltage and current of 40kV and 40mA, respectively. Identification of peaks involved the use of Bruker Eva Software in the X-Ray diffraction equipment, allowing mineral identification from standard X-ray power diffraction patterns set by the Joint Committee on Chemical analysis by Powder Diffraction. Quantitative analysis was done following the Reference Internal Ratio (RIR) method which requires measuring the intensity of one or more peaks for each mineral present and the added internal standard (Hubbard et al. 1976).

2.2.3. X-Ray Fluorescence (XRF)

XRF analysis was performed in material science laboratory in UCL Qatar. Considering the fact that this type of rare pottery has not been analyzed before, both portable and bench-top XRF analysis were performed, as supplementary qualitative and semi-quantitative data to the SEM. High vacuum bench-top ED-XRF (Fischerscope XUV773) with the smaller collimator (diameter 0.6mm), measurements conditions set to 20kV (no filter) and 1000uA current and run time of 482s, was performed for semi-quantitative slip analysis. Furthermore, the handheld ED-XRF Spectrometer (Olympus Innov-X Delta Premium), with Mining Plus-UCL 3mm calibration mode set up, was run for the qualitative bulk analysis on the unprepared ceramic samples. In the both XRF cases, the small collimators were used in order to analyze particular areas in the sample.

2.2.4. Laser Ablation - Inductively Coupled Plasma - Mass Spectrometry (ICP-MS)

The LA-ICP-MS method was chosen as the most suitable one given the fact that the aim was to approach in non-destructive way in order to preserve this rare type of unglazed molded pottery. Analysis was performed using an Agilent 8800 ICP-MS Trip Quad coupled to a CETAC LSX - 213 G²⁺ laser ablation system. The equipment was calibrated prior to the analysis with NIST

612. Elemental fractionation was monitored using the $^{238}\text{U}/^{232}\text{Th}$ ($\cong 105\%$) and the oxide formation was evaluated using $^{248}\text{ThO}/^{232}\text{Th}$ ($< 3\%$) ratio. For the present study, ICP-MS was performed in TRA mode (Time Resolved Analysis) operating with the scan type MS/MS mode. The elements monitored and their integration times, as well as the ICP conditions are showed in the following table.

Acquisition Mode	TRA (Time Resolved Analysis)
Scan Type and Tune Mode	MS/MS, No Gas
Plasma Parameters	
RF Power	1550 W
RF Matching	1.4 V
Sample Depth	4 mm
Dilution Gas (Ar)	0.70 L/min
Plasma Gas (Ar)	15 L/min
Dwell time	Isotopes Measured
5 ms	^{27}Al , ^{28}Si , ^{56}Fe
10 ms	^{23}Na , ^{24}Mg , ^{39}K , $^{42,43,44}\text{Ca}$, ^{47}Ti , ^{51}V , ^{52}Cr , ^{55}Mn , ^{57}Fe , ^{88}Sr , ^{133}Cs , ^{137}Ba ,
20 ms	^{85}Rb , ^{89}Y , ^{90}Zr , ^{93}Nb , ^{178}Hf , ^{181}Ta

The laser conditions used for the analysis were 100 μm spot size, 600 shots per spot, 80% energy, frequency of shot 20Hz, He flow 1L/min. A gas blank of 20s and a washout of 10s were applied per spot. The standard NIST 612 was used as CRM and was analyzed in triplicate after each 12 spots of sample analysis, in order to evaluate the accuracy of the measurements and to check for possible drift of the machine, what did not occur. The percentage of recovery of all elements was performed to check the accuracy of the measurements, which showed to be between 95 and 103%. Glitter® data reduction software was used to convert the intensity of the elements into concentrations in ppm.

CHAPTER 3: RESULTS AND DISCUSSION

3.1. Molded ceramic with slip

As mentioned before, these samples from Mértola were interpreted by archaeologists as molded pottery with a red slip. Production of pottery coated with a red layer has been reported from Neolithic sites in the Iberian Peninsula, and different examples also appear at sites dated to the Bronze and Iron Ages, and to the Roman period, such as terra sigillata. However, a lack of local, slipped – ceramic production has been observed in the Iberian Peninsula from the fifth century AD, so this type of ceramic was probably a tradition imported during the Islamic period.

3.1.1. Specimen CR/MD/004

The SEM images showed visually two distinct layers in the Mértola specimen number CR/MD/004 – body dominated by quartz and the possible slip layer (Figure 11).

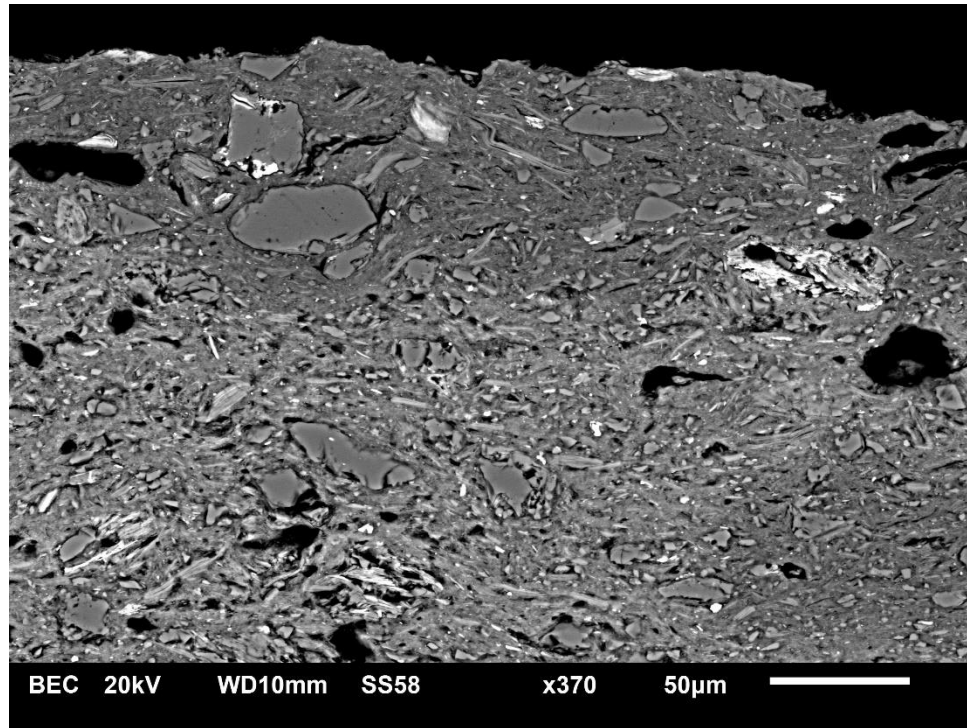


FIGURE 11. BSE IMAGE OF SAMPLE CR/MD/004 WITH VISUALLY DISTINGUISHABLE BODY AND THE SLIP

The results of the chemical composition of slips and bodies are shown in Table 1. The chemical composition of the body revealed that ratios of silica (59 wt% SiO_2) and alumina (25 wt% Al_2O_3) were readily repeatable through three different analyzed bulk areas, together with high contents of potassium (3,95 – 4,05 wt% K_2O) and iron oxides (8,5 - 9 wt% FeO) due to the abundant quartz and feldspar contents in the body (Figure 12). Smaller quantities of soda (0,66 – 0,7 wt% Na_2O), magnesium (0,7-0,8 wt% MgO), calcium (0,67 - 0,69 wt% CaO) and titanium oxides (0,79 - 0,86 wt% TiO_2) completed the composition. On the other hand, chemical composition of the slip (Figure 13) showed that it is made from the same raw materials as the body itself and that there are no significant qualitative and quantitative differences between this two features, although visual differences are present (Table 1). The strongest similarity between the slip and the body was shown in potassium and calcium composition, where the both features are interpreted, according to the data, as non – calcareous matrixes. This characteristic simultaneously points to the fact that in the case of this specimen there is no compositionally distinguishable layers, in other words the presence of the red coating layer is absent.

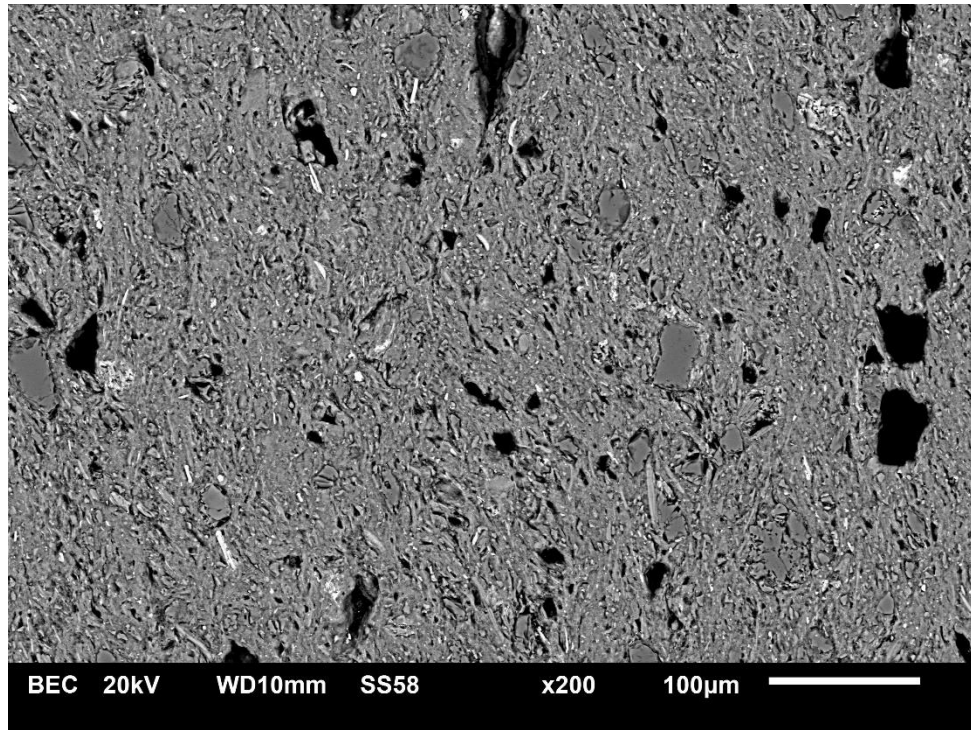


FIGURE 12. BSE IMAGE OF SAMPLE'S CR/MD/004 BODY, AREA ANALYSIS

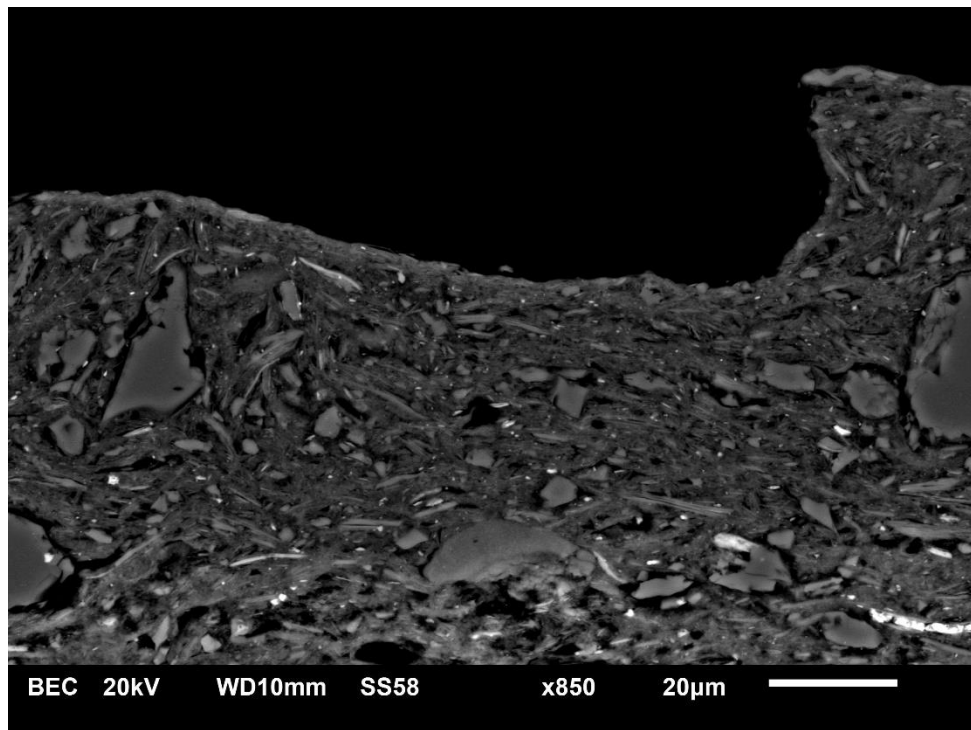


FIGURE 13. BSE IMAGE OF SAMPLE'S CR/MD/004 SLIP AREA ANALYSIS

Furthermore, a comparison of the composition of Mértola specimen (surface layer and body) together with the results of a study conducted on a ceramic material with red coating layer from Zaragoza in Spain (12th century AD) showed significant compositional differences (Arantegui J., Castillo R. 2000). The composition between body and red surface of Zaragoza samples differed in that the body had higher Al₂O₃ to SiO₂ ratio, higher iron and potassium contents and lower calcium and magnesium contents (Table 2). The strongest difference was shown in potassium and calcium composition, resulting in that the coating layer was non-calcareous (1.9-4.0% wt CaO) compared with a very calcareous body matrix (22-28% wt CaO) (Arantegui J., Castillo R. 2000).

TABLE 1. THE BULK BODY AND SLIP SEM-EDS ANALYSIS, SAMPLE CR/MD/04, NORMALIZED TO 100 WT%.

Spectrum label	Na₂O	MgO	Al₂O₃	SiO₂	K₂O	CaO	TiO₂	FeO
Body-area analysis	0,66	0,77	25,29	59,26	3,99	0,67	0,86	8,5
Body-area analysis	0,71	0,82	25,7	58,74	4,05	0,69	0,81	8,48
Body-area analysis	0,67	0,81	25,15	58,77	3,95	0,68	0,79	9,18
Upper slip bulk – area analysis	0,76	1,01	25,44	59,03	3,96	0,74	0,75	8,12
Upper slip bulk – area analysis	0,76	0,99	26,89	57,1	4,11	0,85	0,64	8,46
Upper slip bulk – area analysis	0,57	0,91	24,49	61,14	3,84	0,75	0,56	7,49

Lower slip bulk – area analysis	0,58	0,73	24,03	60,83	4,19	0,67	0,87	7,93
Lower slip bulk – area analysis	1,47	0,66	22,47	63,89	3,38	0,6	0,62	6,78
Lower slip bulk – area analysis	0,62	0,77	26,34	57,51	4,24	0,7	1,11	8,19
Average	0,76	0,83	25,09	59,59	3,97	0,71	0,78	8,13
St. Deviation	0,28	0,12	1,31	2,08	0,25	0,07	0,17	0,68

TABLE 2. CHEMICAL COMPOSITION OF ZARAGOZA CERAMIC SAMPLES (SLIP AND BODY CHEMICAL COMPOSITION) (ARANTEGUI P., CASTILLO R., 2000)

Characterization of red-coloured slips on Islamic ceramics

		MgO		Al ₂ O ₃		SiO ₂		K ₂ O		CaO		TiO ₂		Fe ₂ O ₃	
		x	σ	x	σ	x	σ	x	σ	x	σ	x	σ	x	σ
AL1	Outer red slip	0.98	±0.21	20.7	±0.70	43.4	±2.33	12.2	±0.92	2.94	±1.06	1.55	±0.60	14.9	±1.78
	Inner red slip	0.91	±0.07	21.7	±1.10	45.5	±1.61	10.5	±1.14	1.88	±0.11	1.82	±1.63	17.4	±0.52
	Body	1.31	±0.13	12.1	±1.10	40.4	±2.58	6.86	±0.72	25.6	±3.32	0.79	±0.16	11.3	±0.71
AL2	Outer red slip	0.68	±0.13	16.3	±0.62	32.9	±0.92	28.5	±1.11	6.78	±1.76	0.82	±0.22	13.1	±0.61
	Inner red slip	1.46	±0.17	20.1	±0.57	42.4	±0.92	15.6	±0.31	2.33	±0.51	0.90	±0.16	15.8	±0.44
	Body	1.21	±0.06	11.2	±0.32	43.3	±0.25	5.59	±0.12	27.2	±0.91	0.81	±0.21	9.76	±0.15
AL3	Outer red slip	1.28	±0.15	19.1	±0.85	35.7	±1.98	18.5	±1.53	3.33	±0.84	0.83	±0.16	14.6	±0.69
	Inner red slip	1.00	±0.13	17.6	±1.17	34.5	±1.62	15.7	±2.09	4.04	±1.97	0.80	±0.17	14.0	±0.82
	Body	1.37	±0.22	11.9	±0.54	39.6	±0.18	5.33	±0.03	27.8	±1.69	0.75	±0.24	10.7	±0.22
AL4	Outer red slip	0.93	±0.13	20.7	±2.19	44.2	±3.05	9.61	±1.28	3.14	±2.31	0.79	±0.18	16.8	±1.23
	Inner red slip	1.19	±0.24	19.9	±1.49	41.1	±1.96	13.5	±0.65	3.78	±2.91	0.84	±0.34	15.1	±0.55
	Body	1.35	±0.18	12.2	±0.57	40.8	±1.01	6.62	±0.19	25.7	±1.48	0.89	±0.04	11.3	±1.67
AL5	Outer red slip	1.18	±0.09	21.0	±0.59	48.7	±2.91	9.79	±2.57	2.55	±1.02	0.90	±0.15	15.2	±1.12
	Inner red slip	0.78	±0.75	22.4	±1.24	51.0	±2.48	7.71	±0.94	1.95	±0.21	0.87	±0.46	14.3	±3.12
	Body	1.44	±0.08	12.1	±2.02	45.6	±3.90	6.75	±0.97	22.4	±1.35	0.83	±0.08	9.79	±0.86

x: average value (n = 6); σ: standard deviation.

As minerals are the evidences for stable and metastable solid phases, the determination of mineralogical compositions of the ceramics is the keynote for archaeometric investigation of ancient ceramics (Krapukaitytė 2008). Thus, knowledge of decomposition of present minerals and formation of new phases allow us to estimate the firing temperatures of the studied potteries. This information will also assist to unveil the production techniques and technologies of the Islamic population in Mertola.

In order to characterize the clays and pastes used, as well as the firing temperature more effectively and to combine results obtained with SEM-EDS data, sample CR/MD/004 was analyzed using powder X – Ray diffraction (XRD). The XRD results showed different mineralogical and phase contents in this sample. Quartz (SiO₂), clay mineral: illite [KAl₂Si₃AlO₁₀(OH)₂], feldspars (K-feldspars KAlSi₃O₈) and plagioclase-albite (NaAlSi₃O₈) and iron mineral hematite (Fe₂O₃) were identified (Figure 14.)

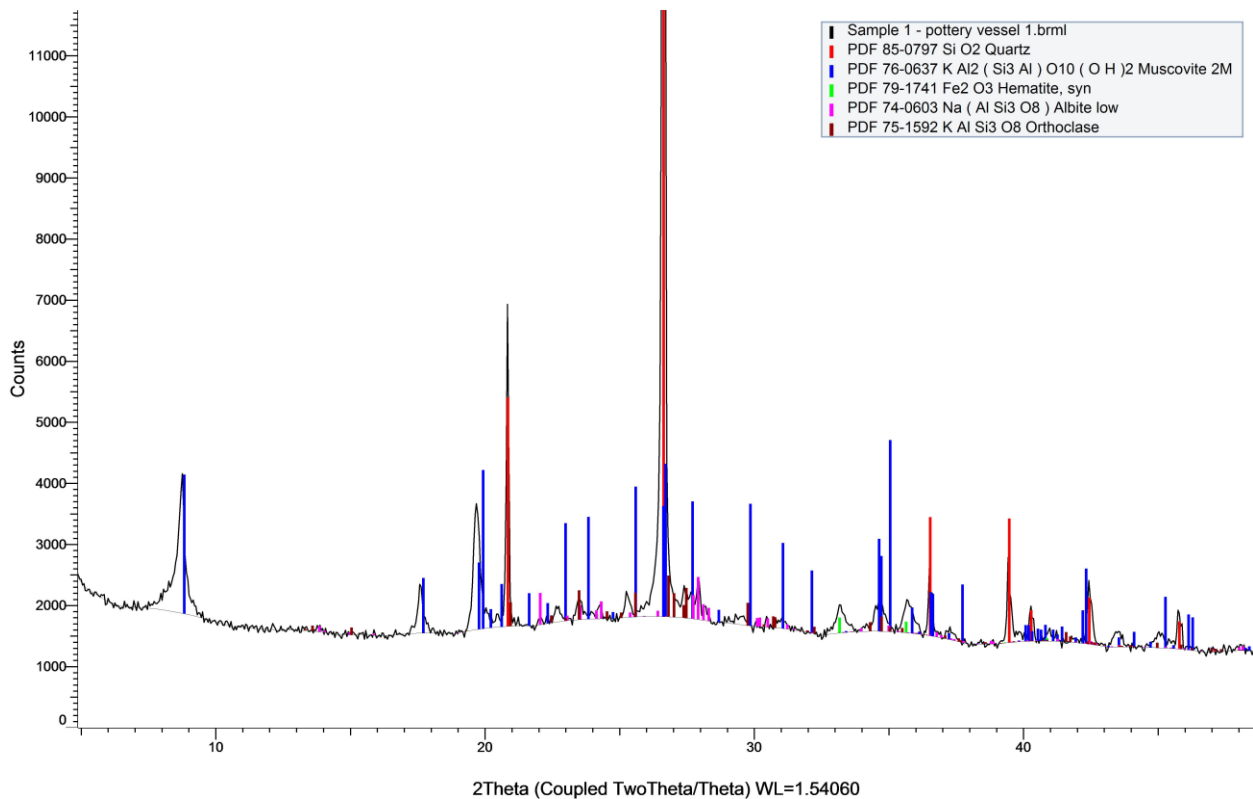


FIGURE 14. X-RAY POWDER DIFFRACTION SPECTRA OF CR/MD/004

As mentioned before, XRD data revealed the presence of illite/muscovite (it is important to note that muscovite can also be result of tempering the vessel by the potter, but at this point we cannot know that for sure without any petrographic observations) as main clay mineral used for manufacture of this particular vessel, which in general agreement with SEM micro-textural observations. In addition, this result can be used for determining firing conditions which can be estimated through observations based on presence or absence of particular mineral phases. Illite has the nominal formula $(K_{0.88} Al_2 (Si_{3.12} Al_{0.88}) O_{10} (OH)_2$ and it is a non-expanding 2:1 clay that is constructed from two tetrahedral sheets that border a central octahedral sheet (Stevenson 2016). The interlayer of K and Na serve to inhibit the presence of water molecules and prevent swelling except for K-deficient varieties which may allow water into the interlayer region (Yates and Rosenberg 1997). The dehydroxylation and phase transformations of illite begins with the condensation of water molecules in the octahedral layer and results from Al-O bond breaking. This is followed by a one-dimensional diffusion of water molecules through the tetrahedral ring into

the interlayer region that can occur at between 350 and 675 °C (McConville and Lee 2005). The crystalline structure is still in place until 700 °C but then begins to break down between 700 and 850 °C. According to several authors complete breakdown of dehydroxylated illite/muscovite structure occurs somewhere between 850-950 °C (Bayazit 2016; Stevenson 2016; Matau 2013; Kramar 2012). Another decisive phase found in this sample are iron minerals which can also allow us to estimate the firing temperature, as well as the atmosphere in which this vessel was manufactured. Traces of hematite were identified in this sample (<0.5%), thus causing vivid red/orange color of the sherd, which further implies that the firing circle of this vessel manufacture was ended under oxidizing conditions (Matau 2013, Kramar 2012). Quartz remains the main abundant phase in all Mertola samples. Quartz is often considered as an indigenous phase found in clay deposits and thus its use as an intentionally-added temper is not always easy to confirm (Papachristodoulou 2006). Quartz temper is more likely to initiate cracking upon firing of the clay paste, owing to the higher expansion rate of the quartz crystal (Hoard 1995; Tite 2001) and as a result, quartz-tempered pottery is less resistant to mechanical and thermal stresses arising during use, when compared with calcite-tempered pottery (Tite 2001). Taking into account that this pottery was made from non-calcareous clay and presence of illite/muscovite and hematite peaks as well as the absence of high-temperature minerals (such as mullite and cristobalite) we can suggest that the maximum firing temperature of this vessel was somewhere between 850-950 °C.

In this respect, we can argue that the original clay body represents illite which remained unaltered because the firing temperatures were not high enough to destroy its crystal structure. This conclusion is in general agreement with SEM-EDS spot microanalysis of Si/Al ratios in sherd matrix, both in the body and “slip” (Table 3). The SiO₂ ratios are 2.58–3.51, 1.53–2.62 and 1 for montmorillonite, illite and kaolinite respectively. In total nine different areas, bulk analysis of ceramic clay matrix showed that Si/Al ratios fall within the scope of illitic clays, which is between 1.53 – 2.62 (Kramar 2012, Newman 1987). For the sake of characterization of the type of raw material used for the manufacture of this particular vessel, it is important to note that three minerals observed in sample CR/MD004 are primary minerals and were originally present in the clay body. We are talking here about quartz, feldspars (albite and orthoclase) and muscovite which can handle any distress related to firing, use and post-use processes because they are highly resistant to

changes at lower firing temperatures and, therefore, we might argue that they are not new phases from the firing, but they represent primary components of the clay matrix.

Table 3. SiO₂/Al₂O₃ ratios of clay body and slip

Spectrum Label	Body bulk	Body bulk	Body bulk	Slip bulk	Slip bulk	Slip bulk	Lower slip bulk	Lower slip bulk	Lower slip bulk
Al ₂ O ₃	25.29	25.7	25.15	25.44	26.89	24.49	26.34	24.03	22.47
SiO ₂	59.26	58.74	58.77	59.03	57.1	61.14	57.51	60.83	63.89
SiO ₂ /Al ₂ O ₃	2.34	2.28	2.33	2.32	2.12	2.49	2.18	2.53	2.84

3.1.2. Specimen CR/MD/003

This pottery vessel was also interpreted as the previous sample (CR/MD/004) as a type of containers coated with a red slip by the archaeologist who excavated medieval Mertola (Gomez 2000). Contrary to this accepted interpretation, SEM images showed highly homogeneous clay body dominated by quartz and feldspar minerals (Figure 15).

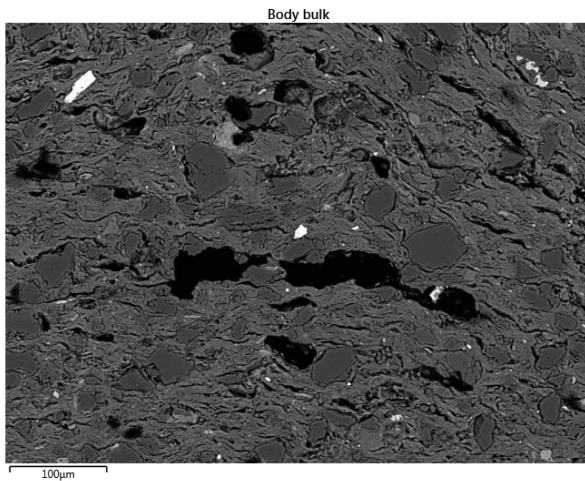


FIGURE 15. BSE IMAGE OF SAMPLE CR/MD/003 BODY

Three different areas (spectrums 52, 53 and 54) were analyzed in order to determine potential differences, as well as to perform characterization of the used raw material in the manufacture of this vessel (Figure 16). The results of the chemical composition of the body is shown in Table 4.

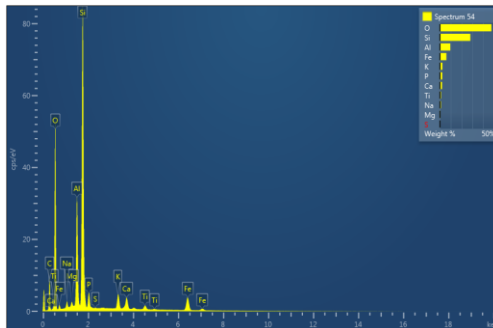
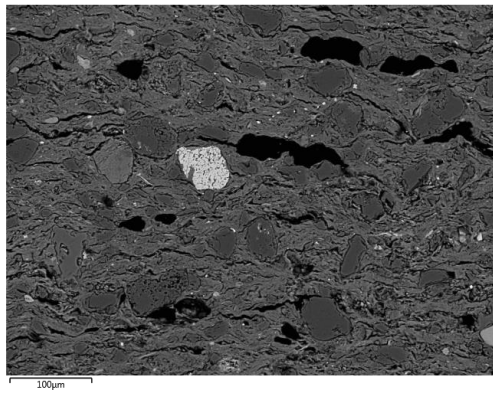
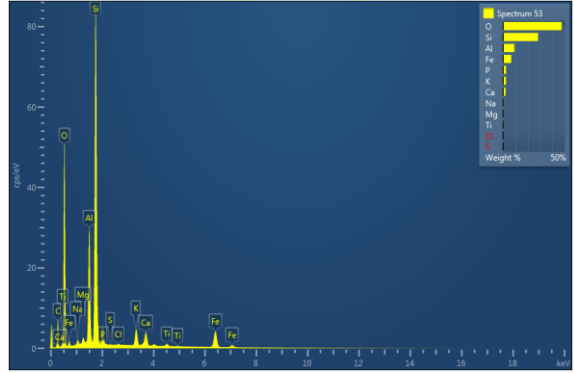
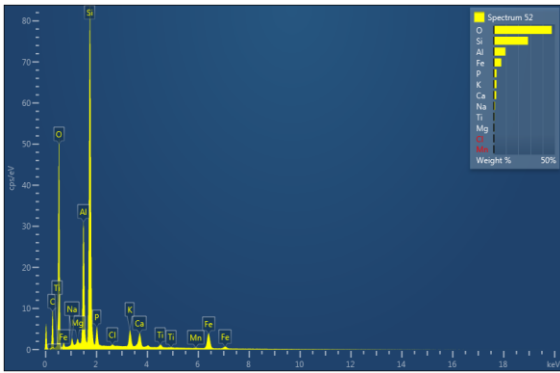
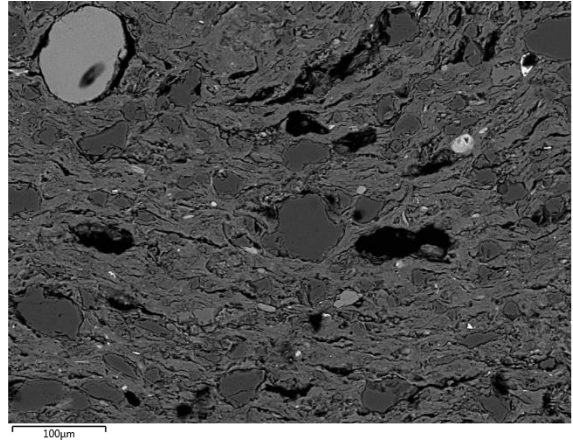
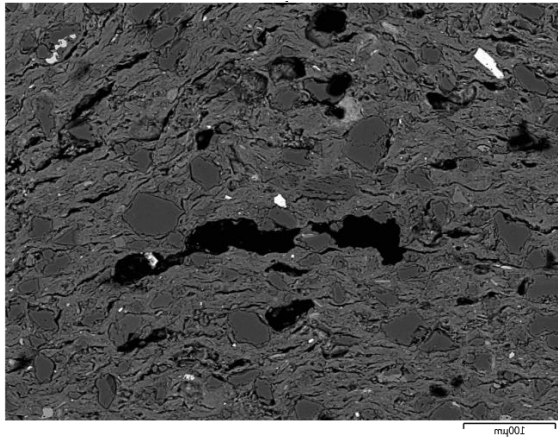


FIGURE 116. BSE IMAGES OF THE SAMPLE CR/MD/005 AND BODY AREA ANALYSIS

TABLE 4. THE BODY AREA SEM-EDS ANALYSIS, SAMPLE CR/MD/003, NORMALIZED TO 100 WT%.

Spectrum Label	Spectrum 54	Spectrum 53	Spectrum 52
Na ₂ O	1.21	0.8	1.24
MgO	0.77	0.84	0.76
Al ₂ O ₃	18.13	17.23	18.05
SiO ₂	60.11	60.62	60.04
P ₂ O ₅	4.93	5.41	5.21
SO ₂	0.15	0.13	
K ₂ O	2.74	2.76	2.66
CaO	2.68	2.82	2.83
TiO ₂	1.6	0.78	0.96
MnO			0.16
FeO	7.68	8.51	7.91
Total	100	99.89	99.83

The chemical composition of the body revealed that ratios of silica (~60 wt% SiO₂) and alumina (~ 18 wt% Al₂O₃) were readily repeatable through three different analyzed bulk areas, together with low contents of potassium (~2.74 wt% K₂O) and high amounts of iron oxides (7.68 – 8.51 wt% FeO) due to the abundant quartz and feldspar contents in the body. Smaller quantities of soda (0.8 – 1.24 wt% Na₂O), magnesium (0,7-0,8 wt% MgO), calcium (2.68 – 2.83 wt% CaO), titanium oxides (0,78 - 1,6 wt% TiO₂) and unlike the previous sample, here are recognized traces of sulphur (~ 0.15 wt% SO₂) and higher amounts of phosphorous (~ 4,93 – 5,41 wt% P₂O₅). Lower concentration of calcium (2.68 – 2.83 wt% CaO) indicates that this pottery was made from a non-calcareous type of clay and SEM-EDS spot microanalysis of Si/Al ratios in five different areas of sherd matrix, bulk analysis showed that SiO₂/ Al₂O₃ ratios fall within the scope of montmorillonite clays (Table 5), which is between 2.58–3.51 (Kramar 2012, Newman 1987). As we can see in the table 5, we have enrichment in SiO₂ which may be coming from small quartz minerals in the clay.

TABLE 5. Si/AL RATIOS OF THE CLAY BODY

Label	Spectrum 54	Spectrum 53	Spectrum 52
SiO ₂	60.11	60.62	60.04
Al ₂ O ₃	18.13	17.23	18.05
SiO ₂ / Al ₂ O ₃ ratios	3.32	3.52	3.33

As we can see, the biggest difference between these two samples of this pottery group is the presence of phosphorous. The presence of phosphorus in samples of soil, sediments and water is traditionally considered to be an important indicator of human activity, either archeological or contemporary. Traditionally, the presence of phosphorus in archeological ceramics is attributed to adsorption from the soil subsequent to the discarding of utensils or the presence of the element in the raw material, although a few authors support the hypothesis of the contamination of pots by food during cooking (Santos Rodrigues 2016: 224). However, studies of the presence of phosphorus in archeological ceramics are relatively scarce, given that the presence of this element, as previously noted, is traditionally attributed to its adsorption from the soil in which the sherds were discarded. Alternatively, phosphorus can be derived from apatite, sometimes in the form of bone fragments, when this mineral is found in the ceramic matrix, which is not the case in our sample. Also, the presence of red slip is arguable. BS images showed neither discontinuity between the ceramic body and the surface nor evidence of vitrification. Therefore, the microscopic examination seemed to point to the absence of a slip in this sample suggesting the use of a simple pottery burnisher to smooth and burnish the vessel exterior.

In order to characterize more precisely the clays and pastes used, as well as the firing temperature more effectively and to combine results obtained with SEM-EDS data, sample CR/MD/003 was analyzed using micro X – Ray diffraction (XRD). The XRD results showed exactly the same mineralogical and phase contents in this sample like in the previous one of this pottery group (sample CR/MD/004). Quartz (SiO₂), clay mineral: illite/muscovite [(K, H₃O) Al₂Si₃AlO₁₀ (OH)₂] / [KAl₂Si₃AlO₁₀(OH)₂], feldspars (K-feldspars KAlSi₃O₈) and plagioclase albite (NaAlSi₃O₈) and iron mineral hematite (Fe₂O₃) were identified (Figure 17). As we can see in the graph below, traces of calcite or neoformed calcium silicates were not identified which is

in general agreement with SEM-EDS data regarding the fact that the potters used non-calcareous type of clay.

Considering the fact that the mineralogical composition is the same as in the previous sample CR/MD/004 (quartz, albite, orthoclase and hematite), in this case we will pay attention only to illite/muscovite peak, because somehow it is contrary to the results obtained with SEM-EDS. The visibility of illite clay in diffraction patterns is in direct conflict with SEM data, where it was determined the use of montmorillonite clay, according to $\text{SiO}_2/\text{Al}_2\text{O}_3$ ratios. There are two possible explanations for this phenomenon. The simplest clarification could be that original clay body indeed represents illite which remained because the firing temperatures were not high enough to destroy its crystalline structure. A bit complicated explanation is related to a transition of original clay body that contained montmorillonite but transformed into an illite-like phase that is observed in fired sherds. Montmorillonite is classified as a specific clay mineral in the smectite family and smectite is known to commonly transition to illite during diagenesis. This process is referred to as “smectite illitization” and represents a sequence that involves initial transformation from smectite to random mixed-layer illite/smectite and ordered mixed layer illite/smectite and finally to illite (Zerai 2015: 59).

Such phenomena are extremely difficult to verify as there are no visible peaks of montmorillonite and an illite/montmorillonite peaks in diffractograms of sample CR/MD/003. That said, we can argue that this pottery was fired at low temperatures, somewhere between 850 – 950°C if consider the facts that this pottery was made from non-calcareous type of clay and presence of illite/muscovite and hematite peaks as well as the absence of high-temperature minerals (such as mullite and cristobalite).

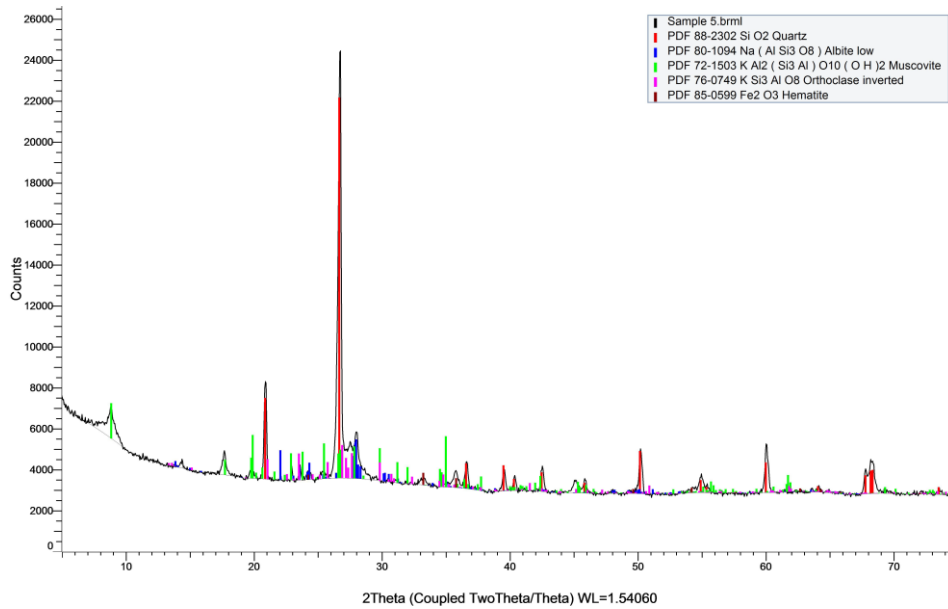


FIGURE 17. X-RAY POWDER DIFFRACTION SPECTRA OF CR/MD/003

3.1.3. Specimen CR/MD/005

The last piece of this ceramic assemblage from Mertola was like the others from this pottery group interpreted as a type of containers coated with a red slip by the archaeologist who excavated medieval Mertola (Gomez 2000). Nevertheless, SEM images failed to show any visual presence of the slip (Figure 18). However, visual observation revealed inconsistencies in the color in the cross section of the ceramic sample. Namely, areas close to the exterior and interior wall were reddish, while, the middle part of the cross section was dark grey or black (Figure 19).

bulk pri dnu fragmenta

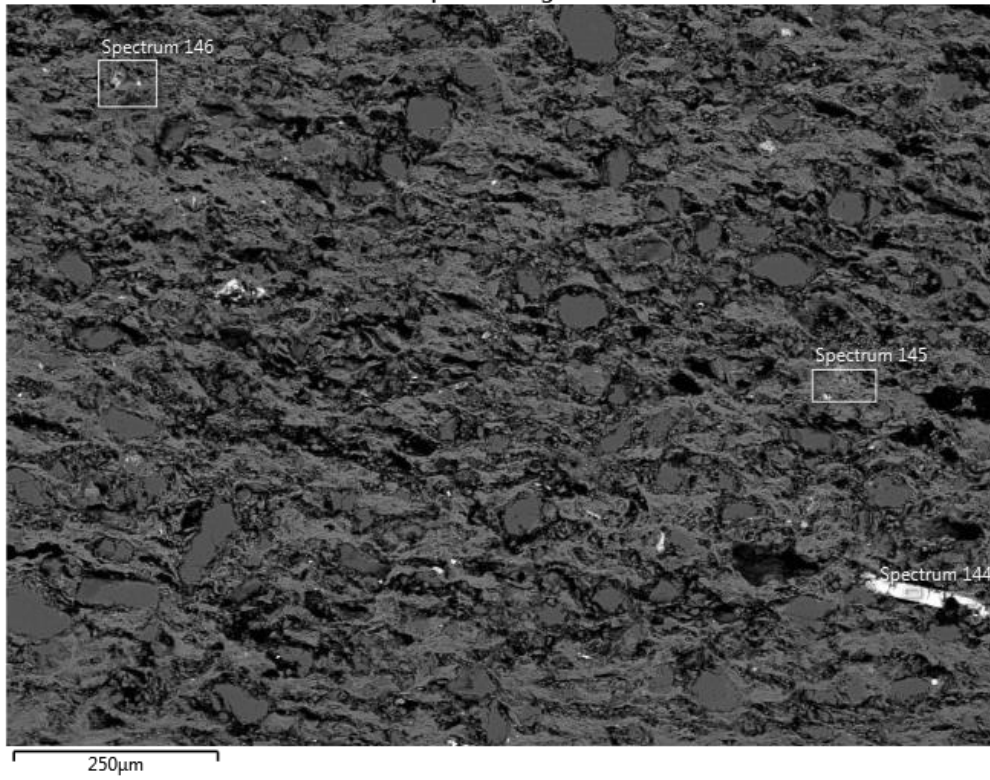
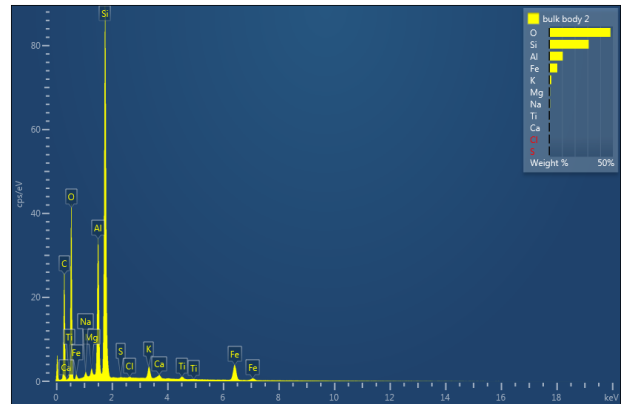
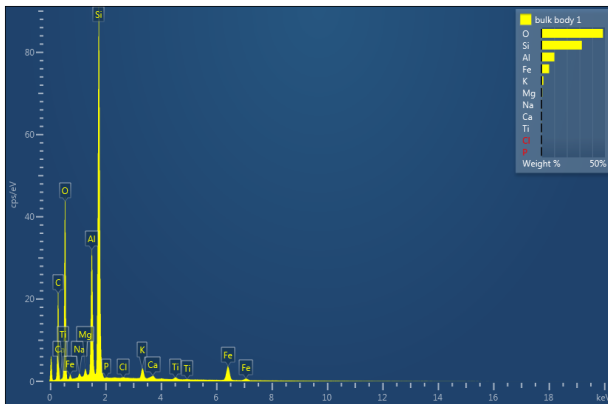
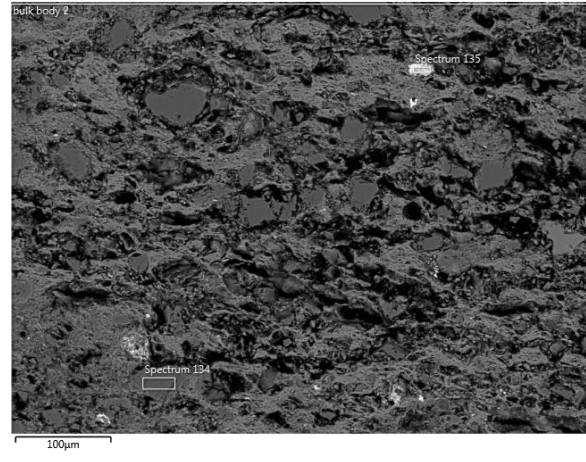
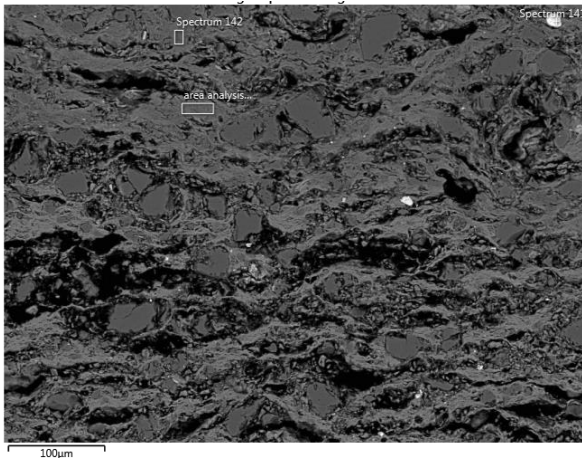


FIGURE 18. BSE IMAGE OF SAMPLE CR/MD/005 BODY



FIGURE 19. CROSS SECTION OF THE SAMPLE CD/MD/005

Three different areas were analyzed (areas close to the exterior/interior wall and in the middle of the sherd) in order to investigate potential differences between these two visually different parts of the sherd, as well as to perform technological characterization of the used raw material in the manufacture of this vessel (Figure 20). The results of the chemical composition of the body is shown in Table 6.



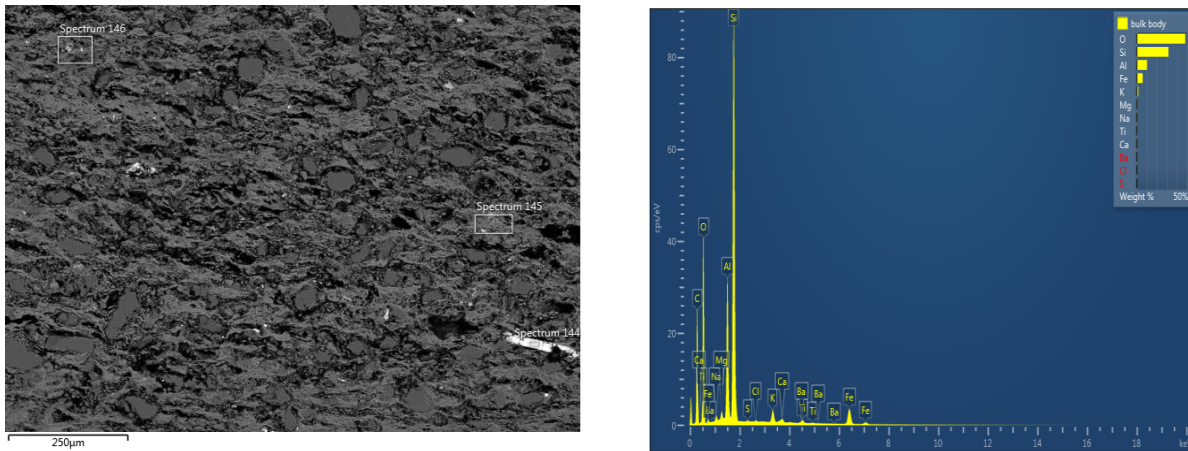


FIGURE 20. BSE IMAGES OF THE SAMPLE CR/MD/005 AND BODY BULK ANALYSIS

TABLE 6. THE BULK BODY SEM-EDS ANALYSIS, SAMPLE CR/MD/005, NORMALIZED TO 100 WT%.

Spectrum Label	Bulk body – Lower reddish part	Bulk body 2 – Middle Grey part	Bulk body 1 – Upper reddish part
Na ₂ O	0.8	0.82	0.65
MgO	1.05	1.02	1.08
Al ₂ O ₃	19.16	20.01	19.15
SiO ₂	67.48	66.31	68.03
SO ₂	0.24	0.15	0.16
K ₂ O	1.88	1.94	1.79
CaO	0.67	0.7	0.64
TiO ₂	0.83	0.86	0.7
FeO	7.52	8.09	7.71
Total	99.88	99.9	99.92

The results of the chemical composition are shown in Table 6. As we can see, there are no significant differences in the composition, therefore presence of the slip has been denied in this case also.

The chemical composition of the body revealed that ratios of silica (~ 68 wt% SiO₂) and alumina (~ 20 wt% Al₂O₃) were readily repeatable through three different analyzed bulk areas,

together with high contents of iron oxides (~ 9 wt% FeO). Unlike previous cases in this group of archaeological findings, concentrations of potassium are rather low (less than 2 wt % K₂O). Smaller quantities of soda (~ 0.8 wt% Na₂O), magnesium (~ 1,08 wt% MgO), calcium (~ 0.7 wt% CaO), sulphur (~ 0,2 wt% SO₂) and titanium oxides (~ 0,86 wt% TiO₂) completed the composition.

Lower concentration of calcium (0,64 – 0,7 wt% CaO) proved that this vessel was made from a non-calcareous type of clay like all the others from this pottery group. SEM-EDS spot microanalysis of SiO₂/ Al₂O₃ ratios of sherd matrix showed that Si/Al ratios fall within the scope of illite clays (spectrum area analysis of the clay; Figure 21; Table 7), which is between 1.53 – 2.62 (Kramar 2012, Newman 1987).

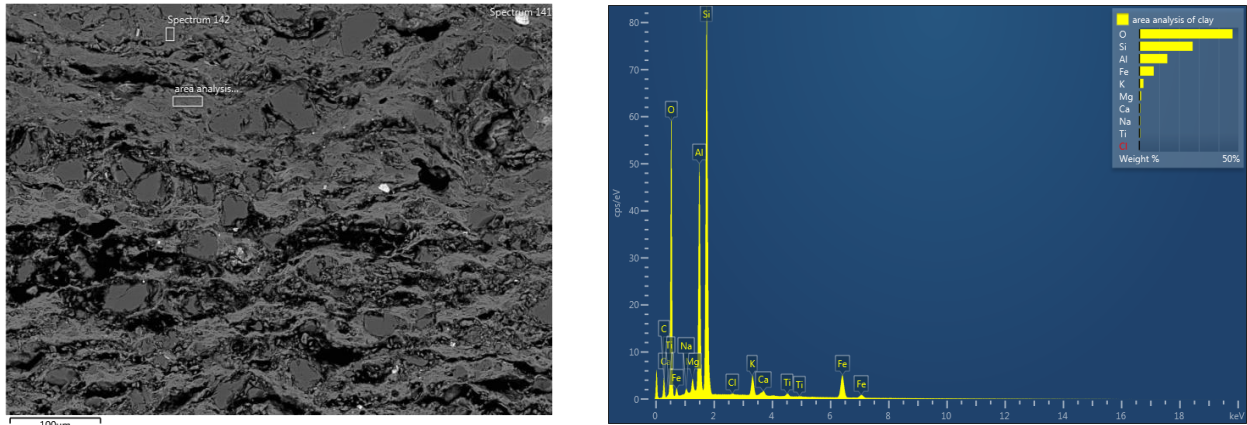


FIGURE 21. BSE IMAGE OF THE SAMPLE CD/MD/005 AND AREA ANALYSIS OF THE CLAY

TABLE 7. Si/AL RATIOS OF THE CLAY BODY

Spectrum Label	Area analysis of clay
SiO ₂	26.74
Al ₂ O ₃	57.57
SiO ₂ / Al ₂ O ₃ ratios	2.15

As for the data obtained by the means of the micro X – Ray diffraction, results showed the same mineralogical composition of this vessel as the previous ones of this pottery group from Mértola.

The uXRD results showed different mineralogical and phase contents in this sample. Quartz (SiO_2), clay mineral: illite/muscovite [$\text{KAl}_2\text{Si}_3\text{AlO}_{10}(\text{OH})_2$], orthoclase (K-feldspars KAlSi_3O_8), plagioclase albite ($\text{NaAlSi}_3\text{O}_8$) and iron mineral hematite (Fe_2O_3) were identified (Figure 22).

As mentioned before, XRD data revealed the presence of illite/muscovite as main clay mineral used for manufacture of this particular vessel, which in general agreement with earlier SEM micro-textural results.

Another decisive phase found in this sample are iron minerals which can allow us to estimate the firing temperature, as well as the atmosphere in which this vessel was manufactured. As previously noted, visual observation revealed inconsistencies in the color of this sherd's cross-section, whilst SEM analysis failed to show use of several different raw materials in the manufacture of this vessel. In this respect, we can look up for explanation in the observation of hematite peaks.

The presence of hematite in this sample suggested that the firing process of this vessel has presumably been ended in oxidizing atmosphere. It is also known that sandwich structured samples (red/brown exterior layer with black/grey interior layer or red/brown margin with a black/grey core) would appear in two ways. First, firing in reducing atmosphere and then cooling in oxidizing atmosphere and second option is that firing was in oxidizing atmosphere with high amounts of organic materials (Bong et al., 2008). That said, we can assume that this vessel was fired in reducing atmosphere and then cooled in oxidizing atmosphere, therefore firing temperature should be somewhere around 850 - 950 °C.

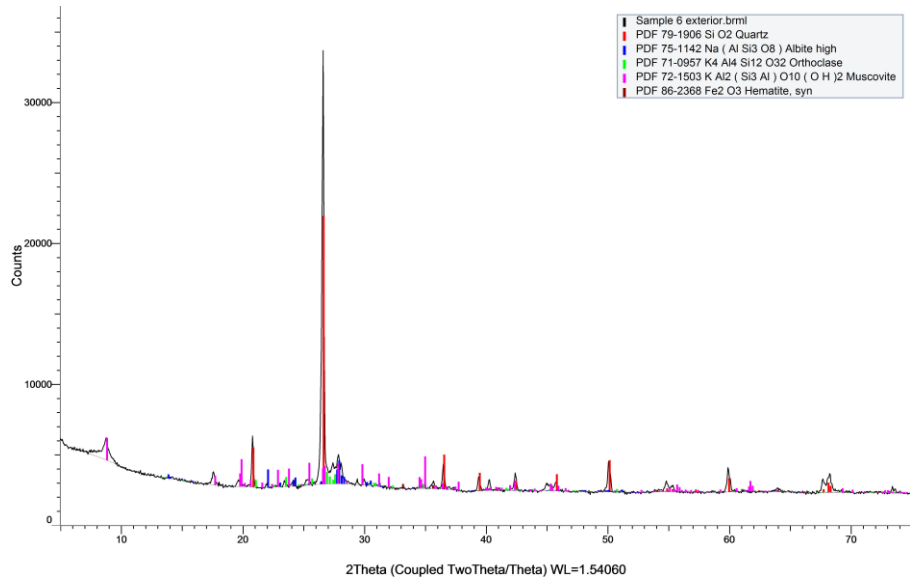


FIGURE 22. X-RAY POWDER DIFFRACTION SPECTRA OF CR/MD/005

3.2. Molded glazed ceramic

The last group of mold-made ceramics from Mertola is formed by the pieces covered with glass, among which the jars with a molded body decorated with metallic ornaments play an important role. Within Mertola complex it was possible to reconstruct the total shape of at least, three vessels that were manufactured with the same type of mold (pieces with inventory number CR/DR/0001, CR/DR/0002 and CR/DR/0023). Vessels were identified as jars with molded edges, inverted conical neck, globular body and vertical handles. For the purposes of this research only vessels CR/DR/0002 and CR/DR/0023 were subjected to the archaeometrical study (Figure 23).



FIGURE 2312. VESSELS CR/DR/0002 AND CR/DR/0023, RESPECTIVELY

3.2.1. Specimen CR/DR/0023

As in the previous pottery group, SEM-EDS analysis was used to determine chemical composition of the body, inclusions and in this case glaze, present in this pottery assemblage as well as to provide insights of their production technology. Compositional mapping and EDS area enabled determination of feldspar composition as well as bulk elemental composition, while XRD was used mainly for identification of mineral phases. This helps to place Mértola's pottery in context locally and regionally. At present, there is no evidence for molded glazed pottery production workshops in Mértola region, and no geological prospection has been carried out on clay sources and other raw material sources that could have been used in production. Therefore, the analysis of glazed molded bodies from Mértola is an original, important and necessary contribution to the study of pottery production in the region – along with Beja, Évora and others.

The SEM images showed two distinguishable layers in the Mértola specimen – body dominated by the angular quartz and feldspars and glaze above it (Figure 24). Also notable is the absence of an engobe, which in case of Islamic glazed pottery serves as some kind of interaction layer between the glaze and the underlying body (Jenkins 1983, Özçatal 2014, Tite 2011).

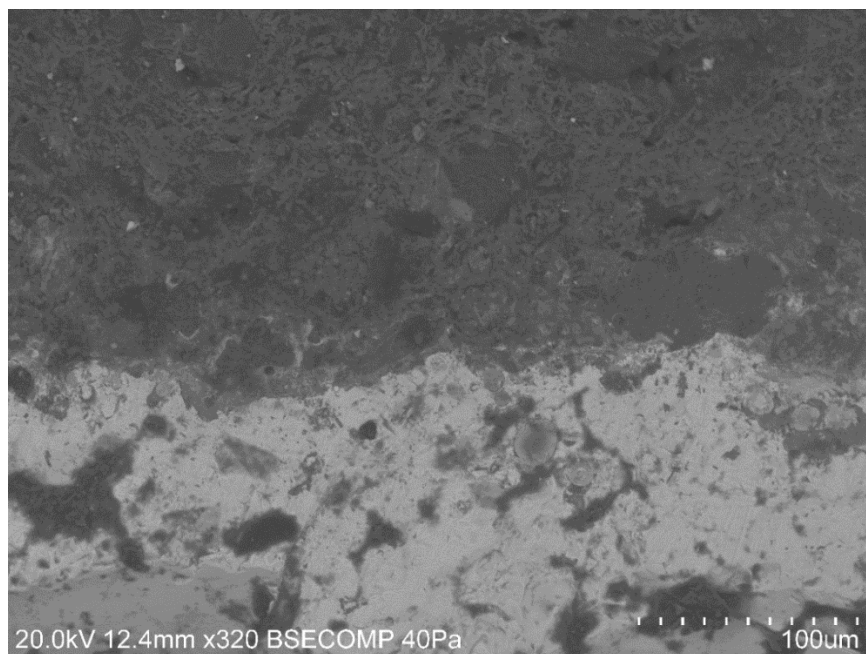


FIGURE 24. BSE IMAGE OF SAMPLE CR/DR/0023 WITH VISUALLY DISTINGUISHABLE BODY AND THE GLAZE

The results of the chemical composition of the body is shown in Table 8. According to the results, bulk analysis of the potsherd revealed an iron-rich composition with FeO quantities changing from 6.2 – 7.15 wt%. Quantities of Na₂O and K₂O were in a moderate range from 0.91 to 1.06 wt% and 2.53 to 2.64 wt%, respectively. Quantities of CaO and MgO were between 20.74 and 21.99 wt% and 2.73 and 2.91 wt%, respectively. What is very interesting and represents a certain difference compared to unglazed ceramics from Mértola is the presence of calcium oxides which in this case goes around ~ 20 wt % CaO which attests to the fact that the potters used extremely calcareous clay for manufacture of this particular vessel. Smaller quantities of soda, titanium, manganese, lead, sulphur, phosphorous and copper completed the composition. These contents could be determined by the conditions of formation of clays in the geological environment. Clay deposits may contain natural ingredients such as quartz, feldspars, iron minerals, calcium-rich materials and organic residues. Na₂O and K₂O quantities should be provided by clay minerals such as illite/muscovite and the other components in clay, especially feldspars.

Spectrum Label	Body bulk	
	Area 1	Area 2
Na ₂ O	0.91	1.06
MgO	2.91	2.73
Al ₂ O ₃	13.26	13.3
SiO ₂	35.16	39.91
P ₂ O ₅	1.57	1.1
SO ₂	0	0.66
K ₂ O	2.64	2.53
CaO	21.99	20.74
TiO ₂	0.63	0.39
MnO	0.26	/
FeO	7.15	6.2
Cu	0.46	/
PbO	1.2	/
Total	100	100

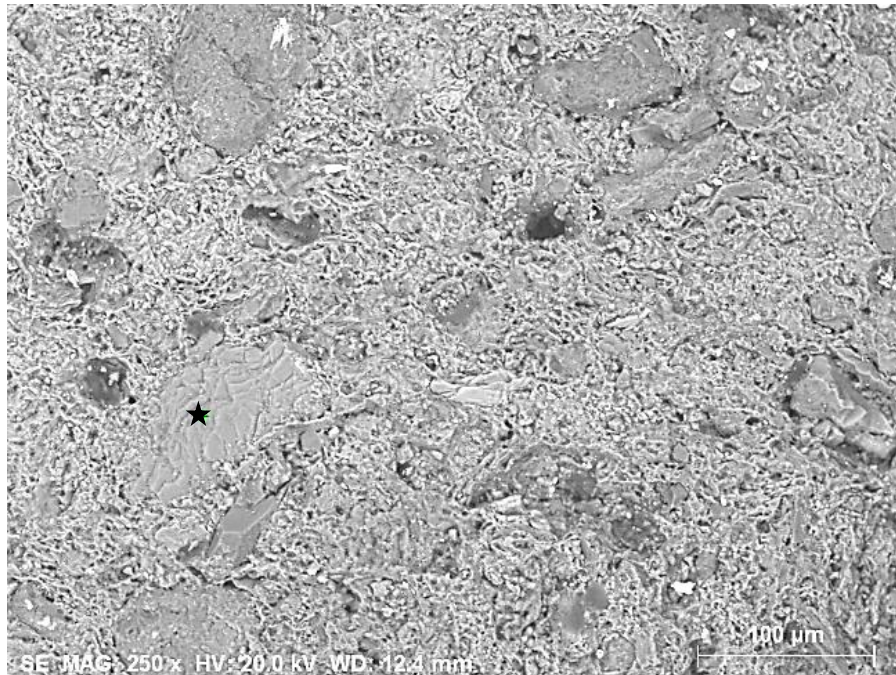
TABLE 8. THE BULK BODY SEM-EDS ANALYSIS, SAMPLE CR/DR/0023, NORMALIZED TO 100 WT%. NOTE THAT WEIGHT PROPORTIONS REPRESENT NORMALIZED WEIGHTS. NORMALIZED WEIGHTS HAVE BEEN CONVERTED TO OXIDES

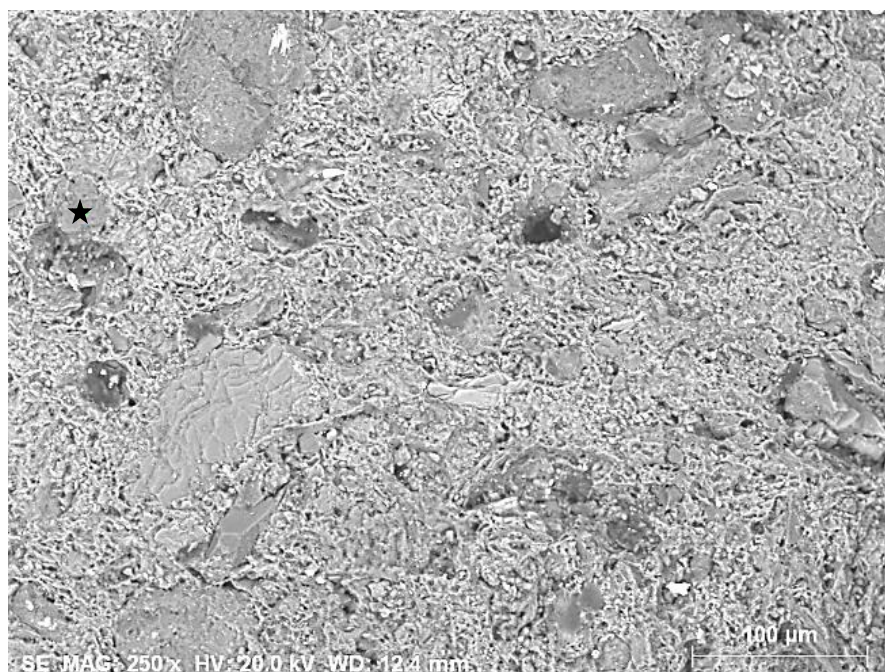
On the other hand, point analysis revealed presence of several types of feldspars, as well as amphiboles. As for the feldspar group, with the help of respective EDS spectra it was feasible to reveal variations in the amounts of sodium, potassium and calcium oxides, thus providing distinction between alkaline feldspars and plagioclases (Table 9).

TABLE 9. SEM – EDS ELEMENTAL CONCENTRATIONS OF FELDSPARS AND AMPHIBOLE IN SAMPLE CR/DR/0023

Spectrum label	SiO ₂	Al ₂ O ₃	K ₂ O	Na ₂ O	CaO	FeO
Point 1	44.13	33.53	9.78	0.74	3.63	2.52
Point 2	58.71	21.78	0.71	11.75	5.87	1.05
Point 3	30.61	14.93	8.75	/	15.66	38.00
Point 4	52.88	19.46	0.42	12.86	2.90	0.82

As we can see in the above table, weight proportions of elements detected from SEM-EDS analysis of sample CR/DR/0023 showed both alkaline feldspar and plagioclase solid solution composition (Point 1, 2, 4 and 5, figure 25).





Element	Normalized wt % in oxides		Element	Normalized wt % in oxides
Na ₂ O	0.74		Na ₂ O	11.75
MgO	2.78		MgO	0.81
Al ₂ O ₃	33.53		Al ₂ O ₃	21.78
SiO ₂	44.13		SiO ₂	58.71
P ₂ O ₅	0.26		P ₂ O ₅	0.48
SO ₂	0.16		SO ₂	1.45
K ₂ O	9.78		K ₂ O	0.71
CaO	3.63		CaO	5.87
FeO	2.53		FeO	1.06
Sum	100		Zinc	0.34
			Sum	100

FIGURE 25. POINT 1 AND 2 RESPECTIVELY, LOCATION AND THEIR ELEMENTAL COMPOSITION

As for the glaze, SEM-EDS analysis was performed to gain information on elemental composition and texture of the outer and inner glaze (Table 10). The chemical analysis of the

glazes determined that they belong to the high-lead type, as results showed that the most prominent component in both glazes is PbO. Its amount is readily repeatable in both inner and outer glaze. The amount of Na₂O and K₂O are in a moderate range from 0.75 – 0.96 and 0.5 – 0.57 wt %, respectively. CaO and MgO amounts are also in a moderate range from 3.11 – 3.63 and 0.46 – 0.61 wt%, respectively. As we can see from the below graph as a coloring agent for the exterior black glaze, most probably MnO was used, while on the other hand for the interior glaze we can deduce that common transparent lead glaze was applied without any coloring agents.

TABLE 10. THE AREA ANALYSIS OF THE GLAZE, SAMPLE CR/DR/0023, NORMALIZED TO 100 WT%. NOTE THAT WEIGHT PROPORTIONS REPRESENT NORMALIZED WEIGHTS. NORMALIZED WEIGHTS HAVE BEEN CONVERTED TO OXIDES

Spectrum Label	Exterior Glaze		Interior glaze	
	Area 1	Area2	Area 1	Area 2
Na ₂ O	0.8	0.96	0.75	0.92
MgO	0.61	0.52	0.46	0.5
Al ₂ O ₃	2.95	3.08	2.31	2.33
SiO ₂	25.06	24.78	22.22	21.69
K ₂ O	0.5	0.55	0.51	0.57
CaO	3.63	3.11	3.28	3.19
MnO	1.39	1.33	/	/
FeO	1.17	1.05	0.71	0.84
PbO	59.44	60.05	62.08	60.76
Total	100	100	100	100

Glazes may be described and classified in many ways; for example, by their maturing temperature, their principal modifier or flux and the wares on which they may be used (Rice 1987, al-Saad 2002). The most informative of these classification systems is the one that is based on principal modifier which is the one that will be used in this study. That said, glazes can be classified with reference to their principal modifiers into three distinct groups: the alkaline glazes, the lead – alkali glazes and the high lead glazes (Palamara 2016, Rice 1987, Tite 1998, Tite 2011). Alkaline glazes are characterized by having significant amounts of soda (average 16.08 wt% Na₂O) which was used as the main flux; lead – alkali glazes have somewhere between 20 – 40 wt% PbO and from 5- 12 wt % Na₂O + K₂O.

Therefore, according to the plot (Figure 26), $\text{Na}_2\text{O} + \text{K}_2\text{O}$ amounts versus that of PbO , identified these glazes as transparent high lead glaze, which normally contain somewhere between 45 – 65 wt % PbO , less than 2 wt% $\text{Na}_2\text{O} + \text{K}_2\text{O}$ and 2 – 7 wt % Al_2O_3 . This type glaze was extensively used throughout the Islamic and Byzantine empires, in the Medieval Europe for both pottery and tiles, and continuing to the present day in both Europe and the Near East (Özçatal 2014, Tite 1998)

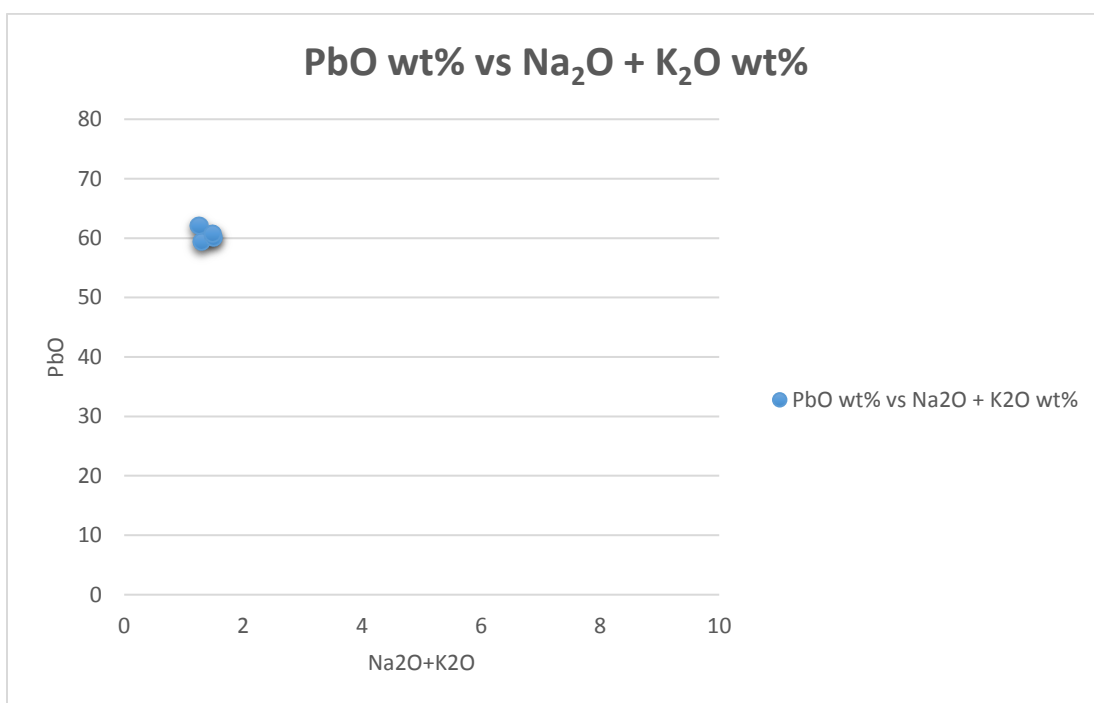


FIGURE 26. **PBO VS NA₂O+K₂O PLOT**

The next important question that seeks to be answered is how the transparent high lead glaze of this vessel was produced. There are several possible methods and the first and simplest method is when a lead compound, such as litharge (PbO), red lead (Pb_3O_4), white lead ($2\text{PbCO}_3 \cdot \text{Pb}(\text{OH})_2$) or galena (PbS), is used by itself, typically as a suspension in water. The lead oxides can be obtained by melting metallic lead in a furnace or a domestic hearth and skimming off the oxide layer. Although the galena which is a common, naturally occurring mineral can be used directly, it is also possible that it was sometimes first roasted to form the oxide (Tite 1998).

In order to provide an adequate answer, whether a lead compound by itself or a lead – silica mixture was used and whether the glaze suspension was applied to an unfired or biscuit – fired body, we must consider the interaction between the glaze mixture and the body (Tite 1998, Molera 2001).

As discussed by Molera (2001), one of the main characteristics of high-lead-content glazes is their relatively low melting temperatures and when firing, the molten glaze reacts with the body, and chemical diffusion of elements from the substrate to the glaze and vice versa occur while the phases forming the clay body decompose. The mineral composition of a clay-based ceramic body (in our case clay minerals, quartz, feldspars, calcite, and iron oxides from a raw clay), and the corresponding sintering products for a fired clay. During the reaction, diffusion of K, Al, Ca, Fe, and Si from the clay body to the glaze and of Pb from the glaze to the body occurs (Tite 1998, Molera 2001, Palamara 2016). In principle, the concentration of potassium-lead-aluminium-silicate crystals at the body-glaze interface of a high lead glaze could provide a criterion for determining whether the glaze was applied to an unfired or a biscuit-fired body (Figure 27). However, the concentration of crystals will also depend on other factors in particular, clay body composition, firing temperature, firing duration and cooling rate, and separation of the effects of all these different variables is likely to prove very difficult.

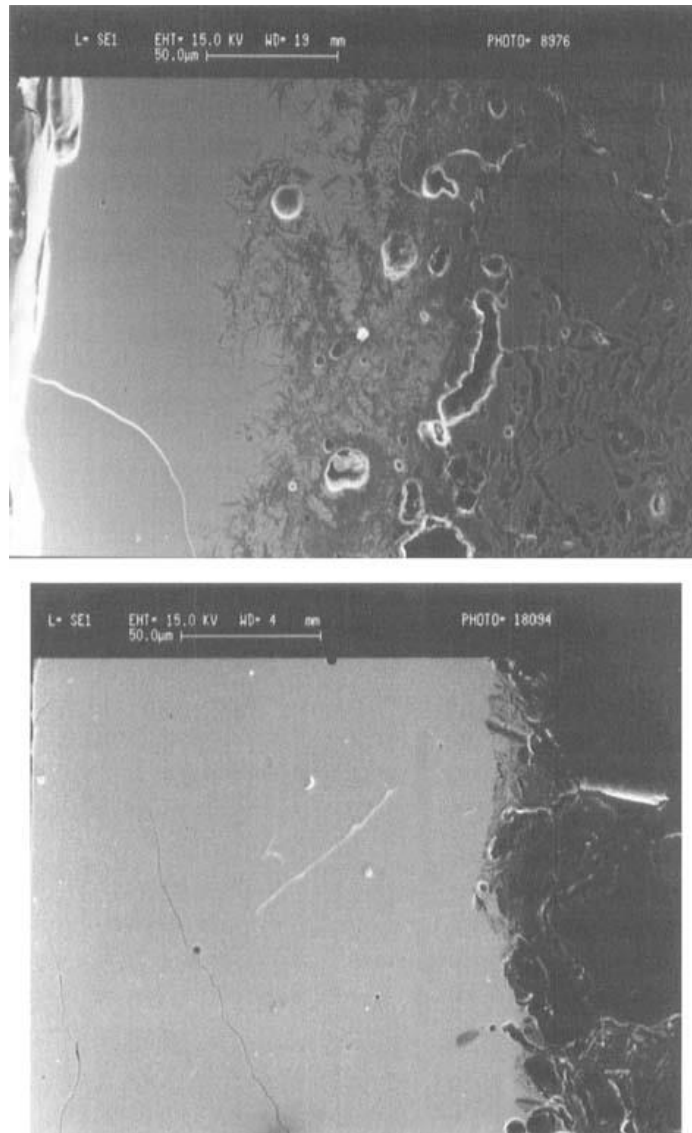


FIGURE 27. SEM PHOTOMICROGRAPHS OF BODY-GLAZE INTERFACES FOR TRANSPARENT HIGH LEAD GLAZES SHOWING (UPPER) THE HIGH CONCENTRATION OF POTASSIUM-LEAD-ALUMINIUM-SILICATE CRYSTALS WHICH ARE CHARACTERISTICALLY FORMED AT THE INTERFACE WHEN THE GLAZE SUSPENSION IS APPLIED TO AN UNFIRED BODY AND (LOWER) THE ABSENCE OF POTASSIUM-LEAD-ALUMINIUM-SILICATE CRYSTALS AT THE INTERFACE WHICH IS CHARACTERISTIC OF THE APPLICATION OF THE GLAZE SUSPENSION TO A BISCUIT-FIRED BODY (TITE 1998)

When we compare SEM image (Figure 28) of sample CR/DR/0023 with the example provided by Tite we can argue that the high lead – silica glaze was applied to an unfired body due to the concentration of potassium-lead-aluminium-silicate crystals which are characteristically formed at the interface when the glaze suspension is applied to an unfired body. Afterwards both glaze and the body were subjected to firing process. Another indicator that goes in favor of this hypothesis is the fact that the body was made of highly calcareous clay with a CaO average percentage of around 20%. It is expected that if the glaze suspension was applied to unfired body, this would result in releasing carbon dioxide due to the decomposition of the calcium carbonate upon firing. This would have resulted in the formation of trapped glaze bubbles in the glaze layer (Figure 20). The absence of such bubbles from the glazes suggests that the glaze suspension was applied to biscuit-fired bodies rather than to unfired bodies, which is not our case.

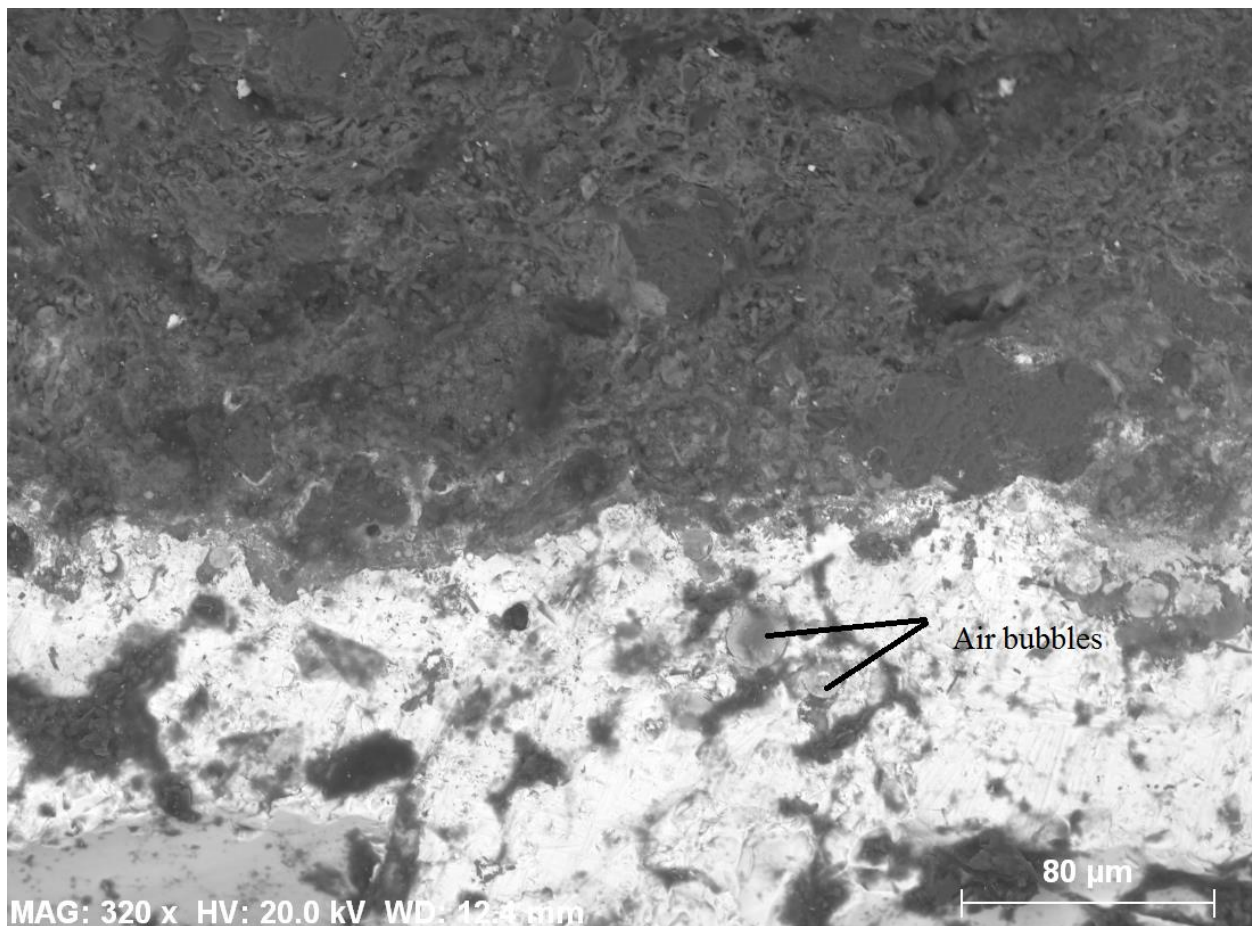


FIGURE 28. PRESENCE OF AIR BUBBLES

Regarding uXRD analysis, results showed that the sample CR/MD/0023 has strikingly distinct mineralogical and phase contents than samples CR/MD/003, CR/MD/004 and CR/MD/005. The uXRD analysis revealed that the ceramic body of the artefact is generally composed of quartz, pyroxenes (diopside and/or augite), potassium (orthoclase) and plagioclase feldspars (anorthite) (Figure 29).

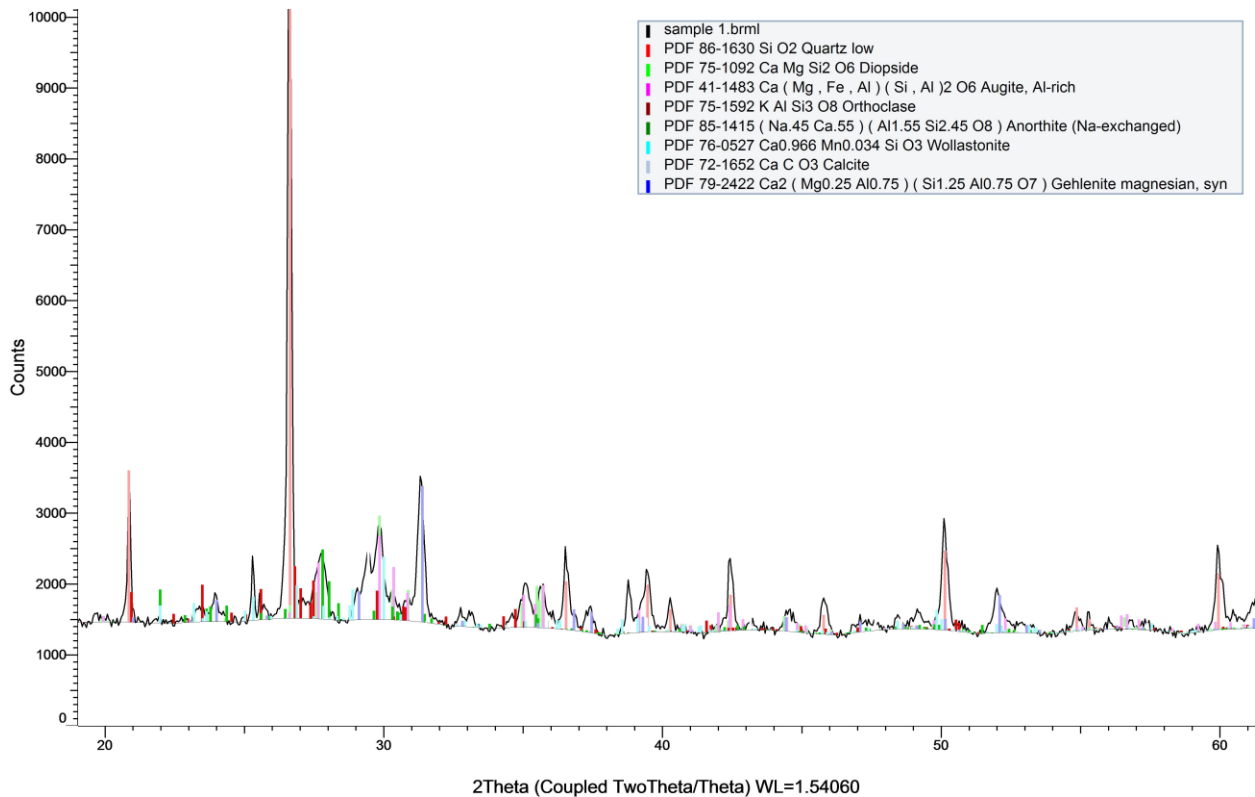


FIGURE 29. X-RAY POWDER DIFFRACTION SPECTRA OF CR/MD/0023

The presence or lack of certain mineral phases in this case can allow us advanced hypothesis on the firing conditions – both temperature and atmosphere – that have been used during manufacture of this specific pottery vessel.

uXRD data failed to show the presence of clay mineral used for manufacture of this particular vessel, which in our case could be illite/muscovite structure if take into consideration

SEM-EDS data. SEM-EDS spot microanalysis of $\text{SiO}_2/\text{Al}_2\text{O}_3$ ratios of sherd matrix showed that $\text{SiO}_2/\text{Al}_2\text{O}_3$ ratios fall within the scope of illitic clays (Figure 30; Table 11), which is between 1.53 – 2.62 (Kramar 2012, Newman 1987).

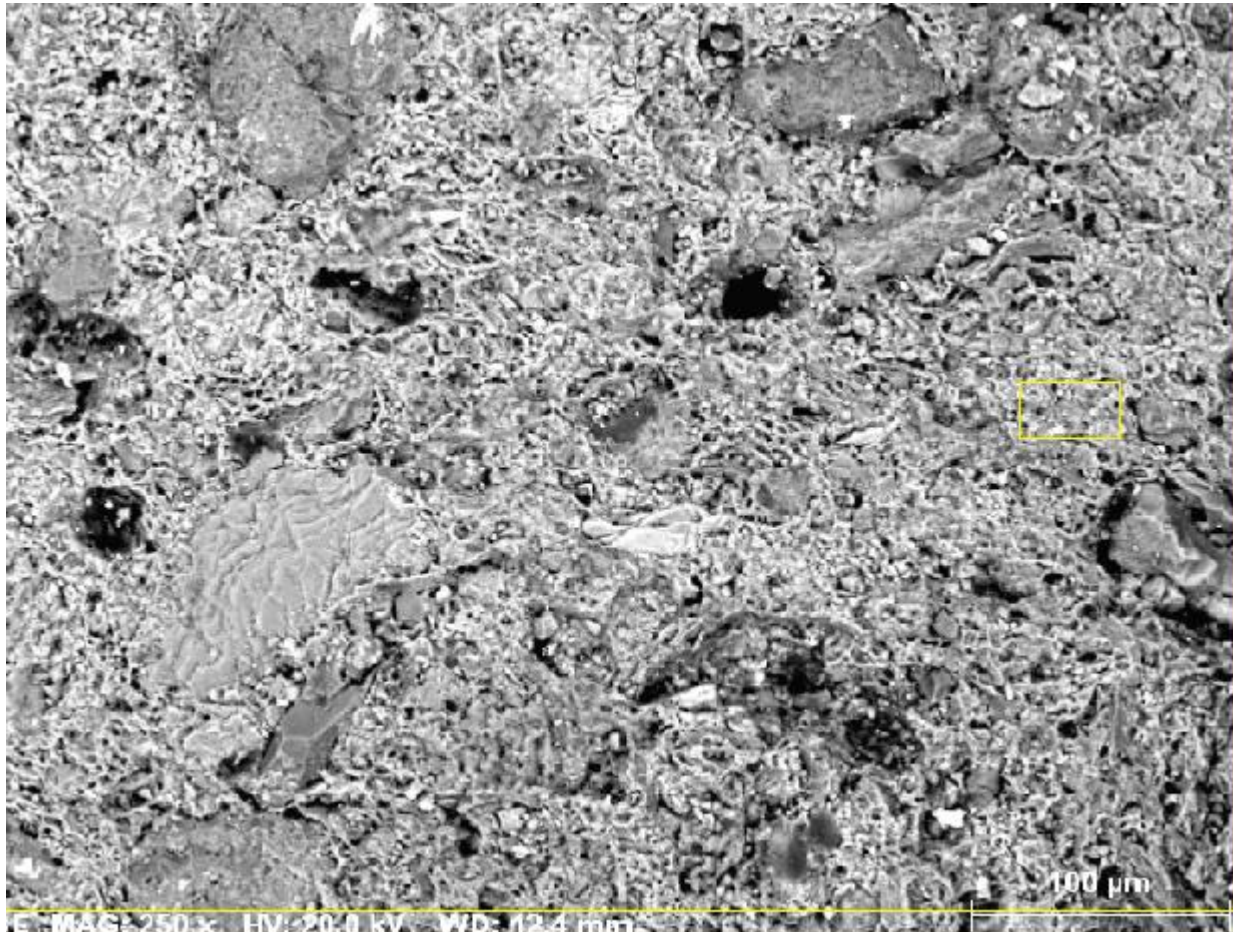


FIGURE 30. BSE IMAGE OF THE SAMPLE CR/MD/0023 AND AREA ANALYSIS OF THE CLAY

TABLE 11. SI/AL RATIOS OF THE CLAY BODY

Label	Spectrum 54
SiO_2	35.17
Al_2O_3	13.45
$\text{SiO}_2/\text{Al}_2\text{O}_3$ ratios	2.61

As noted before illite/muscovite minerals undergo a decomposition process between 700-1000 °C. Depending on the composition of the ceramic body, the complete destruction of illite/muscovite structure occurs somewhere between 950 – 1000 °C and normally ensues the development of diopside and gehlenite peaks, which are confirmed in CR/MD/0023 corresponding diffractogram (Papachristodoulou et al. 2006, Matau et al. 2013, Kramar et al. 2012).

As well as in unglazed samples from Mértola, quartz remains the main abundant phase also in this pottery group. Quartz is often considered as a ubiquitous phase found in clay deposits and thus its use as an intentionally-added temper is not always easy to confirm (Papachristodoulou 2006). Quartz temper is more likely to initiate cracking upon firing of the clay paste, owing to the higher expansion rate of the quartz crystal (Hoard 1995; Tite 2001) and as a result, quartz-tempered pottery is less resistant to mechanical and thermal stresses arising during use, when compared with calcite-tempered pottery (Tite 2001).

The presence of calcite peak in CR/MD/0023 diffractogram, proved to be very useful for the purposes of establishing firing temperatures and/or post-depositional processes of this pottery vessel. As we know, the thermal decomposition of primary calcite to lime (CaO) starts at somewhere around 600 °C and is completed around 800–850 °C releasing CO₂ as a component of the fluid phase in Ca-rich clays, thus giving rise to new “high temperature” minerals. The released fine-grained silica and aluminum from the decomposition of clays and temper (quartz and feldspars) react with free CaO to form calcium silicates such as diopside and wollastonite and calcium aluminum silicates such as anorthite and gehlenite. Gehlenite (melilite group) is stable in a calcium environment and therefore it is formed as a first product around the calcite grains, especially if the calcite was coarse grained (Rathossi et al. 2004). For low SiO₂ concentrations, the stability field of gehlenite + calcite in the presence of low contents of quartz reaches 850 °C, but with increasing SiO₂ content the equilibrium temperature is strongly reduced. Gehlenite, however, is stable at temperatures exceeding 950 °C if coexists with wollastonite, and decomposes to wollastonite and anorthite if there is enough silica to react with.

That said, identified calcite peak cannot be primary mineral because in the same time we have these high temperature minerals such as diopside, gehlenite and wollastonite. So, the logical explanation is that this calcite occurred in this vessel as a result of post-burial deposition processes due to recarbonation of lime (Papachristodoulou 2006).

When we take into consideration lack of illite/muscovite peak and presence of newly formed high temperature minerals, we can argue that firing temperature of this vessel was somewhere between 950-1050 °C.

3.2.2. Specimen CR/DR/0002

The group of archaeological artifacts registered under inventory number CR/DR/0002 is very specific archaeological finding for several reasons. At a time when the excavations of Alcáçova de Mértola occurred in one of the archaeological probes a group of highly fragmented glazed ceramic artefacts were found. In accordance to the existing situation, the archaeological interpretation, which is still up to date, is that these fragments make up one pottery vessel. For the purposes of this study three ceramic fragments were selected (MB0/5A1a, M/82/6c3a, M/79/AA1B) with a primary aim to determine whether these fragments indeed constitute a single vessel or a number of different (Figure 31). Other questions will address issues regarding similarities/differences between CR/DR/0002 and CR/DR/0023.

However, the main focus is still the same and it will concentrate mainly on providing insights about whether unglazed samples have similar chemical and mineralogical composition with these glazed specimens or they are completely different, in order to contribute to the general knowledge of the production technology as well as technological choices applied in the manufacture of this extremely rare type of Islamic material culture.



FIGURE 31. FRAGMENTS MB0/5A1A, M/82/6C3A, M/79/AA1B RESPECTIVELY

As in previous case, SEM images showed two distinguishable layers in Mértola specimens, M/82/6c3a and M/79/AA1B (except sample MB0/5A1a, where no glaze layer was identified!) – body dominated by the angular quartz and feldspars and glaze above it. Also, the absence of an engobe layer was registered as well in these cases.

The clay matrix is highly calcareous, iron-rich and homogeneous, dense, with small, more or less evenly distributed inclusions. There is no evidence of any temper. Traces of organics appear to remain in some pores and as microscopic inclusions (such as seeds, which were probably burned in kiln during firing process), although whether they were present in the raw clay, or added during preparation is unknown.

SEM backscatter electron (BSE) images show the scale of the natural inclusions and pores visible in a cross section of body fabric. Figure 32 shows a typical clay matrix with small, well-evolved inclusions. The medium grey inclusions are quartz and the lighter grey are a silica-alumina-potassium/sodium mineral.

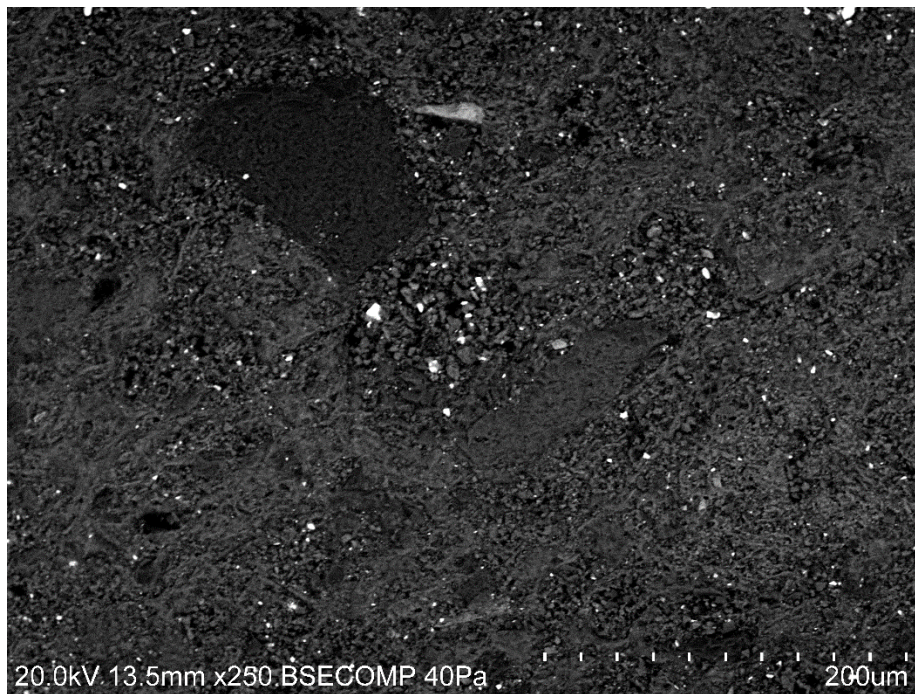


FIGURE 3213. BSE IMAGE OF M/79/AA1B BODY FABRIC AS AN EXAMPLE OF THE INCLUSION CHARACTERISTICS

The results of the chemical composition of the bodies of samples M/82/6c3a, MB0/5AIa and M/79/AA1B are shown in Table 12. According to the results, area analysis of the potsherds indicated almost completely different chemical composition between these three fragments. Therefore, we can safely assume, according to the obtained SEM-EDS data, that in this case we cannot discuss furthermore about the existence of only one vessel, but on at least two and maximum three. Also, we have to take into account that glaze layer was not present in sample MB0/5AIa during SEM observations.

SEM-EDS observations of these three samples revealed an iron-rich composition with FeO quantities ranging from 4.16 – 5.17 wt%. Quantities of Na₂O and K₂O were in a moderate range from 0.8 to 1.33 wt% and 2.06 to 2.9 wt%, respectively. Quantities of CaO and MgO were between 19.36 and 30.11 wt% and 1.89 and 4.41 wt%, respectively. As in previous case (CR/DR/0023), these pottery vessels were made out of highly calcareous clay. Smaller quantities of soda, titanium, sulphur and phosphorous completed the composition. The biggest difference among these three samples is the presence of phosphorous, which was identified in samples M/82/6c3a (9.76 wt%) and M/79/AA1B (0.48 – 0.64 wt%), while in sample MB0/5AIa it was not present. Presence of phosphorous can be explained either as indicator of bone temper in pottery or as contamination caused by secondary factors, such as cooking and/or post - depositional processes. Further, presence of SiO₂ varies through all three samples, as well as CaO and MgO. As for the type of the used clay, SEM-EDS spot microanalysis of SiO₂/Al₂O₃ ratios of sherd matrix showed that SiO₂/Al₂O₃ ratios fall within the scope montmorillonite clays in samples MB0/5AIa and M/79/AA1B (2.58-3.47), while M/82/6c3a indicated presence of illitic clay.

TABLE 12. THE AREA BODY SEM-EDS ANALYSIS, SAMPLE CR/DR/0002, NORMALIZED TO 100 WT%. NOTE THAT WEIGHT PROPORTIONS REPRESENT NORMALIZED WEIGHTS. NORMALIZED WEIGHTS HAVE BEEN CONVERTED TO OXIDES

Spectrum Label	Body area analysis					
	Sample M/82/6c3a	Sample MB0/5A1a			Sample M/79/AA1B	
	Area 1	Area 1	Area 2	Area 3 - clay matrix	Area 1	Area 3
Na ₂ O	1.12	0.8	1.06	1.15	1.33	1.2
MgO	2.38	3.48	3.75	4.41	2.98	1.89
Al ₂ O ₃	10.29	13.09	12.92	12.49	13.53	13.04
SiO ₂	30.08	37.63	36.58	34.72	43.08	42.61
P ₂ O ₅	9.76	/	/	/	0.48	0.64
SO ₂	1.63	/	0.45	0.5	0.5	0.37
K ₂ O	2.06	2.49	2.47	2.41	2.66	2.9
CaO	30.11	23.1	23.06	23.66	19.36	20.54
TiO ₂	0.3	/	/	/	0.83	/
FeO	4.52	4.49	4.16	4.23	5.17	5.15

On the other hand, point analysis revealed presence of several types of feldspars and with the help of respective EDS spectra it was feasible to reveal variations in the amounts of sodium, potassium and calcium oxides, thus providing distinction between alkaline feldspars and plagioclases (Table 13).

TABLE 13. SEM – EDS ELEMENTAL CONCENTRATIONS OF FELDSPARS IN SAMPLES MB0/5A1A, M/82/6C3A AND M/79/AA1B

Spectrum label	SiO ₂	Al ₂ O ₃	K ₂ O	Na ₂ O	CaO	FeO
Sample MB0/5A1a Point 1	55.32	19.88	0.79	10.51	5.95	1.21
Sample MB0/5A1a Point 2	51.83	18.81	11.86	1.78	5.8	1.05
M/82/6c3a Point 1	55.75	19.55	13.62	1.56	5.58	0.66
M/82/6c3a Point 2	43.81	33	12.11	0.99	7.27	2.98
M/79/AA1B Point 4	53.4	19.21	12.3	1.55	3.74	1.67

As for the glaze, SEM-EDS analysis was performed to gain information on elemental composition and texture of the outer and inner glaze of these two samples (Table 14). As mentioned earlier, glaze layer was absent in sample MB0/5A1a. The chemical analysis of the glazes determined that they belong to the high-lead type, as results showed that the most prominent component in both glazes is PbO (same type as CR/DR/0023). Its amount is readily repeatable in both inner and outer glaze. The amount of Na₂O and K₂O are in a moderate range from 1.09 – 2.92 and 1.04 – 1.78 wt %, respectively. CaO and MgO amounts are also in a moderate range from 4.5 – 5.53 and 0.27 – 1.49 wt%, respectively. The biggest difference between samples M/79/AA1B, M/79/AA1B and CR/DR/0023 is the presence of tin oxide in sample M/79/AA1B which was used as opacifier. Therefore, in this case SEM-EDS observations confirmed second type of used glaze within molded glazed pottery from Mértola: tin – opacified high - lead glaze (Figure 33).

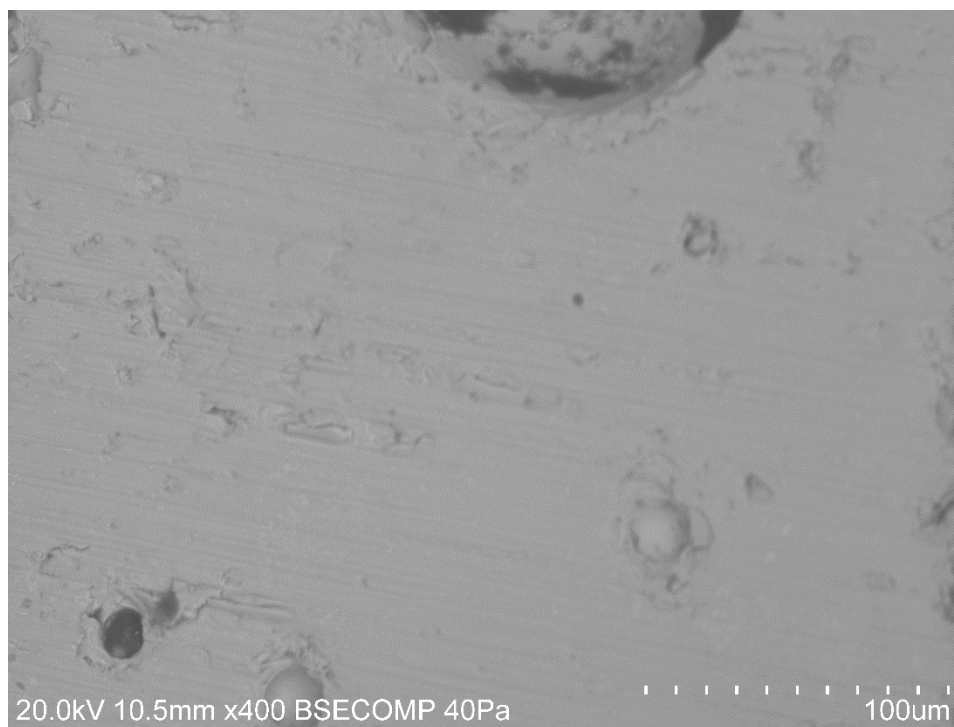


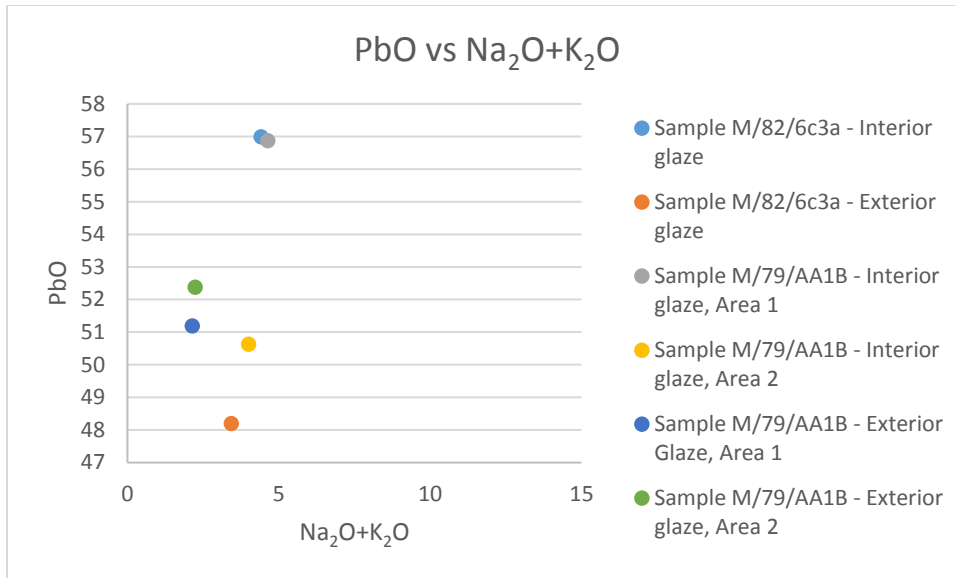
FIGURE 33. BSE IMAGE OF EXTERIOR GLAZE, SAMPLE M/82/6C3A

Tin-opacified glazes, first produced in Iraq in the eighth century AD were initially alkali glazes containing only 1-2% PbO. However, the lead content of these glazes was progressively

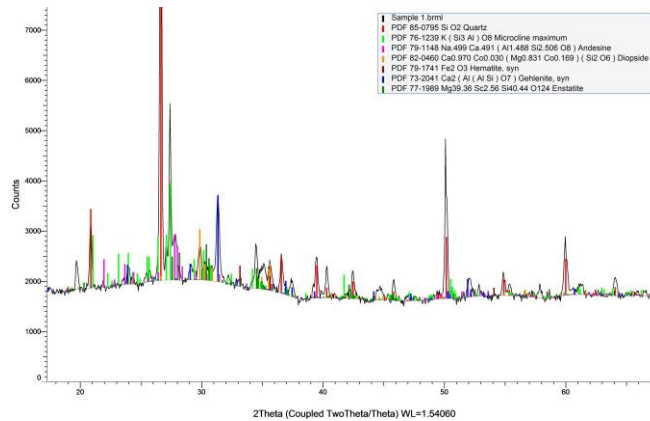
increased until, by the tenth/eleventh century AD, true lead-alkali glazes, containing typically 20-40% PbO and 5-12% alkali, were being used. Subsequently, this glaze type was used almost exclusively for the production of tin-opacified glazes throughout the Near East and Europe. However, in Iberian Peninsula the lead oxide contents tended to be higher (up to about 55% PbO) with correspondingly lower alkali contents (Tite 1998). However, the alumina content of tin-opacified lead-alkali glazes is significantly less than that of high lead glazes (0.5-3% Al₂O₃ as compared to 2-7% Al₂O₃) which is also confirmed in case of sample M/79/AA1B.

TABLE 14. THE AREA ANALYSIS OF THE GLAZES, SAMPLES M/79/AA1B M/79/AA1B AND THE CORRESPONDING PBO VS NA₂O+K₂O PLOT

Spectrum Label	Sample M/82/6c3a		Sample M/79/AA1B			
	Interior glaze	Exterior glaze	Interior glaze		Exterior glaze	
	Area 2	Area 3	Area 1	Area2	Area 1	Area 2
Na ₂ O	2.92	2.39	2.86	2.33	1.09	1.19
MgO	0.48	0.27	0.88	0.8	1.49	1.31
Al ₂ O ₃	0.57	0.32	1.87	2.74	5.22	5.37
SiO ₂	28.49	41.29	29.26	28.73	27.7	27.25
K ₂ O	1.49	1.04	1.78	1.67	1.05	1.05
CaO	4.5	/	4.68	5.53	5.3	4.94
MnO	/	/	/	/	/	/
FeO	/	/	0.9	1.26	2.02	2.22
SnO ₂	4.89	5.61	/	/	/	/
PbO	56.99	48.2	56.87	50.63	51.19	52.38



uXRD analysis showed that the fragments MB0/5A1a, M/82/6c3a, M/79/AA1B all have almost completely different mineralogical (sample M/82/6c3a has no high-temperature minerals such gehlenite and diopside, while the others do; in sample MB0/5A1a the presence of hematite was detected and in others not; sample M/79/AA1B different types of feldspars) and phase contents between them and compared to the other glazed sample (CR/DR/0023). The uXRD results are showed in figure 34.



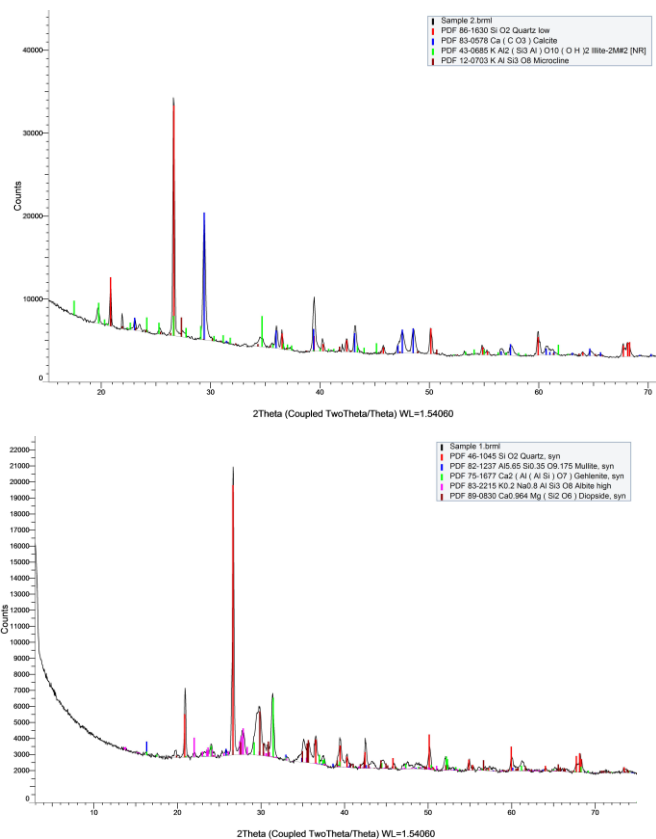


FIGURE 34. XRD SPECTRUMS OF FRAGMENTS MB0/5A1A, M/82/6C3A, M/79/AA1B, RESPECTIVELY

As we can see uXRD data failed to show the presence of clay mineral used for manufacture of vessels MB0/5A1A and M/79/AA1B, while in fragment M/82/6c3a illite structure was identified (which is in general agreement with SEM-EDS data). As noted before illite/muscovite minerals undergo a decomposition process between 700-1000 °C. Depending on the composition of the ceramic body, the complete destruction of illite/muscovite structure occurs somewhere between 950 – 1000 °C and normally ensues the development of diopside and gehlenite peaks, which are not confirmed in M/82/6c3a corresponding micro - diffractogram, thus implying firing temperature below 800-850°C (Papachristodoulou et al. 2006, Matau et al. 2013, Kramar et al. 2012). Also, the calcite peak indicates that the firing temperature was below 800-850 °C because as we know the thermal decomposition of primary calcite to lime (CaO) starts at somewhere around 600 °C and is completed around 800–850 °C releasing CO₂ as a component of the fluid phase in Ca-rich clays,

thus giving rise to new “high temperature” minerals such as diopside and wollastonite which were not identified in corresponding diffractogram.

As for the other two samples (MB0/5AIa and M/79/AA1B), the XRD results showed presence of different kinds of feldspars, both K-feldspars and plagioclases, high – temperature minerals such diopside, gehlenite and mullite released during decomposition of calcite and some iron minerals. Namely, in sample MB0/5AIa, hematite was identified, thus implying that the firing process was finished in oxidizing atmosphere.

When we take into consideration the presence of newly formed high temperature minerals, we can argue that firing temperature of this vessel was somewhere between 950-1050 °C.

If we take into account SEM-EDS data regarding chemical composition as well as XRD results concerning mineralogical composition, we can cautiously argue that fragments MB0/5AIa, M/82/6c3a and M/79/AA1B do not constitute one single unique pottery vessel.

3.3. Laser Ablation - Inductively Coupled Plasma – Mass Spectrometry (ICP – MS)

For the purposes of this study, geochemical analysis LA-ICP-MS, was used to determine whether glazed and unglazed specimens from Mértola were manufactured in the same region or they have origin.

LA-ICP-MS is one of the most important mass spectrometric multi-elemental analytical techniques for the characterization of solid samples in materials science and it is characterized by an accuracy of the determinations as good as that obtained with neutron activation analysis (NAA), commonly used in the past for provenance study of ceramics (Niziolek 2013). There are several applications of ICP-MS in literature for provenance studies, especially for ceramics. This technique provides a concentration “fingerprint” of the sample, which can be used to determine its provenance.

In best case scenario, ceramic chemical data could be statistically clustered into compositional groups that could then be matched with geological sources. However, ceramic material is a complex mixture of paste matrix (the fired clay) and temper (non-plastics naturally occurring or intentionally added to the clay). Further, the numerous choices made by a potter during the production process affect the final chemical composition. Potters may collect clays from primary locations eroding from a parent rock or from secondary locations such as a streambed (Niziolek 2013). Once clays are collected, they can be mixed with other clays, they can be cleaned of their naturally occurring non-plastics and/or they can have one or more non-plastics added to them (Niziolek 2013).

However, in the present work a complete provenance study is not possible because there are not enough reference datasets to compare results obtained from Mértola, therefore information about the origin of these vessels cannot be obtained. But, what we can achieve is to determine whether unglazed samples have the same geochemical signatures as glazed ones as well if unglazed samples share the same source as glazed specimens, thus enabling us to argue about the possible region from where unglazed samples are coming from.

Chemical composition of the unglazed and glazed samples from Mértola obtained by LA-ICP-MS for 20 elements are shown in table 15.

TABLE 15. AVERAGE CONCENTRATION VALUES OF UNGLAZED (CR/MD/003-005) AND GLAZED POTTERY FROM MÉRTOLA. OXIDES ARE GIVEN ON % WHILE MINOR AND TRACE ELEMENTS ARE IN PPM

	Na ₂ O	MgO	Al ₂ O ₃	SiO ₂	K ₂ O	CaO	TiO ₂	MnO	FeO	V	Cr	Rb	Sr	Y	Zr	Nb	Cs	Ba	Hf	Ta
CR/MD/004 - UNGLAZED	0.76	0.99	23.17	53.3	3.92	0.48	0.85	0.02	3	145.35	120.42	151.29	70.077	17.217	116.6	14.153	8.0433	467.69	3.17	1.0367
CR/MD/003 - UNGLAZED	0.68	0.89	15.76	54.34	2.72	1.65	0.69	0.03	4.47	84.767	84.17	92.507	282.4	12.183	61.18	10.013	5.6233	522.9	1.8063	0.7693
CR/MD/005 - UNGLAZED	0.59	1.33	21.21	61.74	1.74	0.37	0.98	0.01	6.2	141.65	106.67	102.2	53.663	13.807	100.93	13.5	6.8367	256.95	2.8667	1.0567
CR/DR/0002 GLAZED- M/82/6C3A	0.79	2.24	12.86	46.57	3.66	14.16	0.56	0.09	3.54	67.488	76.425	97.105	427.69	19.845	137.45	9.8925	4.9775	361.88	3.787	0.661
CR/DR/0002 GLAZED- M/80/5A1A	0.41	6.52	11.61	44.8	2.74	31.03	0.67	0.05	3.69	120.73	77.787	90.793	506.33	18.707	52.947	10.923	5.69	279.91	1.5057	0.7773
CR/DR/0002 GLAZED- M/79/AA1B	1.08	3.05	10.52	41.6	2.62	14.31	0.46	0.07	3.78	81.577	67.967	77.37	368.62	11.08	53.523	7.72	4.3167	315.3	1.4383	0.4897
CR/DR/0023 - GLAZED	1.16	2.55	9.8	42.56	2.21	10.93	0.46	0.07	2.84	50.328	55.425	64.983	325.62	12.515	49.625	7.5375	3.83	299.97	1.4403	0.4745

Major and trace element concentrations of the sherds show clear compositional differences between unglazed and glazed ware from Mértola (Figs. 27a, b and table 15), which is in line with the SEM-EDS and XRD results. Considered as a whole, unglazed ceramics are characterized by low CaO (0.37– 2.18%) and medium - high iron - oxides (from 4.47 up to 6.38 %), Al₂O₃ (15.76– 23.17%) and Na₂O + K₂O ([0.46–1.73] + [1.61–3.92] %) low MgO (0.88–1.33%) concentrations, whereas the glazed vessels show extremely high CaO (10.93–31.03%), low iron oxides (2.84– 3.78%), Al₂O₃ (9.8– 12.86%) and K₂O (2.21–3.66%) concentrations (Figures 34a and 27b). On the basis of their high CaO content, the glazed ceramics are labelled here as a calcareous ceramic group (Kibaroglu 2009).

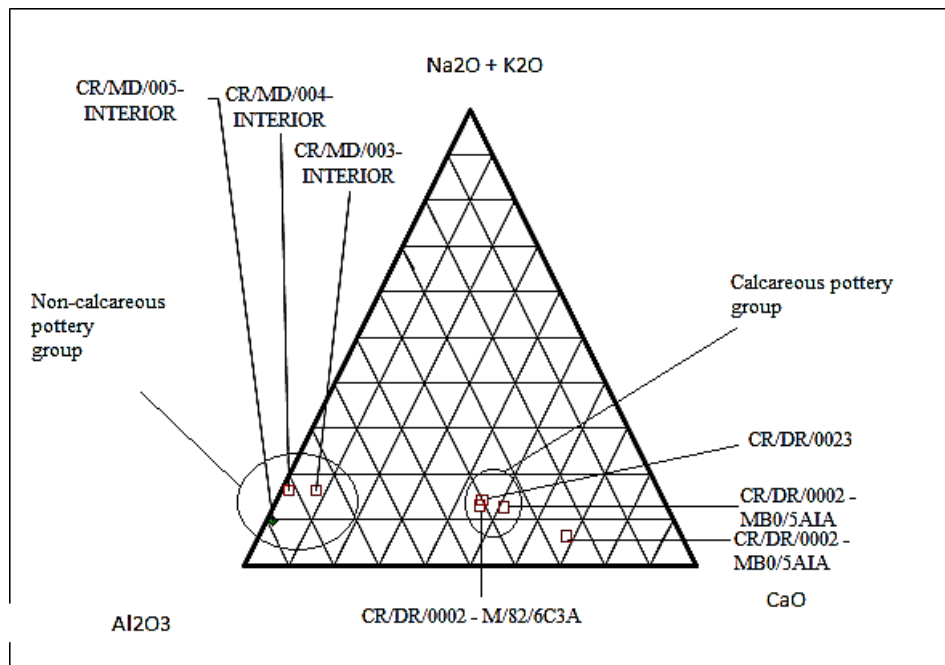
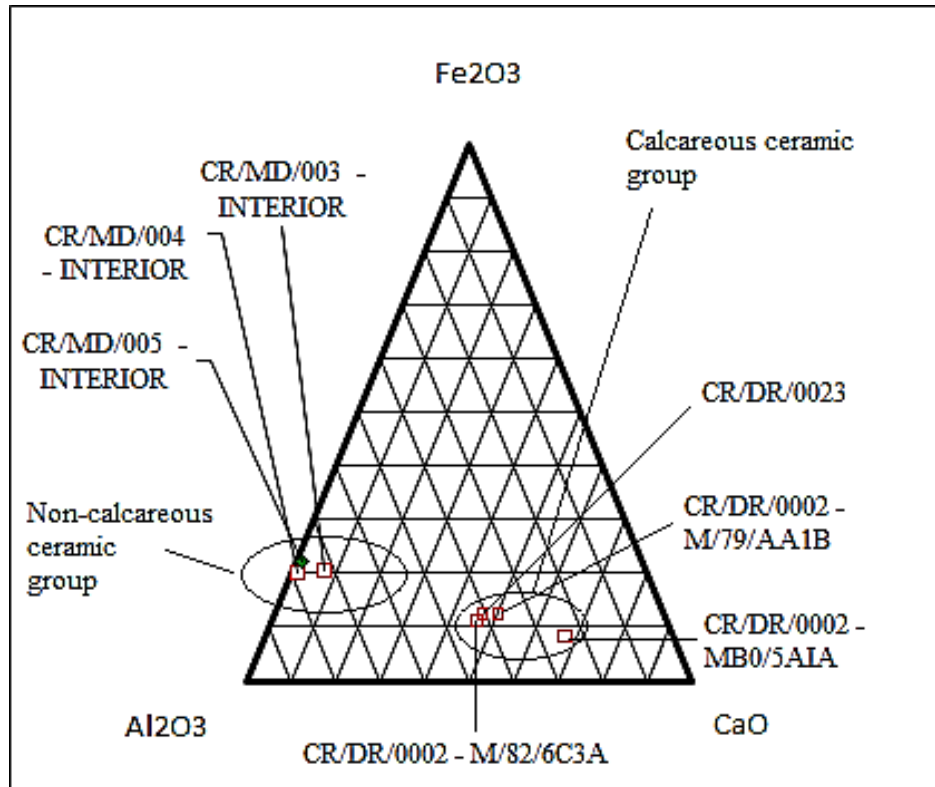


FIGURE 35A,B. TERNARY PLOT OF: (A) Al_2O_3 , CaO , Fe_2O_3 ; AND (B) Al_2O_3 , CaO , $Na_2O + K_2O$ (ALL IN OXIDES %) SHOWING TWO CERAMIC GROUPS WITHIN MERTOLA ; THE NON-CALCAREOUS CERAMIC GROUP AND HIGHLY CALCAREOUS POTTERY ASSEMBLAGE

On the other hand, bivariate plots with trace elements indicate clear differences between glazed and unglazed ceramic vessels from Mértola with enrichment in Sr and depletion in Rb in the first ones (Figure 37). However, its necessary to stress that even when we talk about heterogenous group of unglazed samples, specimen CR/MD/003 somehow groups up with the glazed samples. Namely, geochemical signature of sample CR/MD/003 falls within the group of glazed specimens (Figures 36 and 37).

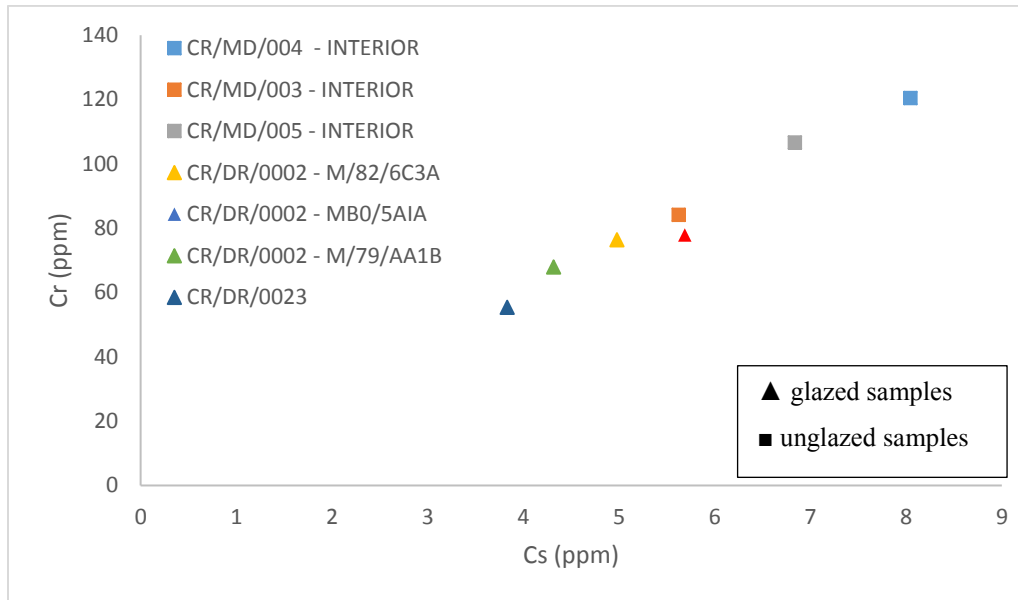


FIGURE 3614. CR VS CS BIVARIATE PLOTS OF ICP-MS DATA. NOTE VALUES ARE GIVEN IN PPM

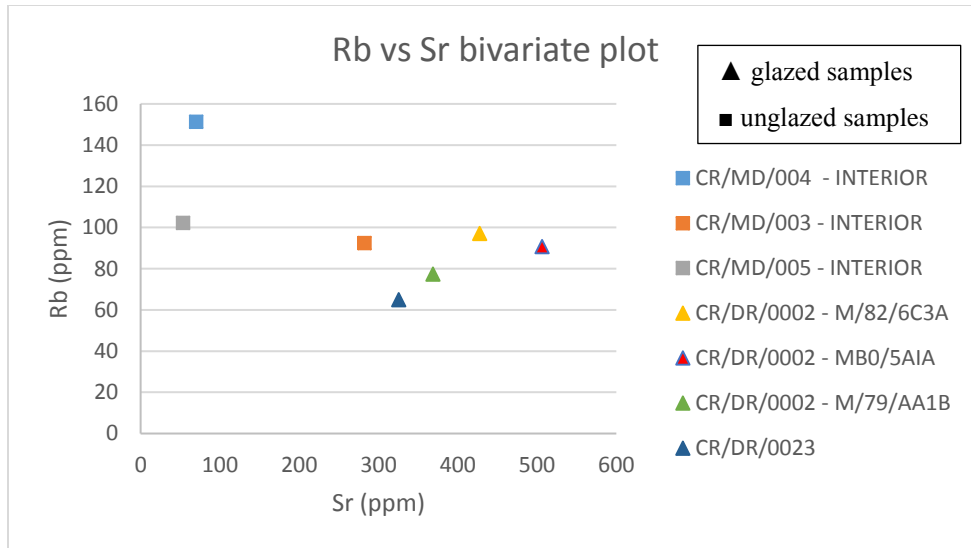
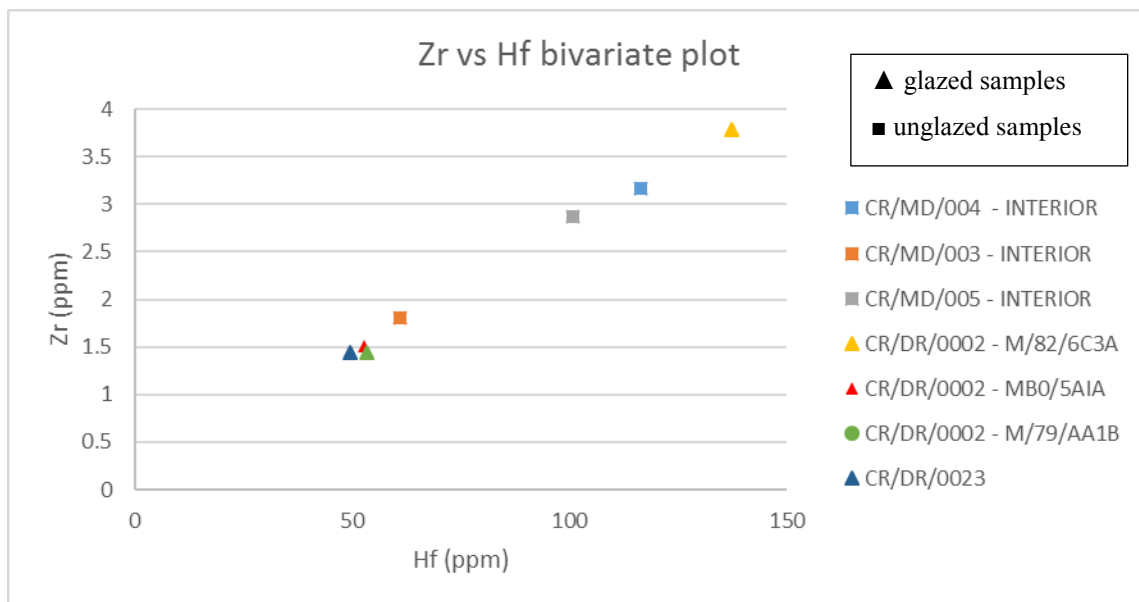
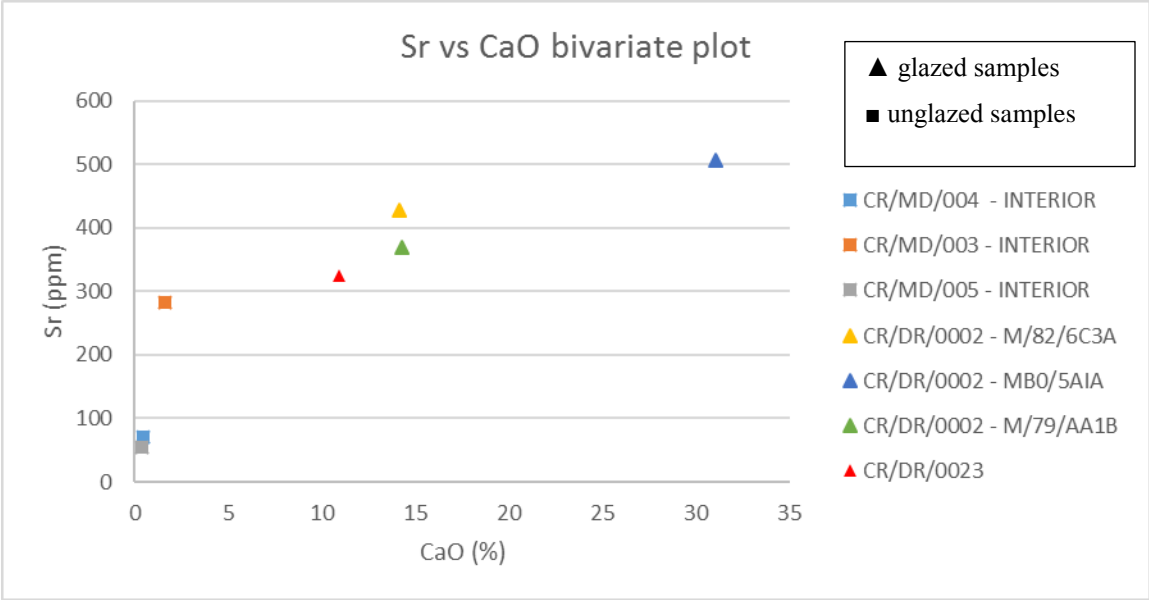


FIGURE 37. RB VS SR BIVARIATE PLOTS OF ICP-MS DATA. NOTE VALUES ARE GIVEN IN PPM





CHAPTER 4: FINAL REMARKS

This master thesis has provided thorough technological insights into the production of unglazed molded pottery from Mértola, touching on a number of issues within southwestern Iberian Islamic archaeological studies. The chosen analytical methods – SEM-EDS, XRF, ICP-MS and XRD – resulted in enhanced understanding and the development of new interpretations concerning the molded pottery of Mértola. The focus of the thesis has been to build a wide-ranging dataset of chemical and mineralogical compositions revealing the nature of clays for this specific and rare type of pottery in order to understand how these artefacts were produced, treated, used and discarded. As the first archaeometric characterization study for this type of pottery, the dataset also provides a basis for comparison to other ceramic assemblages, both intra-site (glazed and unglazed) and inter-site (Beja, Évora, Lisboa). This helps to place the ceramic found in within the wider context of a network of cultural and economic traditions that spanned the western Islamic world during the late Islamic period of 12th/13th century. Greater understanding of the ceramics also leads toward a better understanding of Mértola as a city; its culture, economy, perhaps even a local industry.

The research questions set out at the beginning of this thesis are addressed in the following pages.

What are the characteristics of the Mértola unglazed molded pottery assemblage?

This question was addressed by combining previous archaeological research and undertaking new scientific research on Mértola molded pottery – both glazed and unglazed. This revealed information on technical choices regarding raw material procurement, forming processes, decoration methods and firing conditions. Typological analysis has shown that this molded pottery from Mértola consisted of only one pottery type – jars designed as liquid containers for home use. Taking into account their fragile structure, this interpretation is highly probable. The ornamental decorations are in favor of this statement that these containers were not intended for everyday use.

The body fabrics of both glazed and unglazed pottery was examined with SEM-EDS bulk analysis at relatively low magnifications (x200 – x250) with inclusions analyzed at higher magnifications. Unglazed bodies are non – calcareous and iron-rich, with small inclusions of

quartz, micas and feldspars – quartz by far in the majority, making up 90% or so of all inclusions present. The fabrics are very fine, with inclusions usually less than 20 μm with occasional quartz inclusions as large as 100 μm or less. Non-quartz inclusions are well evolved while the harder quartz inclusions are generally sub-angular to angular. Both, in chemical and mineralogical aspect, the fabrics are very similar across all three samples (CR/MD/003, CR/MD/004 and CR/MD/005), except in the case of sample CR/MD/003 where unusually high percentage of phosphorus (~ 5 wt% P_2O_5) was recorded. As mentioned earlier, the presence of phosphorus in pottery is referred to adsorption from the soil subsequent to the discarding of utensils or to the presence of the element in the raw material, although a few authors support the hypothesis of the contamination of pots by food during cooking. In any case, future research will deal with this issue. Furthermore, SEM-EDS area analysis of clay showed that for the manufacture of these three vessels maybe different types of clay were used during the procurement process, namely illite for samples CR/MD/004 and CR/MD/005 and maybe, montmorillonite for sample CR/MD/003. Nonetheless, we can argue, with certain level of caution, that samples CR/MD/003, CR/MD/004 and CR/MD/005 according to the chemical/mineralogical results and analysis of decoration patterns come from the same production center.

The SEM-EDS bulk analysis comparative work in the glazed molded pottery showed quite the different data. Bodies were made from highly calcareous iron - rich clay, with inclusions of quartz, pyroxenes, feldspars, calcite and certain high temperature minerals such as gehlenite and wollastonite. In the terms of chemical and mineralogical composition, the fabrics are not so similar neither among them nor when compared with unglazed specimens. The largest oscillations in the chemical concentration of these samples (MB0/5A1a, M/82/6c3a, M/79/AA1B) are referring to the values of silicon, aluminum, magnesium, calcium and iron oxides. The glazed molded pottery consisted of both monochrome and polychrome wares. All of these have a typical, high-lead glaze with 45 to 68 wt% PbO content with a corresponding colorant on the exterior wall and colorless in the interior wall and we have a case of tin opacified lead glaze in sample M/82/6c3a. The glazes are thin and smooth, with few bubbles or relict grains and are generally well-preserved. What is astonishing is that the engobe layer was absent among glazed specimens, which may be the result during the process of glaze application. According to SEM-EDS observations on the area where glaze and the body are connected it is implied that the glaze layer was applied before the vessel was fired.

What new interpretations can be derived from the scientific evidence regarding technical and aesthetic style?

The scientific evidence provided certain insights to the process used by the potters of these wares regarding manufacture which to some extent question the current archaeological interpretation. This applies to the samples CR/MD/003, CR/MD/004 and CR/MD/005 where the so-called red “slip” layer was disputed. Also, samples within specimen CR/DR/0002 were interpreted as a part of one single vessel, while, both chemical and mineralogical data question that interpretation. As for the glazes it was impossible to accurately determine ratios of lead to silica in the original recipe, but the high silica content, however, indicates that the glaze was applied as a lead-silica slurry. All the sherds were fired in an oxidized atmosphere (except sample CR/MD/005 where it was reducing atmosphere), although there are differences between the glazed and unglazed wares that indicate different firing methods. The unglazed wares are not as highly oxidized as the glazed wares, and are more likely to show variations in oxidation from one side of the vessel to the other. The lead and alkali glazed wares may have been fired in the same kilns, together, at the same temperature and heating/cooling rate as the lead glazes are well-fired and the alkali glazes somewhat underfired.

What relationships can be seen between the different assemblages present at Mértola?

Pottery production provenance has been of interest to archaeologists studying migration pathways, social and economic interaction, and political organization have all focused-on pottery production provenance. But, in this case we cannot pinpoint the exact location from where unglazed specimens originated because, as previously noted, there are not enough comparable datasets. Nevertheless, we can safely propose that in the studied samples we can distinguish at least two compositional groups that probably used different raw materials for manufacture, therefore different production technology was applied. Namely for the manufacture of unglazed samples non-calcareous clay was used, while for the glazed specimens calcareous clay was applied. That said, it is normal that we expect that these two groups of pottery were fired under different conditions, where unglazed samples were baked under lower temperatures (850-950 °C) and

glazed ones under much higher (950-1050 °C). That can mean that these samples came from different workshops or they were produced in the same but with different raw materials and firing methods.

Priorities for future research.

In order to explore further economic, political and social significance of the pottery industry in Mértola, and the rest of Islamic world in the Iberian Peninsula, additional work is needed regarding the provenance of the vessels. Much larger sample sets must be subjected to XRF, NAA or ICP analysis, on all types of ceramic wares from several sites like Beja, Évora, Lisbon and not only Mértola. Pinning down provenance as closely as possible will bring new avenues to the study of pottery in the region. Density, distribution and exchange all come into play at this point, and may reveal differences between cities regarding their material culture in ways typological analysis cannot. Large data sets can then be cross-checked against technical variations to look for any coordinated patterns of development over time.

BIBLIOGRAPHY

Albero D. 2014. Materiality, techniques and society in pottery production. Warsaw: De Gruyter Open

Arantegui P.J., Castillo R.J. 2000. Characterization of red-colored slips (almagra) on Islamic ceramics in Muslim Spain. *Archaeometry* **42**: pp. 119-128.

Artioli G. 2010. Scientific Methods and Cultural Heritage. Oxford: Oxford University Press.

Barilaro D., et al. 2008. A non-invasive analysis of ‘proto-majolica’ pottery from southern Italy by TOF neutron diffraction. *Journal of physics: Condensed Matter* **20**: pp.1-6.

Barilaro D., et al. 2008. FT-IR absorbance spectroscopy to study Sicilian ‘proto-majolica’ pottery. *Vibrational Spectroscopy* **48-2**: pp. 269-275.

Bayazit M., et al. 2016. Archaeometric investigation of the Late Chalcolithic-Early Bronze Age I and the 1st–2nd millennium BCE potteries from Kuriki-Turkey. *Applied Clay Science* **126**: pp. 180-189.

Bong W.S.K., Matsumura K., Nakai I. 2008. Firing technologies and raw materials of typical early and middle Bronze Age pottery from Kaman-Kalehöyük: a statistical and chemical analysis. *Anatolian Archaeological Studies* **17**: pp. 295–311.

Disney A.R. 2009. *A history of Portugal and the Portuguese Empire*. New York: Cambridge University Press.

Feliu, M.J., Edreira, M.C., Martín J., 2004. Application of physical–chemical analytical techniques in the study of ancient ceramics. *Analytica Chimica Acta* **502**: pp. 241–250.

Fierro M. 2011. The Almohads. In Fierro, M. (Ed.) *The New Cambridge History of Islam*, Vol 2, (pp. 66-106). New York: Cambridge University Press.

Froh, J. 2004 Archaeological Ceramics Studied by Scanning Electron Microscopy. *Hyperfine interactions* **154**: pp. 159-176

Goffer Z. 2007. *Archaeological Chemistry*. Second Ed. John Wiley & Sons, Inc., Hoboken, New Jersey.

Gómez Martínez S. 2000. *Cerámica a molde de época Islámica*. Mértola: Campo Arquelógico de Mértola.

Gómez Martínez S. 2014. *Cerámica Islámica de Mértola*. Mértola: Campo Arquelógico de Mértola.

Hall E.T. 1960. X-ray fluorescent analysis applied to archaeology. *Archaeometry* **3**: 29-37.

Hoard R.J., O'Brien, M.J., 1995. A materials-science approach to understanding limestone-tempered pottery from the Midwestern United States. *Journal of Archaeological Science* **22**: pp. 823–832.

Hubbard C. R., Evans E. H., Smith D.K. 1976. The Reference Intensity Ratio, I/I_c , for Computer Simulated Patterns. *Journal of Applied Crystallography* **9**: pp. 169.

Jenkins M. 1983. *Islamic Pottery: A Brief History*. New York: The Metropolitan Museum of Art

Jones A. 2002. *Archaeological theory and scientific practice*. Cambridge: Cambridge University Press

Jones A. 2004. Archaeometry and materiality: materials-based analysis in theory and practice. *Archaeometry* **46-3**: pp. 327-338.

Kennett D. J. et al. 2002. Compositional Characterization of Prehistoric Ceramics: A New Approach. *Journal of Archaeological Science* **29**: pp. 443–455.

Kiruba S., Ganesan S. 2015. FT-IR and Micro-Raman spectroscopic studies of archaeological potteries recently excavated in Poompuhar, Tamilnadu, India. *Spectrochimica Acta Part A: Molecular and Biomolecular Spectroscopy* **145**: pp. 594-597.

Kramar S., et al. 2012. Mineralogical and geochemical characteristics of Roman pottery from an archaeological site near Mošnje (Slovenia). *Applied Clay Science* **57**: 39-48

Krapukaitytė, A., Tautkus, S., Kareiva, A., Zalieckienė, E., 2008. Thermal analysis - a powerful tool for the characterization of pottery. *Chemija* **19**: pp. 4–8.

Maritan, L., Mazzoli, C., Nodari, L., Russo, U., 2005. Second Iron Age grey pottery from Este (Northeastern Italy): study of provenance and technology. *Applied Clay Science* **29**: pp. 31–44.

Matau F., et al. 2013. Physical study of the Cucuteni pottery technology. *Journal of Archaeological Science* **40**: pp. 914-925

Mason R.B., Tite M. S. 1997. The beginnings of the tin-opacification of pottery glazes. *Archaeometry* **39**: pp. 41-58.

McConville C.J., Lee W.E. 2005. Microstructural Development on Firing Illite and Smectite Clays Compared with that in Kaolinite. *Journal of the American Ceramic Society* **88-8**: pp. 2267-2276

Miller M.L.H. 2007. *Archaeological Approaches to Technology*. London: Elsevier

Molera J., et al. 2001. Interactions between Clay Bodies and Lead Glazes. *Journal of the American Ceramic Society* **84-5**: pp. 1120 – 1128

Moreno M. E. 2011. The Iberian Peninsula and North Africa. In Robinson, C. (Ed.) *The New Cambridge History of Islam*, Vol 1, (pp. 581-623). New York: Cambridge University Press.

Newman A.C.D. 1987. *Chemistry of clays and clay minerals*. London: Wiley

Özçatal M., et al. 2014. *Characterization of lead glazed potteries from Smyrna (Izmir/Turkey) using multiple analytical techniques; Part I: Glaze and engobe*. *Ceramics international* **40**: pp. 2143-2151

Palamara E., et al. 2016. Technology issues of Byzantine glazed pottery from Corinth, Greece. *Microchemical Journal* **129**: pp. 137 – 150.

Papachristodoulou, C., Oikonomou, A., Ioannides, K., Gravani, K., 2006. A study of ancient pottery by means of X-ray fluorescence spectroscopy, multivariate statistics and mineralogical analysis. *Analytica Chimica Acta* **573–574**: pp. 347–353.

Parkes. P.A. 2015. *Current Scientific Techniques in Archaeology*. New York: Routledge

Pollard, A.M., Heron, C. 2008. *Archaeological Chemistry*. Cambridge: RSC Publishing.

Pollard A.M. et al. 2011. *Analytical chemistry in Archaeology*. New York: Cambridge University Press.

Rajaratnam D. 2010. *Instrumental Chemical Analysis: Basic Principles and Techniques*. Department of Chemical and Biomolecular Engineering, Faculty of Engineering. National University of Singapore.

Rathossi C. et al. 2004. Technology and composition of Roman pottery in northwestern Peloponnese, Greece. *Applied Clay Science* **24**: pp. 313-326

Rice P.M. 1987. *Pottery Analysis*. Chicago/London: The University of Chicago Press.

Rodrigues S.F.S., Costa M.L. 2016. Phosphorous in archaeological ceramics as evidence of the use of pots for cooking food. *Applied Clay Science* **123**: pp. 224-231

al-Saad Z. 2002. Chemical Composition and Manufacturing Technology of a Collection of Various Types of Islamic Glazes Excavated from Jordan. *Journal of Archaeological Science* **29**: pp. 803-810

Shackley M.S. 2011. X-ray Fluorescence Spectrometry in Twenty-First Century Archaeology. In Shackley, M.S. (Ed.) *X-ray Fluorescence Spectrometry in (XRF) Geoarchaeology*, (pp. 1-7). New York: Springer.

Sillar B., Tite M.S. 2000. The challenge of „technological choices“ for materials science approaches in archeology. *Archaeometry* **42-1**: pp. 2-20.

Stevenson C., Gurnick M. 2016. Structural collapse in kaolinite, montmorillonite and illite clay and its role in the ceramic rehydroxylation dating of low-fired earthenware. *Journal of Archaeological Science* **69**: pp. 54-63.

Stokes D. 2008. *Principles and Practice of Variable Pressure/Environmental Scanning Electron Microscopy (VP-ESEM)*. Cornwall: John Wiley & Sons Ltd.

Tite M.S., Freestone I., Mason R., Molera J., Vendrell-Saz M., Wood N. 1998. Lead Glazes in Antiquity – Methods of Production and Reasons for Use. *Archaeometry* **40-2**: pp. 241-260.

Tite M.S. 1991. Archaeological science – past achievements and future prospects. *Archaeometry* **33-2**: pp. 139-151.

Tite M.S., Kilikoglou V., Vekinis G., 2001. Strength, toughness and thermal shock resistance of ancient ceramics, and their influence on technological choice. *Archaeometry* **43-3**: pp. 301–324.

Tite M.S. 2008. Ceramic Production, Provenance and Use – A Review. *Archaeometry* **50-2**: pp. 216-231.

Tite M.S. 2011. The technology of glazed Islamic ceramics using data collected by the late Alexander Kaczmarczyk. *Archaeometry* **53-2**: pp. 329 – 339.

Torres C. 1992. O Gharb Al Andaluz. In J. Matoso (dir.), *História de Portugal* (Vol. 5, pp. 363-441). Lisboa: Circulo de Leitores.

Quinn P. 2013. *Ceramic petrography*. Oxford: Archaeopress

Yates M.D., Rosenberg E.P. 1997. Characterization of neoformed illite from hydrothermal experiments at 250 °C. *American Mineralogist* **83**: pp. 1199-1208

Zerai A. 2015. *Archaeometric Study of Lusitanian amphorae from Troia’s Peninsula, Portugal*. Unpublished Master thesis. Universidade de Evora, Portugal.